Finanziato dall'Unione europea NextGenerationEU
Ministero dell'Università e della Ricerca
Italiadomani
UNIVERSITÀ DI SIENA 1240
GIOVANISÌ
Regione Toscana
Consiglio Nazionale delle Ricerche
UNIVERSITÀ DEGLI STUDI FIRENZE Da un secolo, oltre.
ISTITUTO NAZIONALE DI GEOFISICA E VULCANOLOGIA
UNIVERSITÀ DI PISA

UNIVERSITÀ DI SIENA 1240

Dipartimento di Scienze della Vita

Dottorato in Scienze della Vita-Life Sciences

38° Ciclo

Coordinatrice: Prof.ssa Simona Maccherini

Magnetic and chemical air biomonitoring for the preservation of cultural heritage

Settore scientifico disciplinare: *BIOS-01/C*

Candidata
Lisa Grifoni
Via P.A. Mattioli, 4, Siena

Supervisore
Stefano Loppi
Università di Siena

Co-supervisore
Aldo Winkler
Istituto Nazionale di Geofisica e Vulcanologia

Anno accademico di conseguimento del titolo di Dottore di ricerca
2024/25

Table of contents

Abstract

Air pollution poses a challenging threat to cultural heritage: the deposition of particulate matter (PM) on surfaces leads to soiling, colour alteration, and material degradation. Pollution monitoring is therefore central to preventive conservation; however, traditional PM samplers are not always feasible in museums and archaeological sites for aesthetic and operational reasons. This thesis addresses this problem by adopting a nature-based biomonitoring approach—using lichens and tree leaves—to delineate deposition patterns of PM and potentially toxic elements (PTEs) both inside and outside the study contexts.

The three chapters present different applications of magnetic and chemical biomonitoring based on transplants of the lichen *Evernia prunastri* and leaf sampling from site-specific tree species. In the first case study (Peggy Guggenheim Collection, Venice), located in a peculiar aquatic traffic area, lichens showed no substantial indoor bioaccumulation of PM and PTEs (with a limited exception for Zn); outdoors, magnetic measurement highlighted a moderate bioaccumulation only on lichens, that was not evident for *Pittosporum tobira* leaves. The second chapter (Colosseum Archaeological Park, Palatine Hill, Rome) examines an archaeological site in an urban setting: lichen transplants and leaves from several plant species indicate that the horizontal distance from the road source drives PM diffusion more strongly than elevation. Leaves intercept both airborne and resuspended fractions, confirming their potential for preventive mitigation, while lichens are specifically suitable for outlining the airborne component of PM. The third chapter (Museo Nacional de Bellas Artes and Museo Histórico Nacional, Buenos Aires) shows, via magnetic properties and elemental analyses, that most outdoor metallic PM derives from brake abrasion; this signal does not translate into measurable indoor bioaccumulation. Under comparable conditions, *Jacaranda mimosifolia* is more efficient than *Fraxinus americana* at intercepting PM and PTEs.

Overall, the thesis validates an integrated magnetic–chemical biomonitoring approach that identifies vehicle-derived particulate sources, quantifies indoor–outdoor gradients of exposure to PM, and guides vegetation-based mitigation measures to support the preventive conservation of cultural heritage.

Riassunto

L'inquinamento atmosferico rappresenta una criticità rilevante per la tutela del patrimonio culturale: la deposizione del particolato (PM) sulle superfici comporta fenomeni di annerimento e alterazione cromatica, oltre a favorire processi di degrado dei materiali. Il monitoraggio della qualità dell'aria è quindi centrale nelle strategie di conservazione preventiva; tuttavia, per ragioni estetiche e operative, i campionatori tradizionali di PM non sono sempre utilizzabili in musei e siti archeologici. Questa tesi affronta il problema adottando un approccio di biomonitoraggio "nature-based", basato su licheni e foglie di specie arboree, per delineare i *pattern* di deposizione del PM e degli elementi potenzialmente tossici sia all'interno sia all'esterno dei contesti studiati.

I tre capitoli presentano differenti applicazioni di biomonitoraggio magnetico e chimico, utilizzando trapianti del lichene *Evernia prunastri* e campionamenti fogliari delle specie presenti *in situ*. Nel primo caso-studio (Peggy Guggenheim Collection, Venezia), situato in un'area a traffico minimo, i licheni non hanno evidenziato bioaccumulo significativo di PM ed elementi potenzialmente tossici nelle sale espositive (con una limitata eccezione per Zn); all'esterno, le misurazioni magnetiche hanno mostrato un modesto bioaccumulo per i licheni, non evidenziato con le foglie di *Pittosporum tobira*. Il secondo capitolo (Parco Archeologico del Colosseo, Colle Palatino, Roma) analizza un sito archeologico in un contesto urbano: trapianti lichenici e foglie di diverse specie hanno indicato che la distanza dalla sorgente stradale condiziona la diffusione del PM più della quota. Le foglie intercettano sia la frazione aerotrasportata sia quella risospesa, confermandone il potenziale nella mitigazione preventiva, a differenza dei licheni che, invece, intercettano la sola frazione aerotrasportata. Il terzo capitolo (Museo Nacional de Bellas Artes e Museo Histórico Nacional, Buenos Aires) documenta, mediante proprietà magnetiche e analisi degli elementi chimici, che la quota principale di PM metallico esterno deriva dall'abrasione dei freni; tale segnale non si riflette in un bioaccumulo misurabile all'interno. A parità di condizioni, *Jacaranda mimosifolia* è risultata più efficiente di *Fraxinus americana* nell'intercettare PM e PTEs.

Nel complesso, la tesi convalida un approccio integrato di biomonitoraggio magneto-chimico che consente di identificare le sorgenti di particolato di origine veicolare, quantificare i gradienti di esposizione indoor/outdoor al PM e orientare interventi di mitigazione basati sulla vegetazione, a supporto della conservazione preventiva del patrimonio culturale.

Overview of the PhD thesis

This thesis aimed to apply air biomonitoring of particulate matter (PM) and potentially toxic elements (PTEs) to cultural heritage. The main biomonitor used in the experiments was the lichen *Evernia prunastri,* along with the collection of leaves from the available plant species present near each site. The first phase involved the lichen transplants exposure in the absence of vehicle traffic. It was realized at the Peggy Guggenheim Collection in Venice, considering both outdoor and indoor areas. In this particular urban context, where traffic was mainly maritime, the bioaccumulation of PM and PTEs by lichens and leaves was low and outdoors only. Subsequently, a mainly outdoor experiment was conducted at the Palatine Hill, part of the Colosseum Archaeological Park in Rome. In this case, the bioaccumulation of different biomonitors inside and outside the archaeological park was investigated, assessing PM gradients with distance and the role of vegetation as a pollution barrier. In this case, the main source of pollutants was a busy road adjacent to the site, Via dei Cerchi. Different plant species were tested, highlighting the high capacity of leaves from *Quercus ilex* trees to intercept particulate matter and PTEs. Lichens also revealed that the diffusion pattern of traffic-related tracers was influenced more by horizontal distance than by height above road level. In the light of this evidence, a biomonitoring experiment was conducted in two museums exploring indoor–outdoor PM dynamics in a traffic-dominated megacity, Buenos Aires, Argentina, and comparing the pollutant interception capacity of *Jacaranda mimosifolia* and *Fraxinus americana*. In both museums, the Museo Histórico Nacional and the Museo Nacional de Bellas Artes, the concentrations of metallic magnetic particles and PTEs were negligible indoors, whereas elevated concentrations were detected outdoors. Of particular relevance was the bioaccumulation observed in the leaves of *Jacaranda mimosifolia*.

Author contribution for published chapters

Chapter 1 – Grifoni, L., Winkler, A., Lella, L. A. di, Buemi, L. P., Sgamellotti, A., Spagnuolo, L., & Loppi, S. (2024). Magnetic and chemical biomonitoring of particulate matter at cultural heritage sites: The Peggy Guggenheim Collection case study (Venice, Italy). Environmental Advances, 15. Author contribution: **L.G.:** Methodology, Validation, Formal analysis, Investigation, Writing – original draft. **A.W.:** Conceptualization, Methodology, Validation, Formal analysis, Investigation, Writing – original draft, Supervision, Funding acquisition. **L.A.D.L.:** Formal analysis. **L.P.B.:** Investigation, Supervision, Methodology. **A.S.:** Conceptualization, Investigation, Supervision, Methodology. **L.S.:** Formal analysis. **S.L.:** Conceptualization, Methodology, Validation, Formal analysis, Investigation, Writing – original draft, Supervision.

Chapter 2 – Grifoni, L., Winkler, A., Boldrighini, F., di Lella, L. A., Russo, A., Sgamellotti, A., Spagnuolo, L., Strano, G., & Loppi, S. (2024). Nature-based solutions for monitoring the impact of vehicular particulate matter and for the preventive conservation of the Palatine Hill archaeological site in Rome, Italy. Science of The Total Environment, 946, 174358. Author contribution: **L.G.:** Writing – original draft, Visualization, Validation, Methodology, Investigation, Formal analysis, Data curation, Conceptualization. **A.W.:** Writing – original draft, Visualization, Validation, Supervision, Resources, Project administration, Methodology, Investigation, Funding acquisition, Formal analysis, Data curation, Conceptualization. **F.B.:** Supervision, Investigation, Conceptualization. **L.A.D.L.:** Formal analysis, Data curation. **A.R.:** Supervision, Investigation, Conceptualization. **A.S.:** Supervision, Conceptualization. **L.S.:** Validation, Investigation, Data curation. **G.S.:** Supervision, Investigation, Conceptualization. **S.L.:** Writing – original draft, Visualization, Validation, Supervision, Methodology, Investigation, Formal analysis, Data curation, Conceptualization.

Chapter 3 – Grifoni, L., Winkler, A., Chaparro, M. A. E., di Lella, L. A., Marte, F., Sgamellotti, A., Spagnuolo, L., Tascon, M., Buitrago Posada, D., Marié, D. C., Scoccimarro, M., & Loppi, S. (2025). Magnetic and chemical biomonitoring with lichens and vascular plants for the preservation of cultural heritage: A case study at two museums in a megacity (Buenos Aires, Argentina). Science of the Total Environment, 988. Author contribution: **L.G.:** Writing – original draft, Visualization, Validation, Methodology, Investigation, Formal

analysis, Data curation. **A.W.:** Writing – original draft, Visualization, Validation, Supervision, Resources, Project administration, Methodology, Investigation, Funding acquisition, Formal analysis, Data curation, Conceptualization. **M.A.E.C.:** Writing – original draft, Methodology, Investigation, Formal analysis, Data curation. **L.A.D.L.:** Methodology, Formal analysis, Data curation. **F.M.:** Investigation, Conceptualization. **A.S.:** Supervision, Investigation, Conceptualization. **L.S.:** Investigation, Formal analysis, Data curation. **M.T.:** Methodology, Formal analysis, Data curation, Conceptualization. **D.B.P.:** Investigation, Formal analysis, Data curation. **D**.**C.M.:** Investigation, Formal analysis, Data curation. **M.S.:** Formal analysis, Data curation. **S.L.:** Writing – original draft, Validation, Supervision, Methodology, Investigation, Formal analysis, Data curation, Conceptualization.

Thesis introduction

Cultural heritage and air pollution

Cultural heritage is a fundamental component of collective identity and memory, encompassing monuments, artworks, and archaeological sites that reflect a society's history and values. Cultural assets are constantly exposed to environmental agents of deterioration, which threaten their conservation. Among these risk factors, airborne pollutants represent one of the most pervasive and insidious threats, capable of inducing both aesthetic alterations and structural damage (Bonazza et al., 2005). Particulate matter (PM), especially fractions enriched in potentially toxic elements (PTEs), can accumulate on surfaces, leading to soiling, pigments alteration, and reduced surface reflectance. Over time, chemical reactions between deposited pollutants and substrate materials may cause the degradation of organic binders in paintings (Sotiropoulou et al., 2018).

Both outdoor and indoor settings are affected by particulate deposition: outdoor monuments are directly exposed to atmospheric particles, while indoor collections may be impacted by pollutant infiltration through ventilation systems, open access points, or resuspension due to human activity. The risk posed by PM and PTEs is particularly acute in urban areas, where emissions from vehicular traffic, industrial activities, domestic heating, and other anthropogenic sources increase pollutant concentrations (Querol et al., 2004). Even in areas with low traffic, local sources such as boat engines, construction dust, or biomass burning can contribute significantly to airborne pollutant loads. Accurate quantification of these pollutants is essential to mitigate damage before it becomes irreversible (Ashley-Smith, 1999; Camuffo, 2014).

Preventive conservation is a cornerstone of cultural heritage protection. Many materials, including pigments, paper, and metals, undergo chemical and physical alterations that are irreversible once deterioration begins (Schmid et al., 2021), and restoration processes can be time-consuming, costly, and potentially invasive. The presence of airborne pollutants continually increases the risk of deterioration. Therefore, preventive measures are essential to minimize interventions, and institutions must implement robust monitoring and control strategies to ensure the preservation of cultural heritage for future generations.

However, the practical constraints of heritage environments, including architectural sensitivity, budget limitations, and the need for non-intrusive techniques, often preclude the

installation of conventional air quality monitoring equipment. This critical gap in site-specific, high-resolution pollution data represents a major challenge to effective preventive conservation. Integrating biomonitors into atmospheric monitoring frameworks provides a central, cost-effective, and non-intrusive approach to overcoming these limitations.

Air biomonitoring as a conservation tool

Biomonitoring encompasses a suite of techniques that use a wide range of organisms to assess pollutant accumulation over time, thereby detecting the bioaccumulation of contaminants dispersed in the air (Wolterbeek, 2002), water (Gerhardt et al., 2006), and soil (Calzoni et al., 2007). The use of biomonitors, such as lichens and tree leaves, is a well-established and widely applied approach for assessing air quality, owing to their capacity to intercept airborne anthropogenic particulates (Giordano et al., 2005; Levei et al., 2021).

Lichens, in particular, are widely used biomonitors because of their physiology. Lacking roots and a protective cuticle, they absorb nutrients directly from the atmosphere and efficiently bioaccumulate airborne pollutants (Conti & Cecchetti, 2001).

Lichens offer several advantages for air-quality monitoring at cultural heritage sites: (i) high sensitivity to the accumulation of coarse and fine PM, metallic particles, and PTEs from anthropogenic sources; (ii) flexibility, as cleaned samples can be deployed as transplants where fixed monitoring stations are impractical or prohibited; and (iii) cost-effectiveness, owing to low equipment needs and minimal maintenance. *Evernia prunastri* (L.) Ach. (Fig. 1) is a widespread epiphytic lichen of temperate forests in Europe, characterized by a dorsiventral thallus with strap-like lobes, green above and white below. Its suitability as a biomonitor has been extensively demonstrated in both rural and urban settings, including for trace metals (Loppi et al., 1996; Vannini et al., 2019), gaseous pollutants such as NH_3 and NO_2 (Frati et al., 2006), magnetic particles (Winkler et al., 2020), and organic contaminants (Monaci et al., 2020). Evidence of applicability under indoor exposure conditions has been reported (Paoli et al., 2019); therefore, *E. prunastri* was selected as the biomonitor for cultural-heritage environments in this thesis.

A  B 

Figure 1: A. Collection of *E. prunastri* **B.** Lichen transplant of *E. prunastri*

In addition to lichens, vascular plants can also serve as effective biomonitors. The leaves of certain species possess a remarkable ability to intercept airborne pollutants, providing valuable insights into particulate deposition and immobilization (Muhammad et al, 2019).
Different plant species have been studied for their capacity to intercept PTEs (Esposito et al., 2019; Baldantoni et al., 2020), PM (Blanusa et al., 2015), POPs (Odabasi et al., 2015), microplastics (Jafarova et al., 2023), and magnetic particulate (Winkler et al., 2022).
Moreover, tree leaves not only reflect atmospheric pollutant deposition but also provide ecosystem services by acting as green barriers that intercept PM and PTEs, thereby protecting heritage surfaces (Sæbø et al., 2012). Despite the widespread use of vegetation in biomonitoring, only one study (Winkler et al. 2022) combined leaf collection with lichen transplants for magnetic and chemical biomonitoring near cultural heritage sites, underscoring biomonitoring as a key tool for preventive conservation. However, that investigation was conducted under the atypical conditions of the 2020 COVID-19 pandemic (e.g., absence of visitors and routine traffic). Consequently, a critical knowledge gap remains regarding the applicability and efficacy of integrated magnetic–chemical biomonitoring for characterizing typical, high-exposure conditions at active cultural heritage sites and for quantifying the protective role of *in situ* vegetation. There is, therefore, a clear need to advance biomonitoring research within cultural heritage sites, with the dual aim of assessing pollutant bioaccumulation in these areas and evaluating the potential of *in situ* vegetation as a provider of ecosystem services.

Magnetic biomonitoring

Magnetic biomonitoring involves the analysis of the magnetic properties of airborne particulate matter accumulated by biomonitors. The primary parameter considered is magnetic susceptibility by mass (χ), which provides a rapid, non-destructive proxy for the concentration of ferrimagnetic minerals often associated with traffic-related emissions such as brake wear, exhaust particles, and road dust resuspension (Maher et al., 2008). Secondly, the hysteresis parameters are determined through the measurement of the magnetization of a sample during the application of a variable magnetic field. Key parameters include the coercive force (Bc, T), the saturation remanent magnetization by mass (Mrs, or SIRM, Am^2/kg), and the saturation magnetization by mass (Ms, Am^2/kg). These parameters enable the identification of magnetic mineralogy, estimation of grain size, and assessment of magnetic interactions (Maher et al., 2008). Descriptive analyses—particularly the Day plot (Dunlop, 2002a), a plot of the ratios Mrs/Ms versus Bcr/Bc— provide an approximate characterization of domain state, whereas more advanced techniques such as first-order reversal curves (FORCs) yield high-resolution information on magnetic interactions and domain states. Magnetic biomonitoring using roadside tree leaves has emerged as a rapid, cost-effective, and non-destructive technique for mapping the spatial and temporal variation of vehicle-derived particulate loads (Matzka & Maher, 1999). Early investigations showed that the magnetization measured on tree leaves—e.g., *Betula pendula* (Roth)—scaled primarily with proximity to major roads (Matzka & Maher, 1999). Notably, the highest magnetic dust loadings adjacent to uphill road sections implicated vehicle combustion and exhaust emissions as the dominant sources of magnetic particles at those sites, rather than resuspended dust or mechanical wear processes (Matzka & Maher, 1999; Maher et al., 2008).

Coupling concentration dependent magnetic parameters (Ms, Mrs or χ) (SIRM) with elemental analysis has revealed strong correlations between the magnetic signal and concentrations of toxic metals. Complementary advanced morphological analyses and magnetic hysteresis measurements (including FORC analysis) have been applied in specific urban settings, such as Rome, providing essential compositional and morphological characterization of PM (Sagnotti et al., 2009). In that case, the magnetic PM accumulated on *Quercus ilex* (L.) leaves mainly consisted of Fe-rich particles (~0.1–5 μm) with rough surfaces, indicative of mixed vehicular sources where brake-disc abrasion made the dominant contribution to magnetic PM with respect to diesel and gasoline exhaust emissions. High-

resolution imaging further showed that these particles were not merely adhering to the leaf surface but were embedded within the leaf wax layer. Magnetic biomonitoring offers the spatial resolution required to delineate metallic magnetic particles but must be complemented by chemical analyses to fully characterize the composition and sources of complex PM assemblages. Magnetic and chemical analyses were first jointly applied to lichen biomonitoring in a complex anthropogenic setting (Winkler et al., 2019), where native lichens were collected and lichen transplants exposed in an area affected by arson fires. More recently, biomonitors were used to detect airborne magnetic particles at a cultural heritage site, Villa Farnesina in Rome, during the 2020 pandemic, when visitors and nearby traffic were largely absent (Winkler et al., 2022). By integrating the non-destructive, spatially resolved capabilities of magnetic biomonitoring with detailed chemical characterization (e.g., of PTEs), this work seeks to overcome limitations of conventional monitoring. This combined approach delivers high-resolution, actionable insights for preventive conservation, enabling the development of targeted, site-specific strategies to reduce airborne pollutant exposure and safeguard vulnerable cultural heritage materials.

Research question

The primary aim of this thesis is to validate and apply an integrated magnetic–chemical biomonitoring approach to support the preventive conservation of cultural heritage in urban environments. Specifically, this thesis (i) establishes first data on the spatial and temporal distributions of airborne PM and associated PTEs at selected cultural heritage sites under different operational contexts; (ii) compares transplanted lichens (*E. prunastri*) with *in situ* tree leaves as biomonitors of traffic-derived magnetic and chemical particulate; (iii) characterizes the sources and physicochemical nature of deposited particulate using advanced magnetic hysteresis parameters and elemental analysis to identify the most significant conservation threats; and (iv) evaluates the ecosystem-service potential of adjacent vegetation by quantifying its green-barrier function in intercepting airborne pollutants.

CHAPTER 1

Magnetic and chemical biomonitoring of particulate matter at cultural heritage sites: The Peggy Guggenheim Collection case study (Venice, Italy)

Abstract

Cultural heritage (CH) is heavily threatened by air pollution, especially by airborne particulate matter (PM), that acts on the surfaces of fine arts, causing artistic loss. Therefore, the monitoring of air quality assumes a central role for the preventive conservation of CH. In this study, magnetic and chemical biomonitoring of PM was applied at the Peggy Guggenheim Collection, a contemporary and modern art museum in Venice, Italy. It is located in an aquatic context, where the PM sources are considerably different, with respect to the usual vehicular-dominated urban emissions. Lichen biomonitoring is a well-established technique for the assessment of air quality, especially where PM collecting devices cannot be operated for aesthetic and practical reasons. Samples of the lichen species *Evernia prunastri* were collected from a pristine area and exposed for three months (November 2022–February 2023) at increasing distances from the Grand Canal, planning an outdoor vs. indoor sampling design, for outlining the diffusion of airborne PM inside the museum. In combination with lichen exposure, the leaves of *Pittosporum tobira* hedges were sampled for determining their efficiency as bioaccumulators. The magnetic properties of lichens showed a moderate bioaccumulation of magnetite-like particles outdoors. Conversely, the magnetic properties of the indoor samples were like those of the unexposed ones, indicating a negligible accumulation of metallic particles indoors. *Pittosporum tobira* leaves mostly showed diamagnetic properties, resulting an ineffective species for preventing conservation purposes. Chemical analysis did not show any significant difference between unexposed, indoor and outdoor samples. A directional gradient of bioaccumulation was not evident, thus implying that the sources of metallic PM are distant or diffused, with respect to the site. The joint use of magnetic and chemical analyses was useful for evaluating the negligible impact of airborne particulate pollution arising from the Grand Canal towards the Halls of the Collection.

1. Introduction

Biomonitoring of particulate matter (PM) applied to cultural heritage is an innovative strategy of preventive conservation from damage caused by this airborne pollutant.

Atmospheric PM is one of the main causes of degradation of fine arts, damaging their surfaces by different chemical-physical processes (Comite et al., 2019). Historical buildings in urban settlements are directly exposed to airborne pollutants that create “soiling” or “black crusts”, derived from airborne particles deposited on monuments, paintings and masterpieces, generating a thick coating that alters their surfaces and compromises their maintenance. Paintings, frescoes and statues are exposed to damage even if inside a museum. This is because PM can enter or be resuspended by multiple factors, for instance: the air flowing from the conditioning systems, the doors and windows, or the passage of visitors through the rooms. The International Centre for the Study of the Preservation and Restoration of Cultural Property (ICCROM) promotes preventive conservation as a valid instrument against the deterioration of fine arts. In urban contexts, where cultural heritage sites are predominantly located, common sources of these particles are fuel combustion, vehicle brake wearing, industrial activities, heating systems and natural sources, such as wind-blown dusts. This ensemble of particles, widespread in the atmosphere, may contain magnetite-like particles of different grain sizes and magnetic properties, that are mainly connected with anthropogenic activities, especially in trafficked urban areas, where they mainly derive from emission sources like brake abrasion, or iron oxides produced during combustion processes (Hunt et al., 1984; Georgeaud, 1997; Maher et al., 2008; Gonet et al., 2021a, 2021b; Winkler et al., 2020). The use of biomonitors such as mosses (Salo, 2014; Salo and Mäkinen, 2019) lichens and plant leaves is a well-known and widespread technique of air monitoring, owing to the efficacy of these organisms in accumulating even very high loads of airborne anthropogenic particles that in urban areas are enriched in potentially toxic elements (PTEs) such as Fe, Cr, Cu, Sb, Al, Zn, Ba, etc. Biomonitors act as a cost-effective control unit, easy to handle, offering an estimation of air quality in a specific area. Moreover, the use of lichen transplants collected in a remote environment and exposed in the site of interest provides a detailed estimation of the deposition of pollutants over a well-defined time period and knowing the starting composition. The use of lichen transplants offers the further possibility to expose the same biomonitors both outdoors and indoors, considering their successful applications in several indoor case studies too (e.g.: Canha et al. 2014; Protano et al. 2017; Almeida et al. 2011; Paoli et al., 2019). These biomonitors are particularly suitable for the estimation of pollutants close to monuments, museums, or archaeological sites because the exposure of lichen transplants is readily feasible, not easily visible and the risk of biological contamination is minimal. Moreover, lichen and leaves are very effective for providing

experimental high spatial resolution monitoring designs that are not feasible using conventional automated air quality devices. Indeed, biomonitoring gives a different perspective with respect to other methods to assess air pollution, such as modeling based on emission data or measurements of ambient air concentrations of pollutants, providing original parameters based on their biological response and the possible biological effects of harmful emissions. Magnetic biomonitoring techniques provide a proxy for the anthropogenic fraction of PM, that is often linked to the presence of iron oxides, which are well characterizable in terms of composition, concentration and grain-size distribution (Hofman et al., 2017; Chaparro, 2021). The first study about magnetic biomonitoring concerning cultural heritage preventive conservation was drawn at Villa Farnesina, located in a busy area of Rome, where PM distribution from the main street towards the frescoed Lodges was assessed through magnetic and chemical analyses on lichens and leaves (Winkler et al., 2022). Lichens demonstrated to be the best biomonitors, while leaves are worth to be investigated for their PM retention properties and the consequent provision of ecosystem services. This study focuses on the Peggy Guggenheim Collection, a prestigious cultural heritage setting inside the UNESCO World Heritage site of Venice, Italy. Chemical and magnetic analyses were applied to lichens exposed for three months inside and outside the halls of the Collection, with the aim of assessing the impact of outdoor airborne PM on the indoor artworks. Leaves of *Pittosporum tobira* hedges were also collected and subjected to magnetic analysis to characterise the metallic emissions arising from the Grand Canal (the main route of transportation in Venice) towards the Museum's halls, as well as to evaluate the possible use of this plant species for the removal of anthropogenic PM.

2. Materials and methods

2.1. Study area

The Peggy Guggenheim Collection is located in the Venier dei Leoni Palace, along the Grand Canal, in the city centre of Venice. This building was projected in 1749 by the architect Lorenzo Boschetti, and it was inhabited by many families until 1949, when Peggy Guggenheim decided to live there. She was an important American art collector, and her collection hosts masterpieces by Magritte, Picasso, Pollock, Ernst and many other contemporary artists. She decided to open her remarkable collection to the public in 1951, and

since then it has been visited by millions of visitors. The historical building, expected to be on 3 floors and not completed, is based on the ground floor only with a big terrace facing the Grand Canal and a rooftop garden. On the opposite side, the palace has a suggestive garden with trees of the species *Cupressus sempervirens, Cladastris lutea, Tilia americana* and *Betula nigra* and many other plants in hedges and flowerbeds. Hedges of *Pittosporum tobira* figure the railings in the terrace on the Grand Canal and the rooftop garden as well as the entrance in the building from the garden: thus, *P. tobira* is the only ubiquitous plant species available all around the museum.

2.2. Lichen exposure

The lichen *Evernia prunastri* (L.) Ach. was the biomonitor selected according to its suitability in environmental applications (Loppi et al., 1998, 2019a). Thalli of this species were collected in a remote and reasonably pristine area, far from urban settlements and pollution sources, picked at a height >1.5 m to avoid main soil contamination. The material was enveloped in a plastic net (lichen bag) for the exposure. Three samples were left for the analysis not being exposed (unexposed samples). The lichen bags were exposed (three bags per site) at the Peggy Guggenheim Collection's building, along a linear transect from the Grand Canal towards the gardens, passing through two halls of the museum, for a total of six sites on the ground floor and one on the rooftop (Fig. 1): the first one, closest to the Grand Canal, tied to the balcony railing (GC), then on the marble ornaments of the external wall of the building (EW); on the windows railings (OH) close to the staircase of entrance by the side of the Grand Canal; in two halls of the museum, the first one with the Picasso's masterpiece "The Studio", in front of the entrance (H1), and the other, on the left facing the Grand Canal, where Boccioni's "Dynamism of a Speeding Horse" and "The Regular" by Marcoussis are displayed (H2). Another site was located on the rooftop terrace, tied to the railing (RO) and the last one on the branches of three Tilia americana trees, close to the entrance by the garden side (GA). As far as possible, lichen bags were tied avoiding close contact with metallic parts or furniture. The exposure of the samples lasted 3 months (November 4, 2022–February 6, 2023) and during this period the indoor transplants were sprayed with water to keep thalli hydrated. At the end of the exposure period, samples were retrieved, individually stored in paper bags before being dried until the magnetic and chemical analyses.

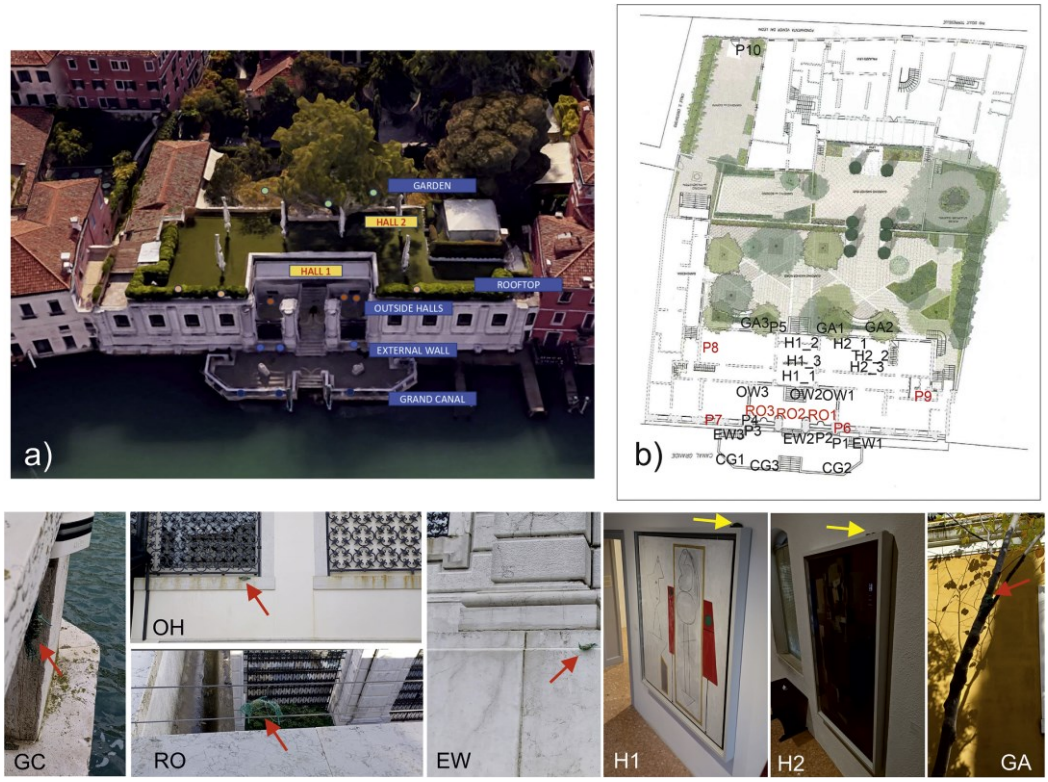

Fig. 1. (a) Google Earth view of the Peggy Guggenheim Collection: the colored dots indicate the lichen bags exposed outdoors (b) lichen and *Pittosporum tobira* sampling sites: the samples at ground level are in black, in red at the rooftop. In the pictures: lichen bags (indicated by red arrows outdoors, yellow indoors) at the sites GC (Grand Canal), OH (Outside Halls), RO (Rooftop), EW (External Wall), H1 (Hall 1 - "The Studio" by Picasso), H2 (Hall 2 - "The Regular" by Marcoussis) and GA (Garden).

2.3. Leaf sampling

Leaves of *P. tobira* were sampled from the available hedges at increasing distances from the Grand Canal at ca. 1 m from the ground: on the terrace with the pier to the Grand Canal (P1, P2, P3), on the opposite side of P3 with respect to the Grand Canal (P4), in the garden, close to the building (P5) and by the side of the street Fondamenta Venier dai Leoni (P10, sampled only in November). In the rooftop, *P. tobira* was sampled at the Grand Canal side (P6, P7), and at the garden side (P8, P9). Two samplings were done: before exposure (4th of November 2022) and at retrieval of lichen samples (6th of February 2023).

2.4. Magnetic analysis

The magnetic properties were measured at the paleomagnetic laboratory of Istituto Nazionale di Geofisica e Vulcanologia in Rome, Italy. Lichens and leaves were dried with a Bionsec Domus plastic desiccator, for at least 24 h, then placed in 8 cm^3 plastic cubes to determine the magnetic susceptibility by mass (χ, m^3 kg^{-1}) with a Agico KLY5 meter. The hysteresis properties, i.e. the coercive force (Bc, T), the saturation remanent magnetization by mass (Mrs, or SIRM, Am^2 kg^{-1}) and the saturation magnetization by mass (Ms, Am^2 kg^{-1}), were investigated on standard gel caps#4 with the magnetic vibrating sample magnetometer Lakeshore 8604 up to a field of 1.0 T in point-by-point discrete sweep mode, at steps of 2.5 mT. Ms and Mrs were determined after subtracting the high field linear trend after saturation, interpolated from 700 to 999 mT. The coercivity of the saturation remanent magnetization (Bcr) was calculated from the logarithmic backfield remagnetization curves up to -1 T, after saturating at 1.0 T. The domain state and magnetic grain size of the samples were compared to theoretical magnetite according to the hysteresis ratios Mrs/Ms and Bcr/Bc in the "Day plot" (Day et al., 1977; Dunlop, 2002a, 2002b). First order reversal curves (FORCs) were measured at steps of 2.5 mT, with 300 ms averaging time and maximum applied field being 1.0 T. FORC diagrams were processed, Variforc smoothed and drawn with the FORCINEL 3.06 Igor Pro routine (Harrison and Feinberg, 2008). FORC diagrams provide information regarding magnetic reversal mechanisms in ferromagnetic minerals (Pike et al., 1999; Roberts et al., 2000) and are used for delineating the distributions of the interaction field (Bu) and coercivity in samples, in order to distinguish between superparamagnetic (SP), single domain (SD), multidomain (MD) and pseudo-single domain/vortex (PSD/V) behaviors, the latter describing the transitional state between SD and MD particles.

2.5. Chemical analysis

Chemical analyses were performed at the University of Siena, Italy. About 250 mg for each lichen sample was weighted and then acid-digested with 3 mL of HNO_3, 0.2 mL of HF and 0.5 mL of H_2O_2 in a microwave digestion system (Ethos 900, Milestone). Afterwards, the samples were analyzed by ICP-MS (NexION 350x, Perkin Elmer) to quantify the content of Fe, Al, Cu, Ba, Cr, Zn and Sb. ICP-OES (Optima 2000 DV, Perkin Elmer) was used to measure S. Analytical quality was verified using the certified reference materials IAEA-336

"Lichen" and GBW07604 "Poplar leaves" for Ni and S, not certified in IAEA-336, and was in the range 98–110 %; precision of the analysis was expressed by the relative standard deviation of 3 replicates and was below 3% for all elements. Three measurements were repeated for each sample and the results were expressed on a dry weight basis.

2.6. Statistical analysis

To disentangle the effect of indoor/outdoor exposure on magnetic and chemical parameters of transplanted lichens, a linear mixed-effects model (LMEM) was fitted for each measured parameter, with exposure as fixed factor and site as random factor. For model validation, the Levene and Shapiro-Wilk tests were used to check for homoscedasticity and normality, respectively. The significance of the models was checked with type II Anova (analysis of deviance) using the Wald chi-square test. All calculations were run using the R software (R Core Team, 2022).

3. Results

3.1. Magnetic properties

The magnetic susceptibility of *P. tobira* leaves (Table 1) ranged -5.37–1.31 × 10^{-9} m^3 kg^{-1} with a mean value of -3.06 ± 0.74 × 10^{-9} m^3 kg^{-1} in November. After 96 days, magnetic susceptibility ranged -2.73–7.01 × 10^{-9} m^3 kg^{-1} with a mean value of 1.62 ± 0.90 × 10^{-9} m^3 kg^{-1}. The magnetic susceptibility values of leaves indicated prevailing diamagnetism, suggesting a negligible accumulation of magnetic particles, which discouraged further magnetic analyses, such as hysteresis loops, that were tested on selected samples and confirmed very weak and unreliable magnetic properties, at the sensitivity limits of the VSM. As a mere qualitative test, leaves of *Acanthus mollis* L. were sampled in close proximity to *P. tobira* P4*,* and their magnetic susceptibility changed from -0.470 to 12.33 × 10^{-9} m^3 kg^{-1} during the same period. The magnetic susceptibility of lichen transplants (Table 1) varied, on average, from 12.90 ± 4.06 × 10^{-9} m^3 kg^{-1} indoor to 26.9 ± 5.30 × 10^{-9} m^3 kg^{-1} outdoor. One of the lichen bags exposed on the branches of *Tilia americana* in the garden showed a χ approximately one order of magnitude larger than the other two samples of the same site (187.00 vs 19.60 and 30.00 × 10^{-9} m^3 kg^{-1}). For this reason, it was disregarded and considered an outlier (Tukey

test), as it was probably contaminated by a point source of pollution, likely a nearby high-power spotlight. The mean χ of unexposed lichen samples was 13.50 ± 5.40 × 10^{-9} m^3 kg^{-1}. Magnetic susceptibility decreased in the following order from outdoors to indoors (Table 1); χ (EW) > χ (OH) > χ (RO) > χ (GA) > χ (GC) > χ (H2) > χ (H1). The mean values of χ of unexposed and indoor samples differ for 2.22 × 10^{-9} m^3 kg^{-1}, while the difference between the mean outdoor and unexposed samples was about six folds, that is 13.20 × 10^{-9} m^3 kg^{-1} (Fig. 2). The hysteresis loops were saturated at relatively low magnetic fields, with Ms, Mrs average values being 1.15 ± 0.46, 1.88 ± 0.66 and 0.16 ± 0.06, 0.21 ± 0.07 mAm^2 kg^{-1}, indoors and outdoors, respectively (Table 1). Bc and Bcr spanned 9.1-10.7 mT and 22.5-34.1 mT, respectively (Table 1), indicating the homogeneous prevalence of low coercivity magnetite-like minerals, under a very limited variation of Bc values. Furtherly, it was calculated the SIRM/χ ratio, as a proxy of the magnetic grain size of the samples; on average the values were 11.5 ± 5.6, 12.4 ± 3.9 and 7.6 ± 1.7 kA/m for unexposed, indoor and outdoor samples, respectively (Table 1). Overall, statistically significant differences ($p < 0.05$) emerged only between lichen samples exposed outdoors and the others: lichen samples exposed indoors were significantly similar to unexposed samples. In the Day Plot (Fig. 3), the mean Mrs/Ms and Bcr/Bc ratios were computed and averaged at site level and compared to the exhaust and non-exhaust vehicular emissions from Sagnotti et al. (2009): all sites lie on the central/PSD region of the plot, not far from the trend lines that represent the mixtures of SD and MD pure magnetite grains. The FORC diagrams were computed for selected samples: in Fig. 4, an unexposed sample (a) is compared to the lichen placed over “The Studio” by Picasso (b), and to another tied to the external wall (c). Despite the relatively low magnetic signal and the use of high smoothing factors, especially at the background, it is evident a shift of magnetic properties from the unexposed sample, that mainly shows PSD/Vortex features, to a slight spreading along the Bu axis of the Picasso’s lichen bag, up to the superimposition of viscous properties in the outdoor sample, that can be ascribed to the accumulation of MD or SP particles, as well as to a tri-lobate geometry that is typical for vortex states and particles that may possibly stray into the MD size range (Roberts et al., 2014; Lascu et al., 2018; Sheik et al., 2023). In the outdoor sample, the high coercivity ridge extending beyond magnetite coercivities suggests the presence of metallic Fe (Sheikh et al., 2022).

Table 1 Mean ± standard deviation of mass specific magnetic susceptibility (χ), saturation magnetization (Ms), remanent magnetization (Mrs), coercivity (Bc), coercivity of the remanence (Bcr) and saturation remanent magnetization to magnetic susceptibility ratio

(SIRM/χ) of the lichen bags and unexposed samples. The asterisk indicates that the Mean ± standard deviation is computed disregarding an outlier.

	χ ($10^{-8}m^3$ kg^{-1})	Ms (mAm^2kg^{-1})	Mrs (mAm^2kg^{-1})	Bc (mT)	Bcr (mT)	SIRM/χ (kAm^{-1})
Unexposed	1.35 ± 0.54	0.93 ± 0.02	0.14 ± 0.01	10.40 ± 0.17	27.52 ± 1.97	11.54 ± 5.61
Hall 1	1.07 ± 0.43	1.10 ± 0.62	0.16 ± 0.05	10.60 ± 0.10	27.81 ± 5.57	14.20 ± 4.32
Hall 2	1.51 ± 0.28	1.19 ± 0.35	0.16 ± 0.01	10.20 ± 0.52	31.16 ± 1.37	10.69 ± 3.06
Outside Halls	2.86 ± 0.43	2.15 ± 0.30	0.24 ± 0.04	9.84 ± 0.31	30.79 ± 1.80	8.43 ± 0.46
External wall	3.19 ± 0.71	2.25 ± 0.80	0.23 ± 0.09	9.33 ± 0.40	32.80 ± 1.19	7.01 ± 1.77
Grand Canal	2.24 ± 0.10	1.40 ± 0.20	0.16 ± 0.01	9.89 ± 0.54	31.27 ± 1.60	7.33 ± 0.53
Garden*	2.48 ± 0.74	1.75 ± 1.12	0.21 ± 0.13	9.80 ± 0.21	30.56 ± 1.38	7.93 ± 3.21
Rooftop	2.59 ± 0.28	1.78 ± 0.87	0.20 ± 0.09	9.82 ± 0.15	32.39 ± 2.14	7.60 ± 2.89

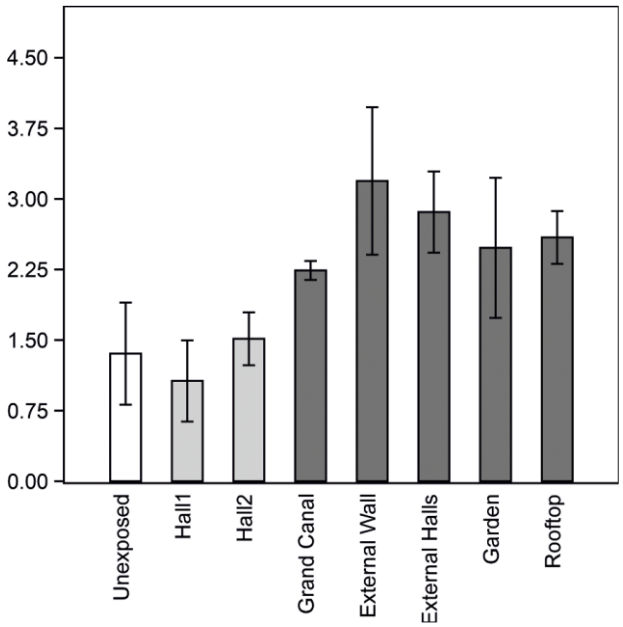

Fig. 2. Mean magnetic susceptibility of lichen transplants, by exposure site (10^{-8} m^3 kg^{-1}, ± standard deviation): outdoor sites in dark grey, indoor sites in light grey, unexposed samples in white.

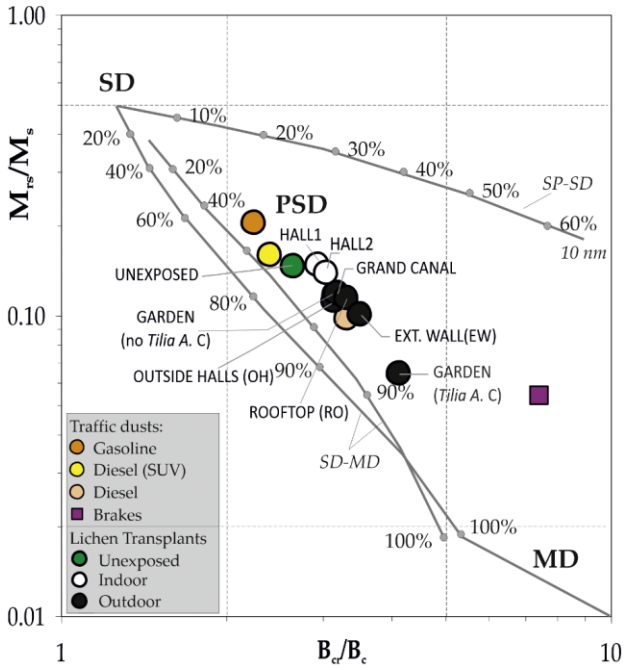

Fig. 3. Bilogarithmic "Day plot" (Day et al., 1977) of the site averaged hysteresis ratios for lichen transplants (black circles for outdoor sites, white circles for indoor sites, green circle for unexposed samples), reported together with the average points for different kinds of fuel exhaust (orange, yellow and pink circles) and brake dust emissions (purple square) calculated from Sagnotti et al. (2009). The SD (single domain), PSD (pseudo-single domain) and MD (multidomain) fields and the theoretical mixing trends for SD-MD and SP-SD pure magnetite particles (SP, superparamagnetic) are from Dunlop (2002a, 2002b).

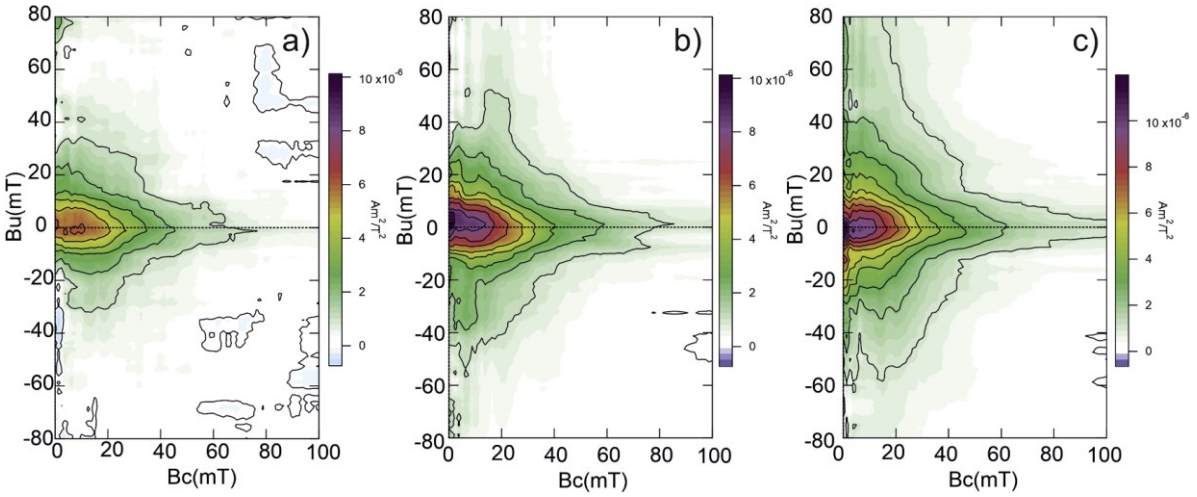

Fig. 4. FORC diagrams, for a selected unexposed lichen bag (a), for the bag exposed over "The Studio" by Picasso (b) and at the external wall (c); averaging time was 300 ms and variforc smoothed up to 12 at the background.

3.2. Content of PTEs

The concentrations of PTEs are reported in Table 2. Indoors, the prevailing element was zinc (Zn), with an accumulation of 107 % in Hall 2, and 79 % in Hall 1; a minor accumulation was found for nickel (Ni). In the outdoor sites, antimony (Sb) prevailed and stood out over the rooftop where it was more than twice the concentration in unexposed samples, then with a decreasing order, close to Grand Canal (GC), on the wall facing the dock (EW), just outside of the museum (OH) and the garden (GA). The net sulphur accumulation stood out close to the Grand Canal (+56 %) but was very low or absent at the other sites. Sites outdoors, close to the museum (EW, OH, RO sites), showed the accumulation of Zn, maximum in RO (142 %), followed by indoor sites (106 % H2, 79 % H1); the accumulation of Zn decreased as the distance from the museum to the Grand Canal increased. The amount of copper (Cu) was relevant in two outdoor sites (EW, RO). The content of Aluminum (Al) varied remarkably just at two sites, GA and RO with an accumulation of 37 % and 38 %, respectively. Iron, Barium and Chromium did not show any particular accumulation (maximum 18 % for Fe at EW). Overall, as opposed to magnetic data, statistically significant differences did not emerge between lichen samples unexposed, or exposed indoors and outdoors.

Table 2

Mean element concentration (µg/g dw, ±standard deviation) in lichen samples. The asterisk indicates that the Mean ± standard deviation is computed disregarding an outlier.

	Al	Ba	Cr	Cu	Fe	Ni	S	Sb	V	Zn
Unexposed	404 ± 79	14.4 ± 1.9	1.8 ± 0.2	6.9 ± 0.7	637 ± 126	2.9 ± 0.6	900 ± 96	0.10 ± 0.02	1.9 ± 0.3	21.8 ± 5.1
Hall 1	433 ± 60	13.3 ± 0.6	1.7 ± 0.6	6.9 ± 0.6	544 ± 128	4.1 ± 1.3	744 ± 26	0.11 ± 0.03	1.7 ± 0.4	39.0 ± 0.8
Hall 2	401 ± 67	15.0 ± 0.3	1.8 ± 0.1	7.3 ± 0.5	652 ± 90	3.5 ± 0.6	963 ± 148	0.11 ± 0.02	1.9 ± 0.3	45.0 ± 14.2
Outside Halls	470 ± 135	19.0 ± 3.8	2.0 ± 0.4	7.5 ± 0.2	749 ± 142	2.2 ± 0.5	898 ± 54	0.20 ± 0.04	2.1 ± 0.6	35.2 ± 7.6
External wall	367 ± 154	14.0 ± 1.8	1.9 ± 0.4	11.9 ± 2.0	621 ± 198	1.7 ± 0.5	843 ± 235	0.22 ± 0.01	1.8 ± 0.5	34.8 ± 8.4
Grand Canal	259 ± 69	14.3 ± 1.3	1.7 ± 0.4	7.9 ± 0.1	460 ± 29	3.3 ± 3.5	1404 ± 269	0.24 ± 0.08	1.5 ± 0.2	21.0 ± 0.7
Garden*	554 ± 232	13.5 ± 1.2	1.7 ± 0.4	7.0 ± 0.0	582 ± 53	1.6 ± 0.6	1002 ± 189	0.16 ± 0.01	1.8 ± 0.1	19.2 ± 1.8
Rooftop	557 ± 49	14.0 ± 0.1	1.9 ± 0.3	11.4 ± 1.8	538 ± 56	2.1 ± 0.2	980 ± 121	0.26 ± 0.03	1.5 ± 0.3	52.8 ± 2.2

4. Discussion

Combined magnetic and chemical analysis of lichen transplants and *P. tobira* leaves provided a complex and detailed overview of the airborne PTEs present indoors and outdoors of the Peggy Guggenheim Collection, by both qualitative and quantitative profiles. Magnetic susceptibility is among the most used parameters in biomagnetic monitoring of airborne PM: it is cost-effective and very sensitive even to very low concentrations of magnetic minerals. χ values can show the accumulation of ferrimagnetic fractions of PM even at barely detectable levels. Despite this, the magnetic susceptibility values of *P. tobira* leaves were so low to consider their bioaccumulation of magnetic particles substantially negligible. In fact, the whole dataset but one sample, in November 2022, was diamagnetic, with a very weak increase in February 2023, that was so limited to reach 7.09×10^{-9} m^3 kg^{-1} as the maximum value. Winkler et al. (2022) discussed the role of tree and shrub leaves for providing preventive conservation services. The concentration dependent magnetic parameters of *Platanus orientalis*' leaves doubled after three months of exposure in Rome, in Lungotevere Farnesina, despite Muhammad et al. (2019) classified the species in the group characterized by the lowest bioaccumulation of magnetic particles. In this study, after three months, *P. tobira* leaves did not substantially change their magnetic susceptibility values, highlighting negligible concentration of airborne magnetic particles or their unsuitability for their immobilization. Conversely, Lorenzini et al. (2006) showed that *P. tobira* is a suitable passive biodeposimeter, useful to assess levels and distribution patterns of inorganic solid pollutants in urban areas. However, during the investigated period, for 20 days out of 90 the daily PM10 concentration levels exceeded the EU limit of 50 $\mu g/m^3$, as recorded by automated monitoring stations of air quality in Venice downtown (https://www.arpa.veneto.it/dati-ambientali/dati-storici/aria/qualita-dellaria-storico-dati-validati). For 6 consecutive days right before sampling the leaves in February, PM_{10} concentration exceeded the limit, reaching values as high as 107 $\mu g/m^3$ along with an event of persistent high pressure that caused abnormally low tide. Thus, it is possible to conclude that, at least in this aquatic lagoon context, *P. tobira* leaves did not behave as efficient bioaccumulator. Moreover, the leaves of *Achantus mollis* that were sampled close to *P. tobira* leaves (P4) on the opposite side of the plant, with respect to the Grand Canal, showed that χ value increased by 12.70×10^{-9} m^3 kg^{-1}, with respect to 4.05×10^{-9} m^3 kg^{-1} of P4, thus confirming the limited bioaccumulation of this species. As far as lichen transplants are concerned, χ values resulted highly correlated with those of Ms and Mrs, the

concentration dependent magnetic parameters determined from hysteresis loops. Considering the higher sensitivity and representativeness of the magnetic susceptibility measurements, carried out on standard 8 cc cubes instead of 0.2 mL gel caps, hysteresis properties were mostly interpreted in the light of magnetic mineralogy analyses, leaving the quantitative aspects to χ. By the comparison of χ values of lichen transplants, a significant statistical difference ($p < 0.05$) was found between the indoor and outdoor sites, with outdoor values, on average, twice those indoors (2.67×10^{-8} m^3 kg^{-1} vs 1.29×10^{-8} m^3 kg^{-1}, respectively), being 1.35×10^{-8} m^3 kg^{-1} the mean of the unexposed samples. Thus, three months of exposure were enough to distinguish two main clusters of samples according to χ values: a statistical difference was found between unexposed samples and outdoor samples but not between unexposed and indoor samples. The same conclusion was confirmed by Ms and Mrs values, the concentration dependent magnetic parameters obtained from hysteresis loops. For what concerns the prevailing magnetic grain-size/domain state, in the "Day plot" all samples fell in the central region of the diagram, where are usually located natural and exhaust vehicular magnetic components, as opposed to non-exhaust emissions that prevail in vehicular traffic urban context, which are placed in the lower-right side of the plot (Sagnotti et al., 2009; Winkler et al., 2020, 2021; Gonet et al., 2021a, b). In detail, the unexposed samples fell in the upper left PSD region of the plot, with the indoor and outdoor sites progressively shifting towards slightly higher proportions of coarser MD particles. The outlier transplant tied to a *Tilia A.* in the garden confirms to be anomalous also for its coarser magnetic grain size. As a reference, the critical magnetic grain-size transitions, theoretically determined for equidimensional magnetite, are about 0.03 μm for SP to SD, 0.08 μm for SD to PSD, and 17 μm for PSD to true MD (Butler et al., 1975), the gradual transition from SD to true MD depending on the spontaneous magnetization, shape and the state of internal stress of a particle (Roberts et al., 2017). This result is also consistent with the features of the FORC diagrams, that showed a progressive increase of vertically spread magnetic components in the indoor and, especially, the outdoor samples, within predominant vortex/PSD general aspects. In Sheikh et al. (2022), the apparent MD signal observed in brake pad residues was attributed to a combination of high-coercivity ridge and a low-coercivity vertically spread signal, which Lappe et al. (2013) considered consistent with the presence of metallic particles in vortex states. It is supposed that the bioaccumulated particles are in the grain-size range from the upper end of the vortex state to MD behavior, with a peak at the origin that can be attributed to an ultrafine SP component, with the high coercivity ridge possibly related to the presence

of metallic Fe. SIRM/χ values confirm this trend too: the mean values of the outdoor samples were lower than those indoor and unexposed, that are very similar, highlighting the relative increased income of coarser magnetic particles. On the whole dataset, χ values were not dependent on the concentration of Fe (Fig. 5), indicating that the most Fe is not directly linked to magnetic minerals, that are the main carriers of magnetic susceptibility. Thus, following the different groups of samples as emerged by the statistical analysis of magnetic susceptibility values, the linear correlation between Fe and χ was tested splitting the dataset into the unexposed + indoor and outdoor samples. In this way, two different and significant linear trends were found (Fig. 5), confirming the different bioaccumulation of magnetic particles outdoors, with respect to the indoor and unexposed samples. It is supposed that the presence of Fe is mainly linked to paramagnetic/weak bioaccumulation conditions in the indoor and unexposed samples, with a moderate supply of further paramagnetic and ferrimagnetic components recorded outdoors. According to the Ms values, that is a grain size independent magnetic parameter, and after the assumption that the magnetic mineralogy is compatible with magnetite-like minerals, whose mass Ms value is 90 Am^2/kg (Dunlop and Ozdemir, 1997), it is possible to calculate the weight percentage (wt%) of magnetite in the samples. Averaged at site level, wt% (EW) > wt% (OH) > wt% (RO) > wt% (GA) > wt% (GC) > wt % (H2) > wt% (H1) > wt% (UN) (Table 3). As a qualitative test, it was evaluated the percentage ratio % ($Fe_{magnetite}/Fe_{tot}$), that is indicative of the percentage fraction of magnetite's iron within the total concentration of Fe. $Fe_{magnetite}$ was calculated according to the weight percentage of iron in magnetite, that is 72%. Under this approach, it was possible to estimate that all the lichen transplants accumulated magnetite, and its associated iron in outdoor samples was about 4 times higher than indoors (Table 3).

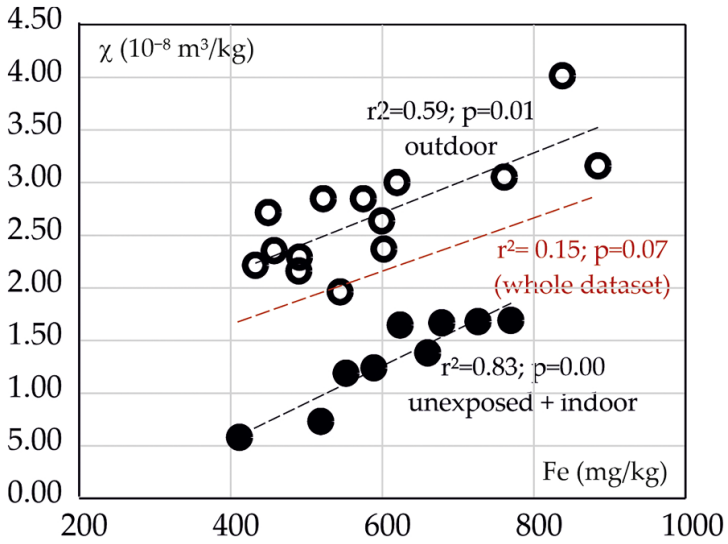

Fig. 5. Relationship between χ and Fe in the whole dataset (red dashed line), and splitting outdoor (white) and indoor+unexposed (black) samples.

Table 3 Weight percentage content of magnetite and elemental Fe, % ratio of the presence of magnetite within the total Fe content and its differential with respect to unexposed samples, indicated as Δ% ($Fe_{magnetite}/Fe_{tot}$). The asterisk indicates that the Mean ± standard deviation is computed disregarding an outlier.

	wt% (magnetite)	wt% (Fe)	% ($Fe_{magnetite}$/ Fe_{tot})	Δ % ($Fe_{magnetite}$/ Fe_{tot})
Unexposed	1.04×10^{-3}	6.37×10^{-2}	1.17	
Hall 1	1.22×10^{-3}	5.54×10^{-2}	1.59	+ 0.42
Hall 2	1.32×10^{-3}	6.52×10^{-2}	1.46	+ 0.29
Outside Halls	2.39×10^{-3}	7.49×10^{-2}	2.29	+ 1.12
External wall	2.50×10^{-3}	6.21×10^{-2}	2.90	+ 1.73
Grand Canal	1.56×10^{-3}	4.60×10^{-2}	2.44	+ 1.27
Garden*	1.95×10^{-3}	5.82×10^{-2}	2.41	+ 1.24
Rooftop	1.98×10^{-3}	5.38×10^{-2}	2.66	+ 1.49

Overall, indoor lichens showed a modest environmental impact: from a magnetic point of view, after three months of exposure, the indoor bioaccumulation of metallic particles was negligible, and barely detectable from a grain-size point of view. Conversely, a moderate bioaccumulation was measured outdoors, corresponding to 2.4 as the maximum ratio between the magnetic susceptibility of outdoor sites (EW) and that of the unexposed samples, which is 17 times lower with respect to the study in Villa Farnesina, where the lichens tied to *Platanus*

trees along the Lungotevere highlighted χ values 39.3 times higher than unexposed samples (Winkler et al., 2022). It should also be noted that the average χ values of the unexposed samples in Villa Farnesina was 0.6×10^{-8} m^3 kg^{-1} while in the present study it was 1.3×10^{-8} m^3 kg^{-1}, thus implying a different baseline and sensitivity in the determination of the relative bioaccumulations. Also the FORC diagrams outlined that relevant magnetic components were already carried by the unexposed samples (Fig. 4a). Outdoors, the Day Plot, the FORC diagrams and the SIRM/χ values highlighted the presence of coarser particles, with respect to the indoor and unexposed samples. Masiol et al. (2014) reported that in the aerosol of a semi-rural coastal site near Venice the anthropogenic elements Fe and Zn in the coarse mode (>4 μm) were well correlated and probably linked to tire and brake wear emissions. S, K, Mn, Cu, Fe and Zn were strongly inter-correlated in the submicrometric (<1 μm) range and Mn, Cu, Zn, Ni in the intermediate mode (1–4 μm), their relationships highlighting the presence of several sources (combustions, secondary aerosol, road traffic). In the intermediate mode, associations having geochemical significance exist between marine (Na, Cl and Mg) and crustal (Si, Mg, Ca, Al, Ti and K) elements. Strong winds favor the formation of sea-spray and the increase of Si in the coarse mode due to the resuspension of sand fine particles. In Prodi et al. (2009), who reviewed the aerosol fine fraction in the Venice Lagoon, the marine aerosol contribution to PM_1 and $PM_{2.5}$ fractions, calculated using Na^+ as a tracer of sea-salts, was estimated to be low, in the range 1–6%. They concluded that Mn and Fe can be partially associated with vehicular traffic, while the high Cr concentration with respect to urban areas is due to industrial activity (e.g. waste incinerator). They also showed that Venice suffers from African dust events, like other Italian cities, that involve much higher concentrations of Si, S, Ca, Ti, P. However, Sagnotti et al. (2006) concluded that the magnetic properties of PM_{10} are not influenced by the presence of high concentration of North African dust, whose magnetic susceptibility is negligible, as well as the marine aerosols, since sea salt is almost diamagnetic. Conversely to that, Larrasoaña et al. (2021) concluded that during intense periods of north African dust transport in southwestern Europe part of the PSD/vortex and MD magnetite grains load is aeolian in origin. For what concerns shipping emissions, they generally derive from the combustion of so-called “bunker fuel”. Most studies have focused on NOx, SO_2, CO and CO_2 as they constitute the majority of ship-derived emissions. Fe-bearing particles occur in the $PM_{2.5}$ fraction in concentrations up to 10 $\mu g/m^3$, usually accompanied by other metals, including V, Ni, Zn, Ca, Na, P, where the Fe-rich particles group, constitutes 3.4% of all PM mass, with smaller portions of Si, S and Ca. Shipping-

derived Fe-bearing particles occur usually in the fraction <100 nm (Popovicheva et al., 2012; Gonet and Maher, 2019). The magnetic fingerprint of airborne particulate matter was significantly detectable only in the lichen samples transplanted outdoors, where the moderate increase of the concentration dependent magnetic parameters is related to the bioaccumulation of relatively coarser particles containing magnetite as the main magnetic mineral, in connection with long range industrial and transportation/traffic related activities that are supposed to be largely diffused and far from the study site. In fact, the homogeneous distribution of the outdoor magnetic parameters is well distinct from the exponential decrease of magnetic susceptibility values that is usually observed within few tens of meters from the emission source of magnetic particles (Szönyi et al., 2008, Winkler et al., 2022). It cannot be excluded that a part of the bioaccumulated dusts is of natural aeolian origin. On the other hand, magnetic measurements well discriminate non-exhausts from other magnetic emissions, but fuel exhausts and fine natural magnetic components are someway difficult to be unmixed (Winkler et al., 2022; Larrasoaña et al., 2021). Irrespective of this indeterminacy, for what concerns the main aim of this study, it can be concluded that the indoor bioaccumulation of airborne magnetic particles was negligible. Biomonitors such as lichens give a biological response in terms of effect (bioaccumulation in this case) of air pollutants, while physico-chemical devices measure the actual atmospheric concentrations of pollutants. It is known that lichen transplants can profitably be used also indoors, since their vitality is preserved and their response is similar to outdoor samples (Paoli et al., 2019). To explain the fact that instrumental monitoring showed a remarkable PM_{10} concentration during the exposure period, while lichens exposed outdoors did not show high levels of PTEs, it may be argued that although massively suspended in the air, the deposition rate of PM was low and hence the ability of lichens to intercept it was reduced, as it is well known that biomonitors provide an accurate estimate of bulk element deposition, but not atmospheric concentration (Loppi and Paoli, 2015; Loppi et al., 2019b; Vannini et al., 2019). On the other hand, another possibility is that high humidity levels, as very commonly experienced in the lagoon of Venice, can lead to leaching, where previously accumulated trace elements within lichen pseudo-tissues can be washed out, resulting in a reduced bioaccumulation, as elements are lost from the lichens. However, the influence of humidity on bioaccumulation is complex and may depend on the interplay of various factors, including local atmospheric composition, wind patterns, and the physiological characteristics of the lichens themselves. Lichen samples exposed outdoors, although not statistically significant, experienced relatively higher values of Sb, which is

usually taken as an indicator of non-exhaust (brake wearing) vehicle pollution. However, in the peculiar environment of Venice, vehicle traffic is extremely limited, and cannot be considered a pollution source worthy of consideration. In fact, outdoor χ and Sb were not at all correlated (R^2=0.00, p = 0.99), thus confirming that Sb is not linked to magnetic emissions from brakes, as opposed to what happens in vehicular traffic contexts (Winkler et al., 2020, 2021). Nevertheless, high Sb levels are common in the Venice lagoon owing to the massive use of this element in traditional artistic venetian glasswork (Formenton et al., 2021). When added to the glass, beside producing a range of colors, especially yellow, the presence of antimony can also affect the refractive index and opacity of the glass, contributing to its aesthetic and artistic qualities. The relatively higher values of Zn measured indoors and at some sites outdoors may be related with the use of zinc oxide which is employed as desiccant in applications related to dehumidification due to its ability to absorb moisture. Zinc oxide's moisture-absorbing properties make it useful in various scenarios where controlling humidity is important, as it is typical in Venice.

5. Conclusions

In this study, a magnetic and chemical biomonitoring approach was tested for assessing the diffusion of metallic PM from the Grand Canal to the halls of the Peggy Guggenheim Collection in Venice, Italy. Lichen bags were exposed outside on both sides of the museum, at increasing distances from the Grand Canal. Indoors, they were located inside two halls, hosting masterpieces by Picasso, Marcoussis and Boccioni. Leaves of *P. tobira* were sampled at the beginning and at the end of the lichen exposure period, in order to evaluate their suitability for providing biomonitoring and ecosystemic services. Lichen transplants were effective for outlining that the bioaccumulation of metallic particles was negligible indoors and moderate outdoors. Indoors, the concentration dependent magnetic parameters were statistically similar to those of unexposed samples. Outdoors, the bioaccumulation of metallic particles was ascribed to magnetic fractions in coarser vortex to multidomain range, with respect to the vortex components already present in the unexposed samples. *P. tobira* leaves mostly showed diamagnetic properties, being unsuited for both magnetic biomonitoring and preventive conservation purposes. The concentration dependent magnetic parameters were mostly homogenous outdoors, with a limited decrease of the magnetic susceptibility values with the distance from the Grand Canal. It is hypothesized that their main sources are diffused

or distant from the study site, as a mixture of anthropogenic and natural far driven dusts. Magnetic biomonitoring demonstrated to be a very sensitive methodology for outlining the impact of metallic emissions, assessed in terms of the composition, concentration and grain-size distribution of iron oxides. Magnetic analyses were so sensitive to detect minimal variations in the concentration levels of Fe, that can be associated with ferrimagnetism and discriminate against different sources of PM, especially when chemical analysis did not reveal any statistically significant difference between lichen bags exposed outdoors and indoors.

Appendix – CHAPTER 1

Research article:

Environmental Advances 15 (2024) 100455

Contents lists available at ScienceDirect

Environmental Advances

journal homepage: www.sciencedirect.com/journal/environmental-advances

Magnetic and chemical biomonitoring of particulate matter at cultural heritage sites: The Peggy Guggenheim Collection case study (Venice, Italy)

Lisa Grifoni [a,b], Aldo Winkler [b,*], Luigi Antonello Di Lella [a], Luciano Pensabene Buemi [c], Antonio Sgamellotti [d], Lilla Spagnuolo [b], Stefano Loppi [a]

[a] Department of Life Sciences, University of Siena, Siena 53100, Italy
[b] Istituto Nazionale di Geofisica e Vulcanologia, Rome 00143, Italy
[c] Peggy Guggenheim Collection, Venice 30123, Italy
[d] Accademia Nazionale dei Lincei, Rome 00165, Italy

***All the authors have agreed for the published article to be used as a chapter of this PhD thesis.**

CHAPTER 2

Nature-based solutions for monitoring the impact of vehicular particulate matter and for the preventive conservation of the Palatine Hill archaeological site in Rome, Italy

Abstract

Magnetic and chemical biomonitoring methodologies were applied to the southern slopes of the Palatine Hill archaeological area in Rome, Italy. Plant leaves and lichen transplants were respectively sampled and exposed between July 2022 and June 2023 to assess the impact of vehicular particulate matter from Via dei Cerchi, a trafficked road coasting Circus Maximus, towards the archaeological area upon the Palatine Hill. The magnetic properties of leaves and lichens, inferred from magnetic susceptibility, hysteresis loops and first order reversal curves, were combined with the concentration of trace elements. It was demonstrated that the bioaccumulation of magnetite-like particles, associated with tracers of vehicular emissions, such as Ba and Sb, decreased with longitudinal distance from the road, without any important influence of elevation from the ground. Lichens demonstrated to be more efficient biomonitors of airborne PM than leaves, irrespective of the plant species. Conversely, leaves intercepted and accumulated all PM fractions, including road dusts and resuspended soil particles. Thus, plant leaves are suitable for providing preventive conservation services that limit the impact of particulate pollution on cultural heritage sites within busy metropolitan contexts.

1. Introduction

A wide array of anthropogenic sources contributes to the diffusion of airborne particulate matter (PM) in urban environments, including vehicular traffic emissions. Particulate matter is one of the most dangerous pollutants to human health and is often associated with chronic illness and an increased risk of death (EEA, 2022). In urban environments, the deposition of airborne PM may also be challenging for monuments (Bonazza et al., 2005; Ozga et al., 2014). Particulate matter, with its associated chemical elements, interacts with artistic and archaeological surfaces, leading to structural degradation (Smith et al., 2008; Tittarelli et al., 2008; Varotsos et al., 2009). Indeed, the so-called “black crusts” are layers of organic and inorganic matter deposited over many years on architectural assets, and it has been

demonstrated that the concentration of trace elements inside these layers is higher than that over the architectural surface, especially for traffic-related elements (TREs) such as Fe, Zn, Cu, Cr, Sb, Pb, V and Ni (Belfiore et al., 2013). Air monitoring plays an important role in determining and evaluating the risk of damage caused by airborne particles. Together with compositional analysis, PM may be well characterised by its magnetic properties, owing to the abundance, compositional and grain-size properties of magnetite-like minerals. Magnetic analysis provides original data for the source apportionment of PM (Maher et al., 2008; Chaparro et al., 2013; Winkler et al., 2019; Gonet et al., 2021a, 2021b). To overcome the limitations of conventional air monitoring using chemico-physical equipment, especially in cultural heritage settings (expensive equipment, power availability, maintenance, and infeasibility of applying a high-density sampling design), air biomonitoring is an effective technique based on the use of cryptogams such as lichens to provide an estimation of the diffusion pattern and bioaccumulation of pollutants. In magnetic and chemical biomonitoring the exposure of lichen transplants is combined to the collection of tree leaves, when available, for analytically testing their capability to offer ecosystem servics (Mori et al., 2015). Lichen transplants can be employed for indoor air quality assessment, as they have been investigated at different sites, such as schools, private houses, offices, and parking spaces (Canha et al., 2012; Gonçalves Da Silva et al., 2021; Demková et al., 2018; Demková et al., 2019; Paoli et al., 2019, 2023). This technique was introduced as a preventive conservation measure near and inside museums by Winkler et al. (2022) and Grifoni et al. (2024). In this study, magnetic and chemical biomonitoring was applied for the first time in an archaeological, mostly open-air, urban environment in Rome, Italy. The southern slopes of the Palatine Hill are an impressive area included in the Archaeological Park of the Colosseum. The slopes are elevated about 8 m above the level of Via dei Cerchi (VDC) road, which separates them from the Circus Maximus; they are divided into two main archaeological sites, Arcate Severiane (AS) and Paedagogium (PA). The AS site is a green area with impressive ruins limiting its northern edge, consisting of a double order of vaulted structures supported by brick pillars, dating back between the 1st and 4th centuries CE. The PA site is located in the complex of Domitian's palace on the Palatine Hill, below the exedra of the façade of Domus Augustana. In its western margin, PA includes the terrace over the Schola Praeconum (SP), which is at the base of the southern slope of the Palatine. Its entrance faces VDC, and its construction dates back to the 3rd century CE. The SP site is characterised by the presence of a rectangular courtyard surrounded by a portico with pillars (no longer legible today except for the open

space that can be walked on). It contains pictorial decoration, dated 200–240 CE and the floor, dated back to the beginning of the 4th century CE, is covered with a large mosaic. The magnetic and chemical properties of *Quercus ilex* (L.) leaves and lichen transplants, respectively sampled and exposed at VDC and at the SP at the ground level of the Palatine Hill, were compared to those of the leaves of several evergreen plant species sampled at different distances from its edge. The hypothesis to be tested was whether and which metallic particles from vehicular traffic at VDC reach the AS and PA archaeological sites at the Palatine Hill, in relationship with the distance from the road and the ecosystem services provided by trees and shrubs, as assessed by means of magnetic and chemical analyses.

2. Materials and methods

2.1. Study area

Via dei Cerchi is a busy (>10,000 vehicles per day) one-way two-lane road. It is particularly congested on its Circus Maximus side, with frequent traffic jams and queues for parking and turning to the left. It is more fluent on its Palatine side, where parking is not allowed and there are no slowdowns for turning, as it continues straight. The southern slopes of the Palatine Hill extend roughly 300 m in the SE-NW direction. AS is the central-eastern sector of the study area and develops for a length of about 100 m and 50 m in width. PA extends for about 150 m in the central-western sector of the sampling area. The geographical information of the area, including the elevation profiles and the lithological units were provided by the Rome Municipality (https://siticatasto.cittametropolitanaroma.it/siticloud/SitiCatastoCloud.jsp?comune=PROV#TAB_0).

2.2. Leaf sampling

Four leaf samplings were carried out at least 10 days after intense rainfall episodes (>10 mm). The first and most extensive sampling took place on the 5th of July 2022. Leaves were collected from eleven *Q. ilex* L. trees - “Qi”, the only recurrent tree species at VDC, 8 of which were distributed homogeneously along the Circus Maximus sidewalk of the road, while the other 3 trees were sampled on the Palatine sidewalk, corresponding to the ground level of the eastern limit of the PA and the central/eastern side of AS. One more “Qi” tree was

sampled at the base of the PA archaeological area at about 6 m from the sidewalk. Leaves from different evergreen species were collected at AS: *Elaeagnus x submacrophylla* Servett. - "Es"*, Laurus nobilis* L. "Ln"*, Nerium Oleander* L. - "No"*, Ligustrum vulgare* L. - "L"*, Rhamnus alaternus* L. - "Ra" and *Olea europaea* L. - "Oe". "Es" were sampled also at the PA for a comparison, being recurrent shrubs (Table 1). The shrubs are arranged in two rows in the eastern part of PA/AS green areas, and they were originally planted and conceived as a natural barrier for containing the diffusion of vehicular PM from the road level (Fig. 1a). Three "Oe" trees were sampled at the Palatine Hill at about 270 m linear distance from Paedagogium, along the pedestrian path from Arco di Tito towards the southern slopes, relatively removed from any vehicular road (Fig. 1s, within the satellite view of the whole area). Leaves were randomly selected from branches at a minimum height of 2 m for the trees, and 1.2 m for the shrubs, then stored in paper bags until drying. For each plant species but one ("Ra", see further) the samples were collected from at least 3 nearby shrubs and stored separately. An isolated "Ra" tree was sampled because of its position at the edge of the Palatine Hill in AS. The "No" shrubs were sampled beyond the security fence of AS. The mean longitudinal distance between the "edge" sampling points and the rows of shrubs was ~7 m. Further leaf samplings were performed on the 28th of February, the 23rd of March and the 26th of June 2023. The sampling of February was aimed at the comparison of sparse "Qi" shrubs with "Es" collected at PA and AS. It also included leaves from "Qi" branches grown at the trunk's base of a tree in the Palatine side of VDC. These leaves were characterised by dark grey layers deposited on their surfaces. The sampling in March concerned the comparison of "Qi" leaves sampled in VDC at 2 and 4 m from ground and was repeated in June, when a "Qi" tree was sampled for comparison with the isolated "Ra", being their leaves in close contact at the edge of AS. Another isolated "Ra" in the inner part of PA was sampled as well. The comparison between "Qi" and "Es" at AS and PA was repeated as well.

Table 1 Leaves sampling detailed: dates, areas, species, acronyms, number of samples.

Date	Area	Species	N
05/07/2022	Via de Cerchi (VDC)	*Q. ilex*	11
	Arcate Severiane (AS)	*Q. ilex*	3
		E. submacrophylla	3
		L. nobilis	3
		L. vulgare	3
		N. oleander	3
		R. alaternus	3
	Paedagogium (PA)	*Q. ilex*	3
		E. submacrophylla	3
	Centre of Palatine Hill	*O. europaea*	3
28/02/2023	Arcate Severiane (AS)	*Q. ilex*	3
		E. submacrophylla	3
	Paedagogium (PA)	*Q. ilex*	3
		E. submacrophylla	3
23/03/2023	Via de Cerchi (VDC)	*Q. ilex*	1
	Via de Cerchi (VDC)	*Q. ilex*	3
26/06/2023	Arcate Severiane (AS)	*Q. ilex*	4
		E. submacrophylla	3
		R. alaternus	3
		Q. ilex	3
		E. submacrophylla	3
	Paedagogium (PA)	*E. submacrophylla*	3
		R. alaternus	1
	Via de Cerchi (VDC)	*Q. ilex*	3

2.3. Lichen exposure

Transplants of the lichen species *Evernia prunastri* (L.) Ach. were exposed, as this species is well known for being suitable in environmental applications (Loppi et al., 1999; Loppi, 2019). Thalli of this species were collected in a reasonably pristine area, far from urban settlements and pollution sources, picked at a height > 2 m to avoid main soil contamination. The material was enveloped in a plastic net (lichen bag) for the exposure. Six samples were left unexposed for comparison. Three lichen bags per site were exposed along a linear transect from VDC to SP, for a total of six sites at the road level and two at the edge of the hill, respectively at the PA and AS sides of the Palatine (Fig. 1b, d). The exposure period lasted from March 23 to June 26, 2023. The duration of exposure of 3 months is regarded as optimal for *E. prunastri*, as reported by Loppi (2019); in addition, this is the same exposure period

used in similar studies (Winkler et al., 2019, 2022; Grifoni et al., 2024). The first site included three transplants tied to the "Qi" branches facing the SP gate on the Circus Maximus (CM) side of VDC. At the second site, three lichen bags were exposed on "Qi" branches just behind the fence that separates the Palatine side of VDC from SP, approximately 5 m from the sidewalk (PS, Fig. 1c). The third site (GS) was located inside a green area surrounding the entrance of SP, and two lichen bags were tied to the railing and one to an isolated pole at an average distance of 25 m from the sidewalk. Two sites were placed inside SP, three lichen bags at the entrance (ES) and three tied to the wooden railing of the stairs to the floor of the hall (RS), approximately five m below the road level. The first site on the edge of the Palatine Hill consisted in three transplants tied to the barrier fence on the border of the PA area over SP (OS, Fig. 1d), at a height of about 10 m and a horizontal distance of 35 m from VDC. Three other transplants were tied to "No" plants on the edge of the AS, at 13 m horizontal distance with respect to VDC and about 5–7 m from the rows of sampled trees.

Fig. 1. (a) Location of the plants sampled in July 2022 at the Palatine Hill and Via dei Cerchi: the colour codes represent *Q. ilex* L. (blue), *L. nobilis* L. (brown), *N. oleander* L. (purple), *L. vulgare* L. (yellow), *R. alaternus* L. (dark blue), *E. submacrophylla* Servett. *(red), O.*

europaea L. are out of the map (modified from Google Earth). (b) Schola Praeconum area, and lichen transplant exposure. Site AS is out of the map. Refer to the text for the acronyms (modified from Google Earth). (c) Lichen bag tied to a *Q. ilex* tree behind the fence of Schola Praeconum. (d) Lichen bag tied to a *N. oleander* L. on the edge of the Arcate Severiane area.

2.4. Magnetic analysis

All leaf and lichen samples were analyzed for their magnetic properties at the Laboratory of Paleomagnetism of Istituto Nazionale di Geofisica e Vulcanologia in Rome, Italy. Lichens and leaves were dried with a Bionsec Domus plastic desiccator and placed in 8 cm^3 plastic cubes to determine the magnetic susceptibility by mass (χ, $m^3\,kg^{-1}$) with a Agico KLY5 meter. The hysteresis properties, i.e. the coercive force (Bc, T), the saturation remanent magnetization by mass (Mrs, $Am^2\,kg^{-1}$) and the saturation magnetization by mass (Ms, $Am^2\,kg^{-1}$), were determined on pharmaceutical gel caps#4 with the vibrating sample magnetometer Lakeshore 8604 up to a field of 1.0 T at steps of 2.5 mT. Ms. and Mrs. were calculated subtracting the high field linear trend after saturation. Lichens and leaves were analyzed after drying for obtaining concentration dependent magnetic parameters that are not influenced by the presence of different quantities of water, that is diamagnetic. Moreover, since lichens and leaves are not planar, mass is better suited than surface for normalizing the concentration dependent magnetic parameters, taking into account that a part of the PM is immobilised inside (Szönyi et al., 2007). The coercivity of the saturation remanent magnetization (Bcr) was calculated from the logarithmic backfield remagnetization curves up to -1.0 T, after saturating at 1.0 T. The domain state and magnetic grain size of the samples were compared to theoretical magnetite according to the hysteresis ratios Mrs./Ms. and Bcr/Bc in the "Day plot" (Day et al., 1977; Dunlop, 2002a, 2002b). First order reversal curve (FORC) diagrams are used for delineating the distributions of the interaction field (Bu) and coercivity in samples, in order to disentangle the superparamagnetic (SP), single domain (SD), multidomain (MD) and pseudo-single domain/vortex (PSD/V) behaviours, the latter describing the transitional state between SD and MD particles (Pike et al., 1999; Roberts et al., 2000). FORCs were measured at steps of 2.5 mT, with 300 ms averaging time and maximum applied field being 1.0 T. FORC diagrams were processed, Variforc smoothed (up to 8 at the ridges and up to 12 for the background) and drawn with the FORCINEL 3.06 Igor Pro routine (Harrison and Feinberg, 2008).

2.5. Chemical analysis

Chemical analyses of all lichen and selected leaf (those collected on 5th of July 2022, $N = 10$) samples were performed at the University of Siena, Italy. Samples were first pulverized with liquid nitrogen using ceramic mortar and pestle, and 250 mg of powder were mineralized with 3 mL of HNO_3, 0.2 mL of HF and 0.5 mL of H_2O_2 in a microwave digestion system (Ethos 900, Milestone). Afterwards, samples were analyzed by inductively coupled plasma – mass spectrometry (ICP-MS, NexION 350x, Perkin Elmer) to quantify the content of potentially toxic elements related with traffic, i.e. Al, Ba, Cr, Cu, Fe, Sb, Zn and expressed on a dry weight basis (mg/kg dw). Analytical quality was verified using the certified reference materials IAEA-336 "Lichen" (International Atomic Energy Agency, 1999) and GBW07604 "Poplar leaves" and indicated recoveries in the range 100–110 %. Precision of the analysis was expressed by the coefficient of variation of 3 replicates and was >95 %.

2.6. Statistical analysis

The dataset was preliminarily checked for outliers using the Tukey test. Since the data did not approach a normal distribution (Shapiro- Wilk test), and it was not even possible to transform them successfully, to check the diffusion pattern of metallic PM from VDC up to the Palatine Hill, a Mann-Whitney *U* test was performed comparing both leaf and lichen samples at the roadside level with those above the archaeological area. Detailed site comparison was achieved by means of Kruskal-Wallis ANOVA followed by the Conover-Iman post hoc test. Correlations were tried using the Spearman rank coefficient. All calculations were run using the R software (R Core Team, 2024).

3. Results

3.1. Leaf magnetic properties

The leaves collected on 5th of July 2022 were investigated through magnetic susceptibility by mass values and hysteresis properties (Table 1s). "Qi" leaves' χ values from the Circus Maximus side of VDC ranged from 6.1×10^{-8} to 51.5×10^{-8} m^3 kg^{-1}, with a mean value of $21.0 \pm 14.7 \times 10^{-8}$ m^3 kg^{-1}. χ values of leaves collected from the Palatine sidewalk of VDC

ranged 5.5 × 10^{-8} - 24.4 × 10^{-8} m^3 kg^{-1} with a mean of χ = 14.8 ± 7.2 × 10^{-8} m^3 kg^{-1}. The overall mean for "Qi" leaves at VDC was χ = 19.1 ± 13.2 × 10^{-8} m^3 kg^{-1}. In the AS area over the Palatine Hill, five different plant species were collected; magnetic susceptibility values ranged from χ = 2.1 × 10^{-8} m^3 kg^{-1} ("L") to 9.8 × 10^{-8} m^3 kg^{-1} for the isolated "Ra" at its edge with a mean of 5.1 ± 2.1 × 10^{-8} m^3 kg^{-1}, whereas in PA, where only the "Es" leaves were collected (with the exception of a single "Qi" sampled at its base), the magnetic susceptibility was 3.0 × 10^{-8} to 3.5 × 10^{-8} m^3 kg^{-1}, the mean 3.3 ± 0.2 × 10^{-8} m^3 kg^{-1}. The hysteresis loops were always saturated well before 1.0 T. Average Ms. and Mrs. were 10.0 ± 6.0 and 1.0 ± 0.6 mAm^2 kg^{-1} at the Palatine sidewalk and 18.1 ± 12.2 and 2.4 ± 1.5 mAm^2 kg^{-1} at the Circus Maximus sidewalk of VDC, respectively. Bc and Bcr were 9.7 ± 1.5 mT and 36.2 ± 1.6 mT at the Palatine side and 12 ± 2.0 and 39.1 ± 1.6 mT at the Circus Maximus side of VDC. At the AS site, the mean Ms. and Mrs. of the five species collected, were 3.5 ± 1.4 and 0.4 ± 0.1 mAm^2 kg^{-1} respectively, with the highest values for "No" (6.4 and 0.6 mAm2 kg^{-1}) and the lowest one for "Es" (1.3 and 0.1 mAm^2 kg^{-1}). Bc ranged 8.1–9.8 mT with a mean value of 9.1 ± 0.7 mT and Bcr varied between 32.5 and 38.5 mT, in mean 35.5 ± 2.3 mT. The "Es" samples from PA showed mean Ms. and Mrs. 2.0 ± 0.3 and 0.3 ± 0.0 mAm^2 kg^{-1}, Bc and Bcr 10.4 ± 3.0 and 36.1 ± 0.5 mT. The concentration independent magnetic parameters (Bc, Bcr) and the low field saturation of hysteresis loops indicated that magnetite-like minerals dominate the ferrimagnetic properties of the bioaccumulated dusts at VDC, AS and PA sites. The comparison between sites AS and VDC showed significant differences in χ (Fig. 2a) and no significant difference between the Circus Maximus and Palatine sides of VDC (Fig. 2b). The comparison between "Es" and "Qi" sampled on February 28th showed no significant differences in χ for the two species (Fig. 2c). In June, the magnetic susceptibility of "Qi" leaves was significantly higher than that of "Es" (Fig. 2d). The magnetic susceptibility of "Qi" leaves collected at VDC during March 2023 at 4 m height was statistically higher than that of leaves collected at 2 m height, but the same was not true for leaves collected during June 2023 (Fig. 2e and f, respectively). In June, the magnetic susceptibility of the "Qi" and "Ra" leaves sampled from trees in close contact and at the edge of AS, was respectively 17.4 × 10^{-8} and 2.1 × 10^{-8} m^3 kg^{-1}, with respect to χ = 0.78 × 10^{-8} for "Ra" in the inner side of PA and χ = 3.1 × 10^{-8} and 1.20 × 10^{-8} m^3 kg^{-1} for "Qi" leaves in AS and PA, respectively. The magnetic susceptibility of the leaves covered by a dark layer, collected at the base of a "Qi" in VDC, was exceptionally high: 109 × 10^{-8} m^3 kg^{-1}, i.e. six times higher than that of "Qi" leaves collected at 2 m height at the same site.

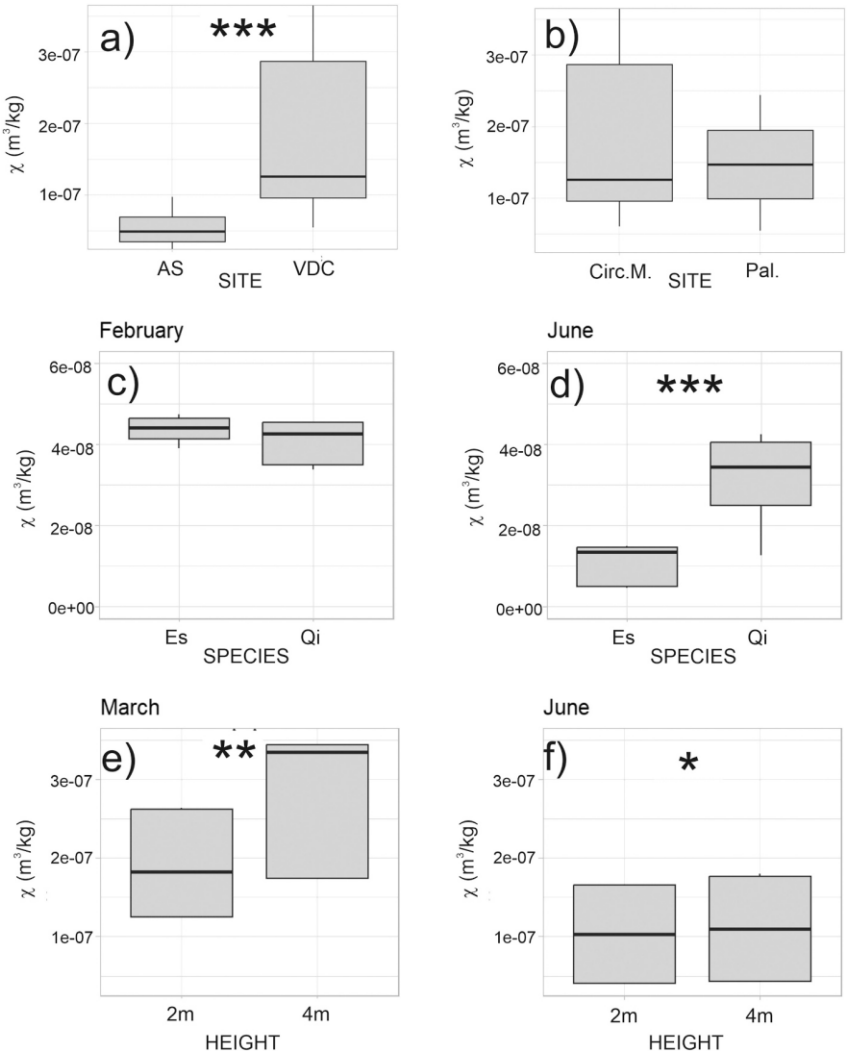

Fig. 2. Boxplots of leaf magnetic susceptibility with respect to site location, plant species and sampling height; statistically significant differences: * = $p < 0.05$, ** = $p < 0.01$, * ** = $p < 0.001$.

3.2. Lichen magnetic properties

Unexposed lichens showed a mean $\chi = 1.9 \pm 0.5 \times 10^{-8}$ m^3 kg^{-1}, Ms = 1.5 ± 0.6 and Mrs. = 0.2 ± 0.01 mAm^2 kg^{-1}, Bc = 8.9 ± 0.4 and Bcr = 33.3 ± 3.6 mT (Table 2s). Exposed lichen transplants showed a decreasing trend of χ from CM to the archaeological area at the ground level (Fig. 3): 10.6 ± 3.4 (CM) > 8.1 ± 2.5 (PS) > 7.1 ± 2.1 (GS) > 3.5 ± 0.7 (RS) > 2.8 ± 0.8 (ES) × 10^{-8} m^3 kg^{-1}. The OS site, overlooking the SP area, showed $\chi = 9.1 \pm 1.2 \times 10^{-8}$ m^3 $kg^{-1}$and higher values were on average revealed at the AS site, where $\chi = 14.8 \pm 1.9 \times 10^{-8}$ m^3 kg^{-1}. Ms. and Mrs. followed the same trend at the ground level, with a maximum value relative to

the CM site, 7.8 ± 1.4 and 0.9 ± 0.2 $mAm^2 kg^{-1}$, respectively, and a minimum indoor value of 2.0 ± 0.3 and 0.20 ± 0.03 $mAm^2 kg^{-1}$, respectively. Bc and Bcr ranged from CM 10.7 ± 0.7 and 39.2 ± 1.1 mT to 8.7 ± 0.2 and 31.4 ± 2.8 mT indoors. The sites at the Palatine Hill reported Ms. = 7.2 ± 1.8 and Mrs. = 0.7 ± 0.1 $mAm^2 kg^{-1}$, Bc = 8.7 ± 0.3 and Bcr = 37.9 ± 0.7 mT at OS site. At AS site, Ms. = 12.6 ± 2.2 and Mrs. = 1.2 ± 0.2 $mAm^2 kg^{-1}$, Bc = 9.0 ± 0.4 and Bcr = 38.5 ± 0.3 mT. Likewise leaves, the concentration independent magnetic parameters (Bc and Bcr) of lichens highlighted the bioaccumulation of magnetite-like magnetic particles. The magnetic susceptibility at the Palatine Hill was not statistically different from that at the outdoor ground level at 9% confidence level ($p = 0.45$). At the same confidence level, the magnetic susceptibility of the unexposed sample was not statistically different from that of the indoor sites ($p = 0.48$ and $p = 0.23$ for ES and RS, respectively), while it was different from that outdoors, p values ranging from 0.00 to 0.03.

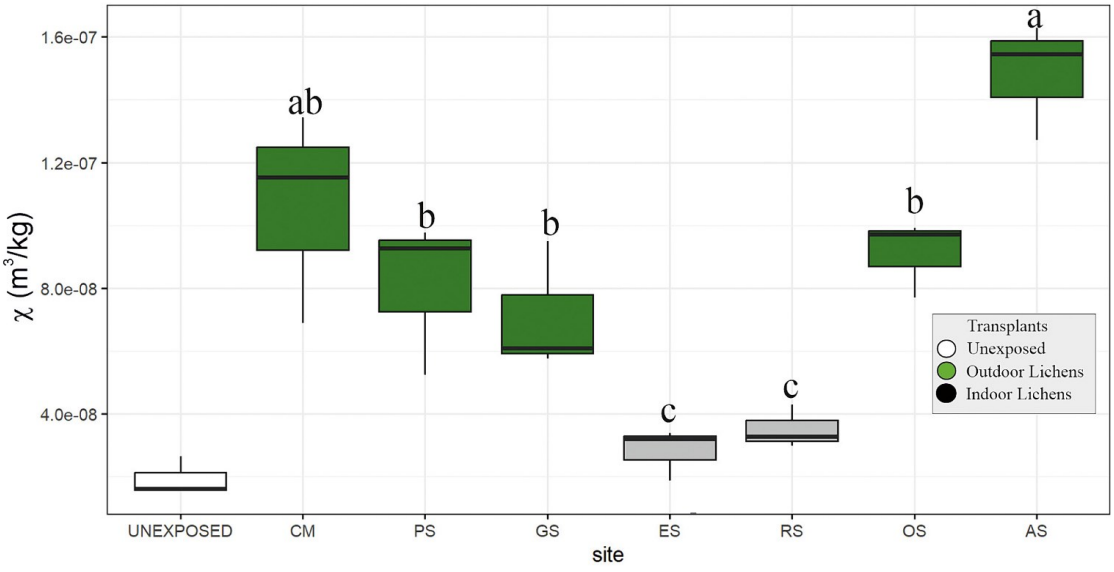

Fig. 3. Boxplots of magnetic susceptibility of lichen samples unexposed and exposed at each sampling site. Different letters indicate statistically significant ($p < 0.05$) differences among sites.

3.3. Magnetic grain-size of leaves and lichens

In the "Day Plot", the site means for leaves, calculated as mean Bcr/ Bc vs mean Mrs./Ms. ratios, were all but "Oe" clustered in the central PSD region of the diagram, (Fig. 4a). The

same behaviour was confirmed for lichens (Fig. 4b), which fell in the same central part of the plot, with a modest linear spread of the points from the indoors (GS and RS, finer) to over Palatine sites (AS, OS, coarser). In the FORC diagrams (Fig. 5), vortex features generally prevail for both leaves and lichens, with variable contributions of SD and MD components. The samples at the AS side of Palatine Hill and VDC (Fig. 5b and h, respectively) highlight, especially for leaves at the road level, a vertical spreading of the distribution along the Bu axis, indicative of an increased contribution of MD grains. The leaf sample at the Circus Maximus side of VDC indicates a relevant presence of non-interacting SD particles (Fig. 5g). Vortex components are prevailing in the indoor and unexposed samples too, in general agreement with the Day Plot. The Oe sample showed SD features, in coherence with its position in the Day Plot (Fig. 2s).

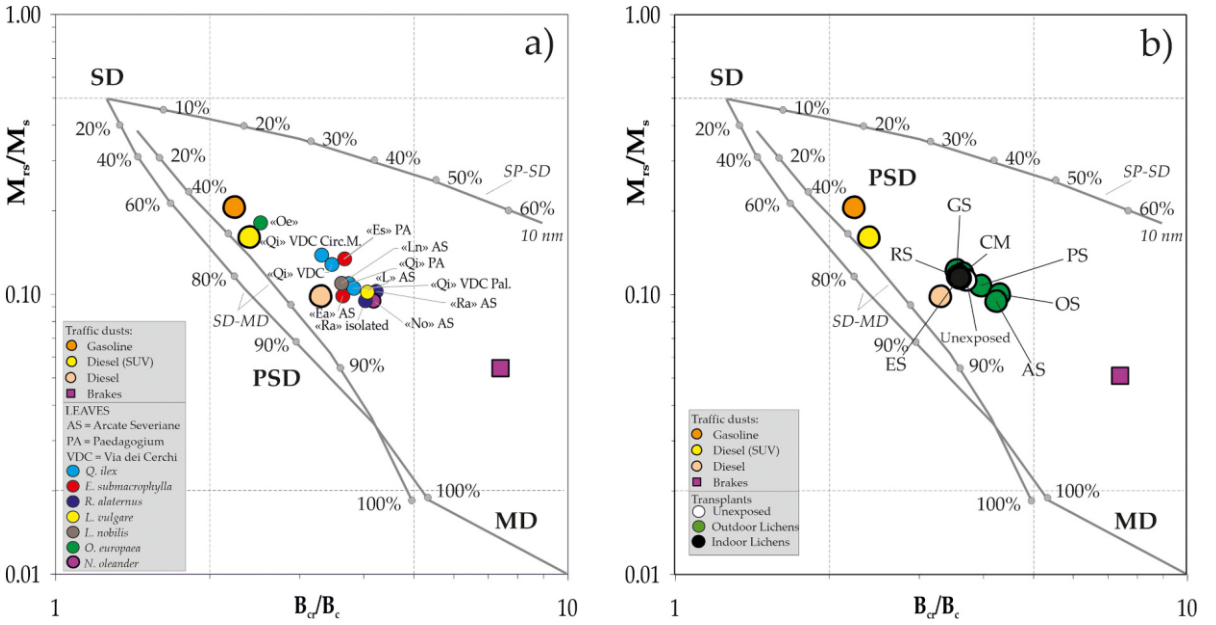

Fig. 4. Bilogarithmic "Day Plot" of the site mean hysteresis ratios for leaves collected in 2022 (a) and lichen transplants (b), reported together with the average points for different kinds of fuel exhaust (orange, yellow and pink circles) and brake dust emissions (purple square) calculated from Sagnotti et al. (2009). The SD (single domain), PSD (pseudo-single domain) and MD (multidomain) fields and the theoretical mixing trends for SD-MD and SP-SD pure magnetite particles (SP, superparamagnetic) are from Dunlop (2002a, 2002b).

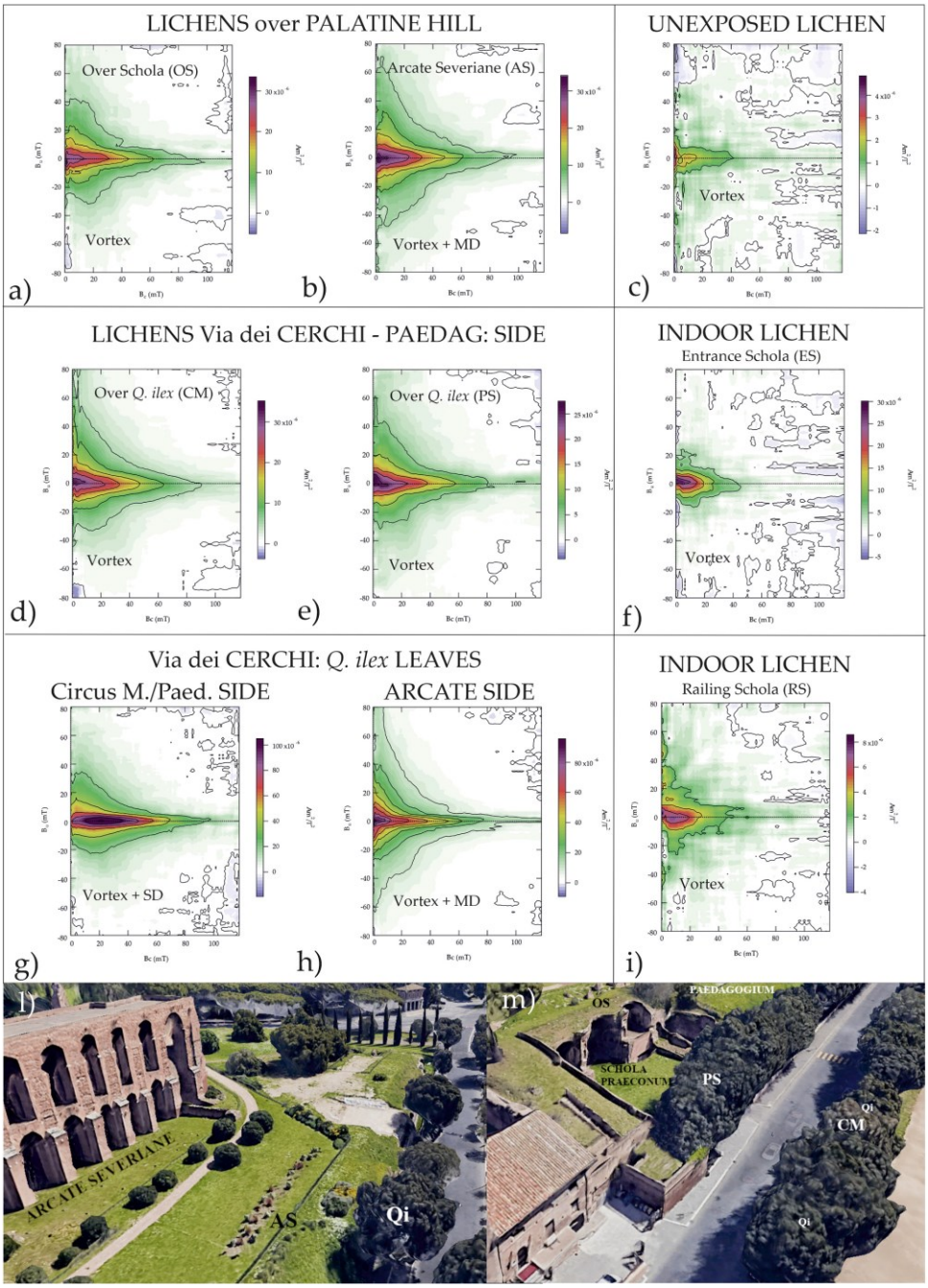

Fig. 5. FORC diagrams for selected lichen bags exposed over Palatine Hill (a, b), unexposed lichen (c), at VDC PA/SP side (d,e), Indoor (f, i) and "Qi" leaves from VDC PA/SP side (g) and AS side (h). Sampling locations in (l) and (m) for AS and PA/SP, respectively (modified from Google Earth). See text for the acronyms.

3.4. Trace element content of leaves and lichens

Leaf samples at VDC2 site were identified as outliers for Cu, Zn and Ba, and these elements were thus excluded from the calculations relative to VDC. Element concentrations in leaf samples collected at VDC showed a remarkable variability, with coefficients of variations exceeding 60% for Al, Ba, Cr, Fe, Sb while on the Palatine Hill variability was much reduced, being <35% for all elements (see Table 3 s for "Qi" at VDC and "Es" at Palatine Hill). Irrespective of the plant species analyzed, trace elements exhibited lower concentrations on the Palatine Hill compared to VDC. All trace elements investigated were accumulated by lichen transplants exposed for three months (Table 4s), as shown by the ratios of the values of exposed-to-unexposed samples (EU ratios; Table 2). Zinc at OS emerged as an outlier and was thus excluded from the calculations. Aluminium was the only element not showing statistically significant differences among sites. Although a decreasing trend was evident from CM to the SP, element accumulation was overall higher on the Palatine Hill (OS and AS) than at VDC. Inside the SP elements did not show any appreciable accumulation.

3.5 Relationship between magnetism and chemistry

The values of χ and Ms., as concentration dependent magnetic parameters, were tried for correlations with the concentration of TREs, both in leaves and lichens. In lichen transplants, magnetic parameters were strongly correlated with all trace elements with the remarkable exception of Al (Fig. 6). Noteworthy, all elements were strongly correlated among them, while Al showed only a weak correlation with Fe (Fig. 3s). In leaves, the relationship between magnetic parameters and trace elements (Fig. 6) depicted a different scenario, with susceptibility being correlated with Al, which was also strongly correlated with Fe (Fig. 3s). Cu and Zn were not correlated with magnetic parameters nor with any other element.

Table 2

Exposed to Unexposed (EU) ratios of trace element concentrations in lichen transplants at each exposure site. Different letters indicate statistically signifi- cant differences ($p < 0.05$) among sites.

	CM	PS	GS	ES	RS	OS	AS
Al	1.30 ± 0.19^{a}	1.02 ± 0.32^{a}	0.92 ± 0.21^{a}	0.95 ± 0.09^{a}	1.49 ± 0.50a	0.93 ± 0.37^{a}	1.21 ± 0.37^{a}
Ba	1.72 ± 0.36^{ab}	1.50 ± 0.24^{b}	1.34 ± 0.25^{bc}	1.03 ± 0.09^{c}	1.29 ± 0.12^{bc}	1.57 ± 0.12^{ab}	2.20 ± 0.25^{a}
Cr	1.27 ± 0.17^{ab}	1.09 ± 0.19^{bc}	0.98 ± 0.12^{bc}	0.82 ± 0.04^{c}	1.20 ± 0.14^{ab}	1.27 ± 0.03^{ab}	1.58 ± 0.23^{a}
Cu	1.23 ± 0.05^{ab}	1.14 ± 0.13^{bc}	1.12 ± 0.04^{bc}	0.93 ± 0.03^{d}	1.05 ± 0.03^{cd}	1.24 ± 0.13^{ab}	1.55 ± 0.15^{a}
Fe	1.58 ± 0.21^{ab}	1.33 ± 0.31^{abc}	1.19 ± 0.21^{bc}	0.96 ± 0.03^{c}	1.49 ± 0.26^{ab}	1.36 ± 0.01^{abc}	1.88 ± 0.35^{a}
Sb	2.24 ± 0.44^{bc}	2.01 ± 0.34^{bc}	1.71 ± 0.28^{cd}	1.04 ± 0.07^{e}	1.30 ± 0.12^{de}	2.48 ± 0.47^{ab}	3.74 ± 0.55^{a}
Zn	1.27 ± 0.34^{bc}	1.10 ± 0.21^{cd}	1.64 ± 0.10^{ab}	0.96 ± 0.01^{d}	1.11 ± 0.11^{cd}		1.47 ± 0.13^{abc}

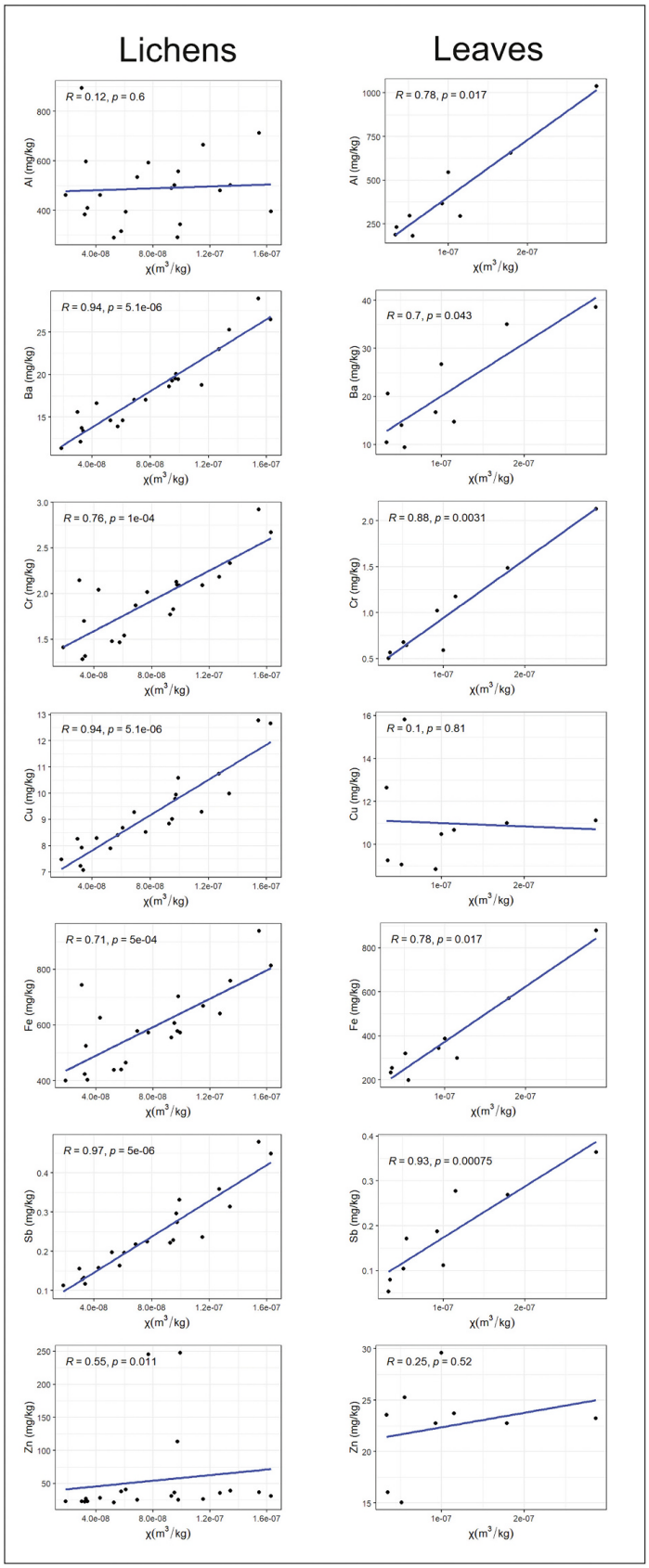

Fig. 6. Relationship between magnetic susceptibility and trace elements in lichens and tree leaves.

4. Discussion

4.1 Concentration dependent magnetic and chemical properties of leaves

The integration of magnetic and chemical analyses provided a comprehensive picture of the presence and distribution of metallic particles throughout the southern part of the archaeological area of the Palatine Hill. Several studies (e.g. Monaci et al., 2000; Sgrigna et al., 2015; Blanusa et al., 2015; Fusaro et al., 2021) have underscored the efficacy of Q. ilex leaves in intercepting PM and accumulating trace elements. This efficacy has been attributed to the evergreen nature, the arrangement of leaves along the branches within the canopy, and specific features such as the epicuticular waxy layer and stellate trichomes on the leaf surface, that maximise the accumulation and immobilisation of particles (Quero et al., 2006; Muhammad et al., 2019). Although Q. ilex may not be recommended in urban greenery based on its peculiar feature of being a strong emitter of VOCs such as monoterpenes (Keenan et al., 2009), this species has been strongly recommended as a key feature of green infrastructures finalized to PM removal because of its high bioaccumulation potential and functional tolerance (Fusaro et al., 2021). In order to test the ability of the plant species that are available over the Palatine Hill to immobilise traffic related particles, magnetic susceptibility was used as a proxy of the concentration of magnetic particles deposited over their leaves, as introduced for cultural heritage settings by Winkler et al. (2022). The average value of χ at VDC was 19.1 ± 13.2 × 10-8 m^3 kg^{-1}; its highest value was 2.7 times higher than the mean and resulted from the "Qi" close to the traffic lights and positioned where vehicles are in stop-and-go regime. Differences in terms of χ did not statistically emerge between the two sides of the road, whereas a statistically significant difference was evident between the leaves collected at VDC and AS. χ values at VDC were in the same range of those measured for "Qi" leaves sampled at other high traffic areas in Rome (Moreno et al., 2003; Fusaro et al., 2021; Szönyi et al., 2008), suggesting that the accumulation of metallic particles by "Qi" leaves remained roughly constant over the last 20 years of magnetic biomonitoring of airborne PM in Rome, under substantial changes of car models and policies of vehicular

emissions (Euro 3 up to Euro 6), and even though nowadays the number Euro 4 to 6 vehicles is 4.6 times greater than that of Euro 0 to 3 (see https://www.comune.roma.it/web-resources/cms/documents/09_Mobilita_Annuario2023_ultimo.pdf). The average interspecies χ value between AS and PA was 4.2×10^{-8} m^3 $kg^{-1,}$ 4.5 times less than "Qi" at VDC, and on the same range of "Qi" leaves sampled at green areas by Fusaro et al. (2021). Despite the lack of recurrent and healthy "Qi" shrubs, that prevented the use of "Qi" for a systematic interspecies comparison over the Palatine Hill, the tests in February and June confirmed that χ values for "Qi" are in the same range as those of "Es" even when the difference between them is significant. The average χ values at Palatine Hill were in the same range of "Oe" (3.1×10^{-8} m^3 kg^{-1}), sampled relatively far from any vehicular source since the nearest street is 225 m away in a straight line. Thus, it can be interpreted as a species-independent magnetic background, arising from the bioaccumulation of local soil and diffused PM. χ is the fastest and most sensitive magnetic property (e.g. Petrovský et al., 2000; Winkler et al., 2020), while Ms. measures the total magnetic signal across all ferrimagnetic grain sizes (Sheikh et al., 2023). Moreover, Ms. is a grain-size independent magnetic parameter, and considering that the magnetic mineralogy of leaves is compatible with magnetite-like minerals with a mass Ms. value of 90 Am^2 kg^{-1} (Dunlop and Ozdemir, 1997), it was calculated the weight percentage (wt%) of magnetite in the samples. At VDC, wt% (Fe_3O_4) = 1.74×10^{-2}, while over the Palatine Hill wt% (Fe_3O_4) = 3.9×10^{-3}, implying a weight concentration of magnetite 4.5 times higher at VDC compared with the Palatine Hill, consistently with χ values. These results confirmed that magnetic susceptibility is a sensitive indicator of the concentration of magnetic particles and that, despite their smaller volume, gel caps are representative of the whole sample as well. The maximum χ and wt% values of the whole dataset were measured in the leaves sampled in February 2023 at the trunk's base of the tree at the Palatine side of VDC where $\chi = 109 \times 10^{-8}$ m^3 kg-1 and wt% = 0.1%, thus highlighting the impressive magnetic content in the dark grey layer deposited over the leaves. The highest value for "Qi" leaves was $\chi = 44.6 \times 10^{-8}$ m3 kg^{-1} in a previous extensive study that covered different districts of Rome (Fusaro et al., 2021). The trace elements were

accumulated in relatively high concentration along the street. Indeed, Al was accumulated in higher concentration compared to other studies in urban settlements, i.e. 375 mg/kg in Salerno (Baldantoni et al., 2020) and 309 mg/kg in Abbadia San Salvatore (Monaci et al., 2023), 385–416 mg/kg in Siena (Fantozzi et al., 2013; Monaci and Bargagli, 1997). Traffic-related tracers such as Ba, Cr, and Sb were detected in elevated levels compared to those recorded at the AS site. Ba concentrations in VDC "Qi", 24.9 mg/kg, were akin to those reported in Abbadia San Salvatore, 23.0 mg/kg (Monaci et al., 2023), in Siena, in fast-moving traffic areas, 23.1 mg/kg (Monaci and Bargagli, 1997) and Florence, 22.6 mg/kg (Monaci et al., 2000). However, Cr concentrations were found to be lower than those observed by Fantozzi et al. (2013) at 2.5 mg/kg and Ugolini et al. (2013) at 3.1 mg/ kg, yet higher than those documented by Monaci et al. (2023) at 1.06 mg/kg and Baldantoni et al. (2020) at 1.11 mg/kg. Sb accumulation by leaves was quantified as three times higher along the street than in the Palatine area, where the amount of Sb was equal to that observed by Monaci et al. (2023), 0.08 mg/kg. All this evidence strongly suggests that the slow-moving vehicular traffic at VDC is an important source of airborne PTEs and causes street dust resuspension. However, there is also evidence that the Palatine area is only partly affected by the deposition of metallic particles. In Fusaro et al. (2021), the element concentration of "Qi" leaves was reported for the soluble fraction of the dust deposited over the leaf surface. The ratios between the element concentration in VDC and the average values of the soluble fraction from the high traffic area described above were Al > Fe > Ba > Cr > Zn > Sb > Cu, indicating that Al is the most bioaccumulated element with respect to the soluble fraction (Fusaro et al., 2021). In fact, a strong correlation emerged between Fe and Al, highlighting that the leaves were contaminated by resuspended soils and road dusts (Loppi et al., 1999). The bioaccumulation of metallic particles in plant leaves decreased from VDC to the Palatine Hill. It should anyway be noted that the rows of shrubs at AS and PA were at least 5 m from the edge of the hill. As a qualitative comparison, in July 2022 χ of the isolated "Ra" at the edge of AS was 1.5 folds that of "Ra" inside AS. In June 2023, the leaves of the isolated "Qi" sampled at the edge of AS highlighted an impressive bioaccumulation of metallic particles. The χ value was 8 folds that of the adjacent "Ra", that was in turn 3

folds higher than the "Ra" inside PA. These results confirmed that "Qi" is an efficient accumulator, especially when as a mature tree. Irrespective of the species, the accumulation of metallic particles from the road was largely abated across the longitudinal distance between the edge of the Palatine and the shrubs, as also qualitatively verified by the comparison of the χ values of "Ra" leaves at the edge and inside the Palatine hill. The minor influence of the vertical distance from the road was confirmed by the χ values of "Qi" leaves sampled at 2 m above the ground, that resulted in lower (March) or similar (June) values to those at 4 m, as it was further investigated with lichens.

4.2 Concentration dependent magnetic and chemical properties of lichens

Given the close relationship between the magnetic susceptibility and the bioaccumulation of several TREs such as Fe, Sb, Cr, Cu and Zn (Winkler et al., 2020), the magnetic susceptibility of lichen transplants was measured to verify the diffusion of magnetic particles from VDC along seven exposure sites. Magnetic susceptibility values decreased from CM to the indoor SP, pointing out different values of χ among Circus Maximus and Palatino sides, despite their similar distance with respect to the center of VDC. This result is consistent with the different types of traffic on the two lanes. On the Circus Maximus side, cars form a queue and slow down for turning left and parking on the only allowed lane. Conversely, on the Palatine side, cars proceed straight towards a large road. The decrease in magnetic susceptibility at VDC was verified within 30 m separating Circus Maximus from inside Schola Praeconum. This result is in line with those found at Lungotevere Farnesina, where lichen transplants demonstrated that the lodges of Villa Farnesina were prevented from large inputs of vehicular emissions (Winkler et al., 2022). The wt% (Fe_3O_4) ranged from 8.71×10^{-3} at CM to 2.47×10^{-3} as the average value for the indoor transplants at SP, anyway, indicating accumulation compared with unexposed samples (1.64×10^{-3}) and highlighting a bioaccumulation of magnetite up to 5.3 folds with respect to unexposed samples. This result is in the same range of the ratio between leaves sampled at VDC and AS. Noteworthy, wt% at VDC was 3.5 times higher than the maximum wt% determined outside the Guggenheim Collection in Venice, where the aquatic context prevented the diffusion of vehicular emissions (Grifoni et al., 2024). Comparing EU ratios of trace elements measured in the present study with those recorded at Villa Farnesina (Winkler et al., 2022), it emerged that at the road sites, all trace

elements were accumulated in higher amounts along Lungotevere Farnesina than at VDC. Bioaccumulation was approximately 4 folds (9.2 vs 2.2) higher for Sb, 3 folds higher for Cu (3.9 vs 1.2) and Cr (3.7 vs 1.3), 2 folds higher for Zn (2.7 vs 1.3) at Villa Farnesina than at VDC. Al and Cr bioaccumulations at the gardens of Villa Farnesina were twice those at PS (1.9 vs 0.9 and 2.2 vs 1.0 respectively), whereas Zn was similar at PS and Villa Farnesina's garden (1.6 vs 1.4). These differences may be connected with experimental features (e. g. season and year of lichen exposure, topology and air circulation of the sites), but also with the different road characteristics. In fact, VDC is a 500 m long per 10 m wide road, where parking is allowed at a single lane portion, while Lungotevere Farnesina is 15 m wide and part of a long road that runs almost straight for >1 km, where parking is allowed at both sides. So, these differences well explain why biomonitoring can provide site specific, time-averaged and high spatial resolution PTE diffusion and concentration patterns, that are tailored for preventive conservation services. This information cannot emerge from the available daily PM10 concentration data from instrumental monitoring, which is based just on one station located between the two sites. The Palatine Hill, especially at AS, resulted as the most enhanced in both χ and trace elements. Several lichen surveys have shown a decrease in the concentration of NOx and TREs within a few tens of meters from roads (e.g. Frati et al., 2006; Contardo et al., 2020), and that angular exposure on the tree trunk is not a key factor (Paoli et al., 2013). At the AS site the bioaccumulation was severe (according to the scale suggested by Frati et al., 2005) for TREs such as Fe, Ba and Sb. Despite the height of about 8 m with respect to the road, AS is a barrier-free area, open on three sides to air mass flows and separated from the street just by the crown of one "Qi" tree. Vehicular emissions by the cars passing in front of the area were intercepted by the lichens tied to "No" plants. This result was confirmed by the bioaccumulation of magnetite as deduced from its wt%, that was 2 folds at AS with respect to OS, with a possible influence also from the longer longitudinal distance from the road at OS. The intense bioaccumulation at AS demonstrated that lichens are much better biomonitors than leaves. In fact, the magnetic susceptibility for lichens exposed for three months at AS was 2.5 folds that of "No" evergreen leaves, whose χ value was among the highest for leaves, due to their position at the edge of the Palatine Hill. The strong correlations emerged for lichens between magnetic parameters and elements such as Fe, Sb, Cu, Cr and Ba, which are well known tracers of exhaust and non-exhaust vehicle emission (Hulskotte et al., 2007; Winkler et al., 2020), suggest that traffic flow in Rome is a remarkable source of atmospheric PM pollution. In addition, tire-wear particles are a known

source of Zn, which is 1% by weight of tire composition (Councell et al., 2004; Jeong, 2022). Al, which has no known metabolic role in lichens and is commonly regarded as a tracer of soil input (Loppi et al., 1999), and the lack of correlation of this element with magnetic parameters suggests that soil has not or has only a very limited contribution to the metallic load of lichen samples. This is further confirmed by the modest relationship between the content of Al and Fe, which suggests that soil is responsible for about 25% of the total load of lichen transplants. Lichens better demonstrated what was supposed for leaves: the longitudinal distance with respect to the road influences the diffusion of vehicular emissions much more than the vertical distance above ground. Moreover, the lack of correlation between χ and Al in lichens is a clear indication that these organisms bioaccumulate airborne PM with no or very limited influence from soil and road dusts. Thus, the combined use of lichens and leaves may provide original and complementary data for disentangling airborne PM with respect to street dusts and resuspended soils. So, lichens are undoubtedly valuable biomonitors of airborne PM, while leaves accumulate and limit the diffusion of the airborne and the resuspended/soil fraction of PM.

4.3. A model based on the magnetic grain-size

In the "Day plot" all samples but "Oe", irrespective of plant species and VDC or Palatine sites, were clustered in the central PSD region of the diagram, near to the theoretical trend for mixtures of SD and MD grains of pure magnetite. The points qualitatively approached those obtained for diesel emission and were far from the brake dust (Sagnotti et al., 2009). Conversely, in previous studies carried out near busy roads in Rome, leaves were placed near brake emissions (Sagnotti et al., 2009; Fusaro et al., 2021; Winkler et al., 2022). PM filters from air quality networks confirmed the same result (Winkler et al., 2021), demonstrating that near trafficked roads the metallic PM mainly arises from brake abrasion (Gonet et al., 2021a, 2021b). "Oe" was relatively removed from any vehicular source and its position as well as its FORC diagram may represent the prevailing SD features of soils and diffused PM in the area. The "pure emissions" points in Sagnotti et al. (2009) and Sagnotti and Winkler (2012) were recently reviewed by Letaïef et al. (2024), who demonstrated that for newer cars the positions in the "Day Plot" of brake dusts and diesel exhaust remained similar. Conversely, gasoline exhausts resulted more scattered as a function of the Euro emission categories. In Letaïef et al. (2024) street dust falls in the central region of the Day Plot. This result can explain the

position of our leaves, that chemical analyses demonstrated to be contaminated by road dusts and resuspended soil particles. Lichen transplants confirmed the same result of leaves, highlighting a general prevalence of PSD/Vortex features. In fact, the site means were all clustered in the PSD region of the plot, where also the unexposed and indoor bags were located. Conversely to leaves, lichens were not, or very modestly contaminated by soil particles. Thus, lichens and leaves bioaccumulated metallic particles mostly in the PSD/Vortex grain-size range, or as combination of fine SD and coarser MD particles, with variable inputs of road dust and natural contributions from the soil and North African dust. In fact, in SW Europe, a minor part of the PSD/vortex and MD magnetite grains load is of Aeolian origin (Larrasoaña et al., 2021). FORC diagrams furtherly disentangled the magnetic grain-size. Within the prevalence of vortex components, a minor difference emerged between the Paedagogium/Schola Praeconum and the Arcate sides of VDC and Palatine Hill. In fact, the increased contribution of MD components at AS and at the south-eastern side of VDC could be related to the different traffic regime of the first half of the road, where brakes are used for slowing down the cars before reaching the queues due to the parking and the traffic light. In the second half of the road, slow or start and stop traffic prevail, with emission of SD and PSD finer particles linked to fuel exhaust (Fig. 7). MD features and a sharp tail extending to higher coercivities were associated with brakes in Sagnotti et al. (2009). Conversely, SD and PSD features were attributed to gasoline and diesel exhaust emissions, respectively. Sheikh et al. (2022) concluded that FORC diagrams of brake-pad residue specimens show a combination of narrow central ridge and vertically spread signal, attributed to vortex behaviour of metallic Fe. Conversely, exhaust-pipe residue displays a more conventional "magnetite-like" signal and a tri-lobate signal attributed to vortex state. Finally, Letaïef et al. (2024) confirmed that MD features are connected to brakes, with some difference between pads and dusts and for what concerns the exhaust pipes, variable contributions of MD particles according to the EURO rules. The same authors concluded that in the street dusts the magnetic particles are in the PSD + SD grain-size range, likewise the leaves sampled at Circus Maximus side of VDC (Fig. 5g). As a summary, the combination of chemical and magnetic data pointed out that vehicular traffic in VDC is the main source of the magnetic particles bioaccumulated by lichen transplants and "Qi" leaves. The particles were mostly in the PSD/Vortex grain size range, as a combination of exhaust emissions and road dusts, the latter influencing only leaves. FORC diagrams well reflected the different traffic regimes between the smoother traffic conditions of the first half of VDC (AS) and the congested

situation at the second half (PA), according to the different occurrence of MD particles connected to brakes and to SD particles from fuels (Fig. 7). The contribution of brake emissions was highlighted by the concentration of tracers such as Sb and Ba. For what concerns the provision of preventive ecosystem services, *Q. ilex* leaves demonstrated, once more, to be an efficient accumulator (Muhammad et al., 2019), when compared to other Mediterranean plant species sampled over the Palatine Hill. Moreover, the longitudinal distance from the road was a key element, with respect to the height from ground. This is a key point that suggests installing green barriers as close as possible to the road for providing the most effective protection service and to maximise the interception and immobilisation of the vehicular metallic particles. This suggestion is in agreement with Sheikh et al., 2023, who concluded by means of magnetic measurements that properly designed tredges (i.e., in terms of species, leaf density, and height) installed close to the locally derived PM source can effectively mitigate exposure to airborne PM.

Fig. 7. (a) Grain-size model of the vehicular emissions at Via dei Cerchi: car queues from the traffic light to the Paedagogium and Schola Praeconum sides of the road: prevalence of Single Domain (SD) and Pseudo Single Domain (PSD) fine particles connected to exhaust emissions (modified from Google Earth). Smooth traffic conditions at the Arcate Severiane side of the road mixture of MD and PSD particles respectively connected to brakes and fuel emissions.

(b) A queue at the traffic light. The delimited lane is reserved to bikes. (c) The queue forming between the Paedagogium and Arcate sides of Via dei Cerchi.

5. Conclusions

In this study, a multidisciplinary biomonitoring approach was applied for testing the diffusion of vehicular metallic particles from Via dei Cerchi, a busy road coasting the Circus Maximus, towards the Palatine Hill, an archaeological area elevated about 8 m with respect to the road level. The main conclusions of this study are:

1) Metallic particles bioaccumulated by lichens and leaves are related to vehicular traffic, their concentration being dependent on the longitudinal distance from the road, with no or limited influence of the height with respect to the road level. Consequently, for the provision of the best preventive ecosystem services, trees should be placed at the shortest longitudinal distance from the road.

2) Vehicular metallic particles accumulated by leaves and lichens arise from a mixture of exhaust and non-exhaust emissions, which depend on the different types of traffic regimes at Via dei Cerchi. Leaves highlighted the relevant contribution of road dusts among the overall PM, while lichens bioaccumulated airborne PM with no or very limited influence from the soil. The multidisciplinary approach outlined that the physicochemical nature of particulate matter at the archaeological site of Palatine Hill was related to the complex pattern of diffusion and resuspension of vehicular emissions. The results indicated that leaves accumulate the overall fractions of PM, thus limiting the adverse effects of all its components, be they airborne or related to soil and resuspension, while lichens are better biomonitors of the airborne component of PM.

APPENDIX – CHAPTER 2

Table 1s

Site mean, standard deviation, minimum and maximum values of mass specific magnetic susceptibility (χ), saturation magnetization (Ms), remanent magnetization (Mrs), coercivity (Bc), coercivity of the remanence (Bcr) of leaves sampled on July 2022

Samples		χ (10^{-8} m^3 kg^{-1})	Ms (10^{-3} Am^2/kg)	Mrs (10^{-3} Am^2/kg)	Bc (mT)	Bcr (mT)
***Quercus ilex*_VDC Palatine Side**	**Mean**	14.8	85.9	8.9	9.7	36.2
	sd	7.2	56.5	5.6	1.4	1.6
	Min	5.5	38.4	4.0	8.5	34.1
	Max	24.4	164.6	16.9	11.8	37.8
***Quercus ilex*_VDC Circus Maximus side**	**Mean**	16.6	151.3	19.8	12.1	39.1
	sd	14.8	106.5	13.0	2.0	1.6
	Min	9.6	6.8	7.2	9.3	37.1
	Max	51.5	337.3	33.9	15.2	40.7
***O. europea*_Palatine**	**Mean**	3.1	24.9	4.1	14.1	35.1
	sd	1.1	17.0	2.0	1.4	1.2
	Min	2.2	10.0	1.9	12.6	34.0
	Max	4.5	43.4	5.8	15.5	36.4
***N. oleander*_AS**	**Mean**	5.8	48.8	4.6	9.3	38.5
	sd	1.7	7.4	0.6	0.8	1.2
	Min	7.1	43.8	4.2	8.7	37.3
	Max	3.4	57.3	5.3	10.2	39.7
***Ligustrum*_AS**	**Mean**	2.8	24.4	2.4	8.1	32.5
	sd	0.9	1.2	0.4	1.0	4.0
	Min	2.1	23.1	2.1	7.5	28.8
	Max	4.1	25.5	2.8	9.3	36.8
***L. nobilis*_AS**	**Mean**	4.1	19.0	2.0	9.8	34.5
	sd	1.4	11.9	0.9	1.8	2.4
	Min	2.6	11.6	1.3	8.7	32.8
	Max	5.9	32.7	3.0	11.9	37.3
***R. alaternus*_AS**	**Mean**	6.9	41.1	4.2	8.8	36.8
	sd	0.7	3.8	0.5	0.6	0.8
	Min	5.9	38.6	3.8	8.3	35.9
	Max	7.7	45.5	4.7	9.5	37.3
***Elaeagnus x sub.*_AS**	**Mean**	4.5	19.2	2.0	9.7	35.0
	sd	0.7	7.8	1.2	1.1	2.3
	Min	3.5	12.2	0.9	8.7	31.8
	Max	5.2	26.5	3.2	10.9	37.0
***Elaeagnus x sub.*_PA**	**Mean**	3.3	18.9	2.5	10.4	36.1
	sd	0.2	3.4	0.4	3.0	0.5
	Min	3.0	15.9	2.1	8.3	35.6
	Max	3.5	22.6	2.9	13.8	36.5

***R. alaternus*_isolated**	**Mean**	9.7	61.2	5.8	9.2	36.7
***Quercus ilex*_PA**	**Mean**	9.3	5.2	0.6	10.0	37.2

Table 2s

Site mean, standard deviation, minimum and maximum values of mass specific magnetic susceptibility (χ), saturation magnetization (Ms), remanent magnetization (Mrs), coercivity (Bc), coercivity of the remanence (Bcr) of lichen transplants

Samples		χ (10^{-8} m^3 kg^{-1})	Ms (10^{-3} Am^2/kg)	Mrs (10^{-3} Am^2/kg)	Bc (mT)	Bcr (mT)
CM	**Mean**	10.62	7.84	0.93	10.7	39.2
	sd	3.37	1.42	0.19	0.7	1.1
	Min	6.89	6.21	0.71	9.9	38.6
	Max	13.44	8.80	1.04	11.1	40.5
PS	**Mean**	8.10	6.62	0.71	9.5	37.8
	sd	2.48	1.36	0.16	0.6	0.9
	Min	5.25	5.07	0.53	8.9	36.8
	Max	9.77	7.62	0.84	10.1	38.5
AS	**Mean**	14.82	12.60	1.19	9.0	38.5
	sd	1.87	2.24	0.21	0.4	0.3
	Min	12.71	10.35	1.01	8.6	38.1
	Max	16.29	14.83	1.42	9.3	38.7
GS	**Mean**	7.12	6.12	0.74	10.2	36.5
	sd	2.07	1.70	0.28	1.0	1.2
	Min	5.77	4.59	0.54	9.2	35.3
	Max	9.50	7.95	1.05	11.1	37.8
OS	**Mean**	9.11	7.17	0.71	8.7	37.9
	sd	1.23	1.83	0.14	0.3	0.7
	Min	7.69	5.69	0.61	8.4	37.2
	Max	9.92	9.22	0.87	8.9	38.7
ES	**Mean**	2.82	2.49	0.29	8.7	31.4
	sd	0.83	0.55	0.09	0.2	2.8
	Min	1.87	1.88	0.21	8.6	28.2
	Max	3.39	2.94	0.40	8.9	33.3
RS	**Mean**	3.52	1.95	0.21	9.0	34.4
	sd	0.69	0.32	0.03	0.4	1.6
	Min	2.99	1.62	0.18	8.7	32.6
	Max	4.30	2.26	0.24	9.4	35.5
Unexposed	**Mean**	1.91	1.47	0.16	8.9	33.3
	sd	0.45	0.57	0.06	0.4	3.6
	Min	1.51	0.90	0.11	8.5	26.7
	Max	2.65	2.36	0.25	9.6	36.8

Table 3s

Mean element concentration, standard deviation (µg/g dw) and coefficients of variation (CV%) for the element content of *Quercus ilex* leaves from VDC and *Elaeagnus x submacrophylla* leaves from Palatine Hill (sites AS and PA)

		Mean	sd	CV%
Fe	**VDC**	604	412	68
	Palatine Hill	269	45	17
Al	**VDC**	743	574	77
	Palatine Hill	238	54	23
Cu	**VDC**	11.8	2.3	19
	Palatine Hill	10.3	2.0	20
Zn	**VDC**	24.9	2.8	11
	Palatine Hill	18.2	4.7	26
Ba	**VDC**	24.9	12.6	51
	Palatine Hill	15.1	5.1	34
Cr	**VDC**	1.53	0.98	64
	Palatine Hill	0.58	0.09	15
Sb	**VDC**	0.29	0.16	53
	Palatine Hill	0.08	0.03	32

Table 4s

Site mean element concentration, standard deviation, minimum and maximum concentration (µg/g dw) in lichen transplants.

Samples		Al	Ba	Cr	Cu	Fe	Sb	Zn
CM	**Mean**	567	20.4	2.10	9.5	669	0.26	30.2
	sd	86	4.3	0.23	0.4	91	0.05	7.7
	Min	502	17.1	1.87	9.3	578	0.22	25.3
	Max	664	25.3	2.33	10.0	759	0.31	39.0
PS	**Mean**	446	17.8	1.78	8.9	565	0.23	25.8
	sd	139	2.8	0.31	1.0	132	0.04	4.9
	Min	290	14.6	1.48	7.9	439	0.20	21.3
	Max	558	20.1	2.10	9.9	702	0.27	31.0
AS	**Mean**	530	26.1	2.59	12.1	797	0.43	34.4
	sd	164	3.0	0.38	1.1	149	0.06	3.1
	Min	396	23.0	2.18	10.7	641	0.36	30.8
	Max	713	29.0	2.92	12.8	938	0.48	36.7
GS	**Mean**	404	15.9	1.61	8.7	504	0.20	38.5
	sd	94	2.9	0.19	0.3	90	0.03	2.4
	Min	315	13.9	1.47	8.4	439	0.16	36.3
	Max	502	19.3	1.83	9.0	607	0.23	41.0

OS	**Mean**	409	18.7	2.08	9.6	574	0.28	
	sd	161	1.4	0.06	1.0	3	0.05	
	Min	291	17.0	2.02	8.5	572	0.22	
	Max	592	19.5	2.13	10.6	578	0.33	28.1
ES	**Mean**	419	12.3	1.34	7.3	409	0.12	22.5
	sd	40	1.0	0.07	0.2	12	0.01	0.3
	Min	384	11.4	1.28	7.1	401	0.11	22.1
	Max	462	13.4	1.41	7.5	423	0.13	22.7
RS	**Mean**	651	15.3	1.96	8.2	631	0.15	26.1
	sd	221	1.5	0.23	0.2	110	0.01	2.7
	Min	462	13.7	1.70	7.9	524	0.13	23.0
	Max	895	16.6	2.14	8.3	744	0.16	28.0
Unexposed	**Mean**	511	12.0	1.73	7.9	431	0.12	23.8
	sd	212	1.2	0.46	1.3	61	0.01	3.0
	Min	272	10.6	1.30	6.8	345	0.10	19.0
	Max	820	13.2	2.54	10.1	525	0.13	27.8

Figure 1s - Full view of the Archaeological Park of the Colosseum and location of the *Olea europaea* L. sampled trees (modified from Google Earth)

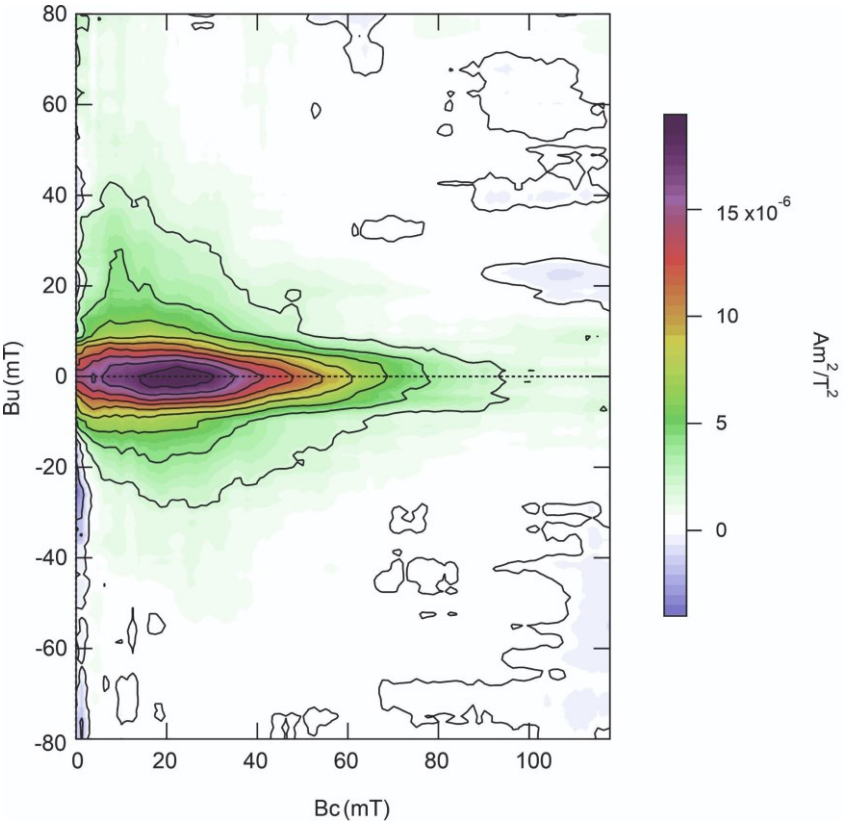

Figure 2s - FORC diagram of *Olea europaea* L.leaves, indicating a prevailing low interaction SD component peaked at ~25 mT

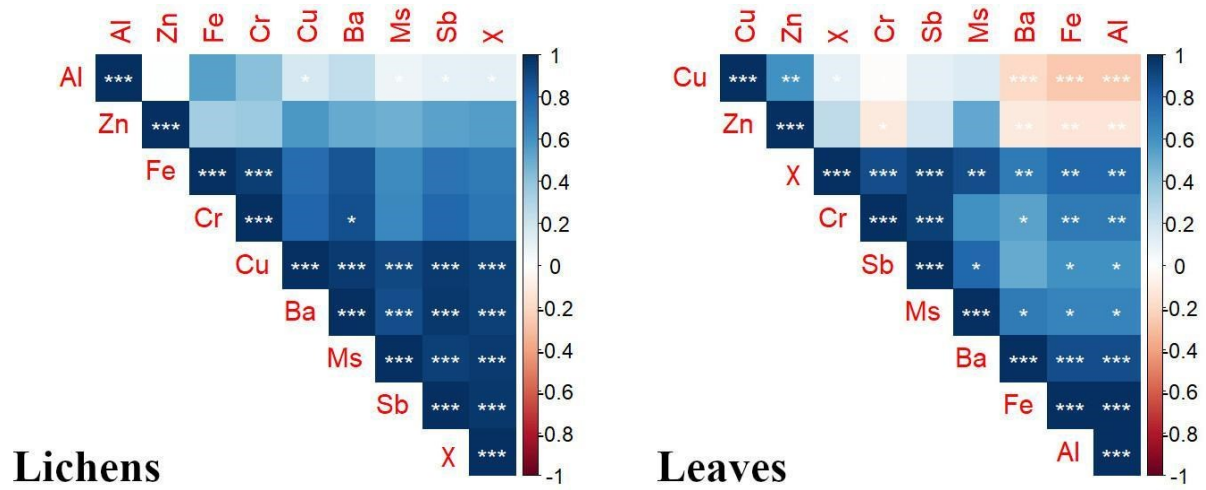

Figure 3s - Correlation matrix of element content, mass specific magnetic susceptibility (χ) and saturation magnetization (Ms). The asterisks indicate statistically significant correlations: *p<0.05, **p<0.01, ***p < 0.001.

Research article:

Science of the Total Environment 946 (2024) 174358

Contents lists available at ScienceDirect

Science of the Total Environment

journal homepage: www.elsevier.com/locate/scitotenv

Nature-based solutions for monitoring the impact of vehicular particulate matter and for the preventive conservation of the Palatine Hill archaeological site in Rome, Italy

Lisa Grifoni [a,b], Aldo Winkler [a,*], Francesca Boldrighini [c], Luigi Antonello Di Lella [b], Alfonsina Russo [c], Antonio Sgamellotti [d], Lilla Spagnuolo [a], Gabriella Strano [c], Stefano Loppi [b]

[a] Istituto Nazionale di Geofisica e Vulcanologia, Rome, Italy
[b] Department of Life Sciences, University of Siena, Italy
[c] Parco Archeologico del Colosseo, Rome, Italy
[d] Accademia Nazionale dei Lincei, Rome, Italy

***All the authors have agreed for the published article to be used as a chapter of this PhD thesis.**

CHAPTER 3

Magnetic and chemical biomonitoring with lichens and vascular plants for the preservation of cultural heritage: A case study at two museums in a megacity (Buenos Aires, Argentina)

Abstract

Magnetic and chemical biomonitoring was applied at Museo Nacional de Bellas Artes and Museo Histórico Nacional, two museums facing busy roads in Buenos Aires, Argentina. Plant leaves (*Jacaranda mimosifolia* and *Fraxinus americana*) and lichens (*Evernia prunastri*) were sampled and transplanted, respectively, from November 2022 to March 2023 for assessing the diffusion of vehicular metallic particulate matter (PM) and potentially toxic elements (PTEs) inside the museum's halls. The magnetic properties of leaves and lichens, deduced from magnetic susceptibility values, hysteresis parameters and first-order reversal curve (FORC) diagrams, were compared to the concentration of PTEs (Al, Ba, Cd, Cr, Cu, Fe, Mn, Sb and Zn), showing that most of outdoor metallic PM was sourced from vehicular brake abrasion and did not bioaccumulate inside the museums. Lichens confirmed to be reliable biomonitors of airborne PM. PTEs were accumulated in higher concentration by *J. mimosifolia* with respect to *F. americana* leaves, thus providing more efficient and sustainable nature-based solutions for the preventive conservation of cultural heritage.

1. Introduction

The degradation of urban air quality prompts for improved conservation of cultural heritage. The increasing exposure of museums, collections and archaeological sites to air pollutants is exacerbated by vibrations, deposition of organic and inorganic contaminants and biological degradation (Mitsos et al., 2022; Comite et al., 2019). In urban settlements, vehicular traffic is the main source of particulate matter (PM), which is the main contributor to the deterioration of artistic surfaces (Vidal et al., 2019). PM, which is composed of carbonaceous and metal-rich particles, causes corrosion due to its hygroscopicity and is the main cause of surface darkening (Mitsos et al., 2022). In urban settlements, air pollution monitoring by chemico-physical equipment is usually carried out in high-traffic areas and rarely involves cultural heritage. Monitoring with living organisms (biomonitoring) is a very flexible and cost-effective tool to evaluate the deposition patterns of air pollutants such as PM and to obtain

information on their biological effects. Moreover, biomonitoring is very useful in areas not covered by conventional monitoring networks. Traditional monitoring methods often face significant limitations - especially in cultural heritage contexts - due to the high cost of technological equipment, limited power availability, ongoing maintenance requirements and reduced practicality in both field and indoor applications. Biomonitoring is a nature-based solution, i.e. a natural tool to address societal challenges, including air pollution, providing ecosystem services. In the context of cultural heritage protection, lichen and plant leaves offer promising and low-impact approaches to monitor and mitigate the effects of air pollution. Lichen transplants, exposed in both indoor and outdoor environments, reveal differences in pollutant accumulation, while the canopies of vascular plants are effective in intercepting and capturing particulate matter that may pose a threat to artworks. Indeed, lichens have a long history as biomonitors of air pollutants (Loppi et al., 1998) and the potential of different plant species to capture atmospheric contaminants has been the subject of several studies (Dzierzanowski et al., 2011; Mori et al., 2015). In recent years, chemical and magnetic biomonitoring using lichens and plant leaves has been employed for the preventive conservation of cultural heritage. In these studies, samples of the lichen *Evernia prunastri* collected from a remote unpolluted area were exposed outside and inside museums (Winkler et al., 2022; Grifoni et al., 2024a) or archaeological sites (Grifoni et al., 2024b). The characterization of magnetic particles along with the measurement of lichens' chemical composition highlighted that non-exhaust emissions from vehicles are usually the main source of metallic PM in the air and have demonstrated that magnetic susceptibility is especially suited for discriminating outdoor and indoor environments, even in cases of missing vehicular traffic contribution such as in Venice (Grifoni et al., 2024a). Moreover, the results of these studies indicated that plant leaves accumulate both the diffused and resuspended components of PM, thus limiting their adverse effects, while lichens are better biomonitors of the airborne component alone (Grifoni et al., 2024b). The aim of this study was to estimate the exposure to metallic PM and potentially toxic elements (PTEs) of artworks exhibited in two national museums in Buenos Aires, one of South America's largest megacities, where vehicle traffic is the main cause of poor air quality (Accorinti et al., 2023). Our hypothesis was that there is a significant difference in the chemical and magnetic properties of lichens between outdoors and indoors. Moreover, the analysis of leaves from local trees aimed at selecting the most suitable plant species offering ecosystem services in terms of green barrier trapping airborne PM and PTEs for the preventive conservation of cultural heritage.

2. Materials and methods

2.1. Study sites

This study was performed in parallel at two museums of Buenos Aires, both located in the eastern area of the city and facing busy roads with different densities of vehicular traffic (Fig. 1). The Museo Nacional de Bellas Artes (MNBA), located in the historical neighborhood of Recoleta, exhibits numerous masterpieces from the Middle Ages to present by Argentinian and international artists, and hosts temporary exhibitions and events. This building overlooks the Avenida del Libertador, a busy six-lanes boulevard, in the south-west direction, and is surrounded by green areas. The most widespread tree species in this area is *Jacaranda mimosifolia* D. Don. The Museo Histórico Nacional (MHN) dates to the XIX century and was founded in the neighborhood of San Telmo, where Buenos Aires originated. After being employed for different purposes, it was converted into a museum in 1897, and nowadays exhibits important Argentinian historical masterpieces, an archive, a library and an education area. The museum is surrounded by a park on its North, East and South sides, and by Defensa street on its West side, where *Fraxinus americana* L. trees are present. Defensa street is narrower than Avenida del Libertador and experiences heavy traffic jams from cars and buses.

2.2. Lichen exposure

Based on past experience, it was preferred using the same lichen species, *Evernia prunastri* (L.) Ach., already used in similar studies (Winkler et al., 2022; Grifoni et al., 2024b), even if not spontaneously present in South America, to allow direct comparison and owing to its well-known ability to accumulate airborne particles and PTEs (Loppi et al., 1998; Loppi and Paoli, 2015). Lichen thalli were collected from a remote area, far from any local source of air pollution, in the province of Siena (Italy) from tree branches at a minimum of 1.5 m from ground, selecting samples larger than 5 cm. Samples were roughly cleaned removing pieces of barks, other lichens or mosses and invertebrates embedded. The transplants, each of about 2 g, were wrapped in plastic nets (lichen bags), and bound at the two ends. Lichen bags were exposed in triplicate, both inside and outside of the two museums (Table 1, Fig. 1), and three unexposed samples were stored for later analysis as controls. The exposure lasted three months, from late November 2022 to early March 2023. At MNBA, two indoor sites consisted of three lichen bags located at the Entrance Hall (EH) and at Badii Hall (BH). One more site consisted of lichen bags placed over the frames of renowned paintings by Paul

Gauguin and Édouard Manet at Impressionist Hall (IH). Outdoors, lichen bags were tied to *J. mimosifolia* trees at different distances from the facade of the museum (10, 35 and 65 m; sites MU, OP and PK, respectively) and at the external frames of the windows (EW). At MHN, one site consisted of lichen bags over paintings depicting historical figures (H_1) and two more sites (H_2, H_3) were set near historical relics such as the Poncho of the dignitary José de San Martín. Outdoors, lichen bags were tied to the external frames of the museum windows facing Defensa street (EW) and to *F. americana* trees at both sidewalks (OP, MU).

Table 1. Exposure sites at the Museo Nacional de Bellas Artes (MNBA) and the Museo Histórico Nacional (MHN).

Museum	Site	Biomonitor	Distance from the interface museum/road	Acronym
MNBA	urban park	*E. prunastri* - *J. mimosifolia*	65 m outdoor	PK
MNBA	opposite side museum	*E. prunastri* - *J. mimosifolia*	35 m outdoor	OP
MNBA	roadside museum	*E. prunastri* - *J. mimosifolia*	10 m outdoor	MU
MNBA	external windows museum	*E. prunastri*	0 m outdoor	EW
MNBA	Entrance Hall	*E. prunastri*	5 m indoor	EH
MNBA	Badii hall	*E. prunastri*	10 m indoor	BH
MNBA	Impressionist hall	*E. prunastri*	15 m indoor	IH
MHN	opposite side museum	*E. prunastri* - *F. americana*	15 m outdoor	OP
MHN	roadside museum	*E. prunastri* - *F. americana*	3 m outdoor	MU
MHN	external windows museum	*E. prunastri*	0 m outdoor	EW
MHN	Hall_1	*E. prunastri*	2 m indoor	H_1
MHN	Hall_2	*E. prunastri*	3 m indoor	H_2
MHN	Hall_3	*E. prunastri*	3 m indoor	H_3

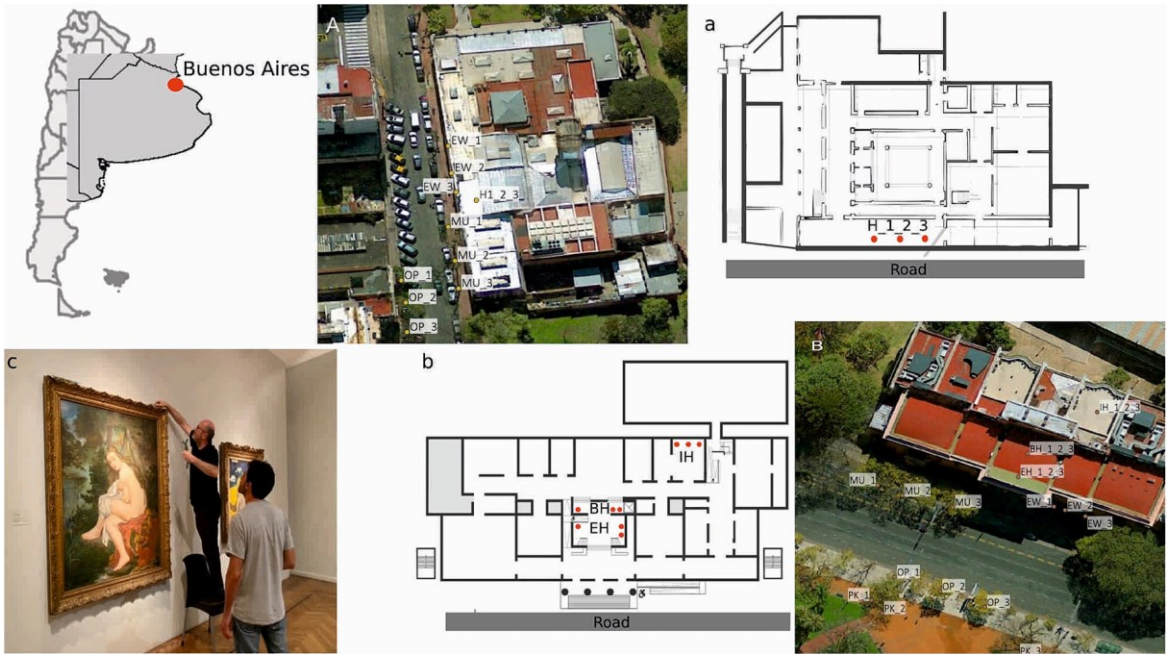

Fig. 1. (A) Museo Histórico Nacional and (a) indoor exposure sites; (B) Museo Nacional de Bellas Artes and (b) indoor exposure sites. Lichen bag placed over the frame of ´Edouard Manet's "La Ninfa Sorprendida" at MNBA (c). The aerial views in (A) and (B) are modified from Google Earth (scale 1:400).

2.3. Leaf sampling

At each outdoor site where lichen bags were tied, 3 trees (*J. mimosifolia* at MNBA and *F. americana* at MHN) were randomly selected. Leaf sampling occurred twice: when lichen bags were deployed (late November 2022) and when they were retrieved (early March 2023). Leaves were randomly collected at least 2 m from the ground, air-dried and stored in paper bags until analysis. Overall, the sampling and exposure activities started on 29 November 2022 and ended on 8 March 2023.

2.4. Magnetic analysis

Leaf and lichen samples were dried in a plastic desiccator at 40 °C and tested for magnetic susceptibility and hysteresis measurements. The mass and volume magnetic susceptibilities (χ and k, respectively) were determined with an Agico KLY5 meter applying a magnetic field of 400 A/m (1220 Hz) and placing the samples inside 8 cm^3 paleomagnetic plastic cubes. The hysteresis properties, such as the coercive force (Bc), the remanence coercivity (Bcr), the saturation remanent magnetization by mass (Mrs or SIRM) and the saturation magnetization by mass (Ms) were measured on sample fragments placed in pharmaceutical gel caps #4 with

a vibrating sample magnetometer (VSM Lakeshore 8604) at a maximum field of 1.0 T and calculated subtracting the high field paramagnetic linear trend before dividing the magnetic moments for the net weight of the samples. The coercivity of remanence (Bcr) values were interpolated from backfield remagnetization curves up to - 1 T, after saturating at 1 T field. The domain state and magnetic grain-size of the samples were compared to theoretical magnetite according to the hysteresis ratios Mrs. / Ms. vs. Bcr / Bc in the "Day plot" (Day et al., 1977; Dunlop, 2002a; Dunlop, 2002b). First-order reversal curve (FORC) diagrams were used for delineating the distribution of the interaction field (Bu) and coercivity in selected samples, to disentangle the single domain (SD), multidomain (MD) and pseudo-single domain/vortex (PSD/V) behaviors (Pike et al., 1999; Roberts et al., 2000). FORCs were measured at steps of 2.5 mT, with 300 ms averaging time and maximum applied field 1.0 T. The diagrams were processed, Variforc smoothed (up to 10 at the ridges and up to 12 for the background) and drawn with the FORCINEL 3.08 Igor Pro routine (Harrison and Feinberg, 2008).

2.5. Chemical analysis

Leaf and lichen samples were homogenized and 250 mg were acid digested with a mixture of 3 mL HNO_3 (70 %), 0.2 mL HF, and 0.5 mL H_2O_2 in a microwave digestion system (Ethos 900, Milestone, Bergamo, Italy). PTEs, namely Al, Ba, Cd, Cr, Cu, Fe, Mn, Sb and Zn were detected by ICP-MS (NexION 350×, Perkin Elmer, Waltham, MA, USA). The analytical quality was checked using procedural blanks and the certified reference materials, Lichen "IAEA 336", Poplar leaves "GBW 07604" and Bushes and leaves "GBW 07603".

2.6. Statistical analysis

To disentangle the effect of indoor preservation on the accumulation of PTEs by lichens, as well as to select the most suitable plant species for the protection of cultural heritage from PTEs, linear mixed-effects model (LMEM) was fitted for each PTE and magnetic susceptibility with indoor/outdoor or plant species as fixed factor and museum and/or site as random factors. Significance of the models was checked with type II Anova (analysis of deviance) using the Wald chi-square test. Correlations between elements and magnetic parameters were tried using the Spearman correlation coefficient. All calculations were run using the R software (R Core Team, 2025).

3. Results

Mean χ values and the concentrations of PTEs measured in lichen transplants and leaf samples are reported in Table 2and Table 3, respectively. LMEM analysis (Table 4) showed that both χ and the concentration of all PTEs analyzed except Al are significantly higher outdoors, and that *J. mimosifolia* showed significantly higher values than *F. americana* for χ and PTEs, except for Ba and Mn.

3.1. Magnetic properties

3.1.1. Lichens

The baseline unexposed mean (±SD) mass magnetic susceptibility (χ) was relatively low (0.9±0.2 $\times 10^{-8}$ m^3 kg^{-1}), as were Ms. (1.19 ±0.09 mAm^2 kg^{-1}) and Mrs. (0.18±0.02 mAm^2 kg^{-1}). The unexposed coercivities were Bc =10.3±0.5 mT and Bcr =27.6±2.4 mT. After three months of outdoor exposure at MNBA, lichen transplants showed a remarkable accumulation of magnetic particles (Table s1), with χ in the range 2.67 $\times 10^{-8}$ m^3 kg^{-1} to 16.0 $\times 10^{-8}$ m^3 kg^{-1} and a mean (±SD) value of 13.3±3.9 $\times 10^{-8}$ m^3 kg^{-1}. The highest χ value was measured in the lichens exposed at the two sides of the road (15.1±8.1 $\times 10^{-8}$ m^3 kg^{-1} at OP and 16.0±4.5 $\times 10^{-8}$ m^3 kg^{-1} at MU and dropped to 2.7±0.4 $\times 10^{-8}$ m^3 kg^{-1} (6 times lower) at just 10 m away from the road, for the transplants tied to the museum windows. For indoor samples, χ ranged from 0.8±0.1 $\times 10^{-8}$ m^3 kg^{-1} to 1.3±0.1 $\times 10^{-8}$ m^3 kg^{-1} with a mean (±SD) value of 1.1±0.3 $\times 10^{-8}$ m^3 kg^{-1}. Mean (±SD) values of 1.3±0.3 and 11.9±6.9, respectively for indoor and outdoor samples, emerged when χ values are expressed as exposed/unexposed ratios. After three months of outdoor exposure at MHN, lichen transplants showed a remarkable accumulation of magnetic particles (Table s2), with mean (±SD) χ values in the range 5.2±0.1 $\times 10^{-8}$ to 17.4±0.2 $\times 10^{-8}$ m^3 kg^{-1} (MU >OP >EW) and a mean (±SD) value of 10±6 $\times 10^{-8}$ m^3 kg^{-1}. For indoor samples, χ showed a mean (±SD) value of 0.9±0.3 $\times 10^{-8}$ m^3 kg^{-1}. Mean (±SD) values of 1.1±0.4 and 11.3±6.5, respectively for indoor and outdoor samples, emerged when χ values are expressed as exposed/unexposed ratios.

3.1.2. Plant leaves

Magnetic susceptibility of *J. mimosifolia* ranged from 3.6±1.6 ×v to 17±4 $\times 10^{-8}$ m^3 kg^{-1}, with a mean (±SD) value of 10 ±8 $\times 10^{-8}$ m^3 kg^{-1} for the leaves sampled in November 2022 and from 19±2 $\times 10^{-8}$ m^3 kg^{-1} to 31±9 $\times 10^{-8}$ m^3 kg^{-1}, with a mean (±SD) value of 25±8 $\times 10^{-8}$ m^3 kg^{-1} for the leaves collected in March 2023 (Tables s3 and s4). In both samplings, the highest χ values were measured at the roadside sites. At OP_MNBA χ was 17.4±2.0 $\times 10^{-8}$ m^3 kg^{-1} in November and 30.7±5.0 $\times 10^{-8}$ m^3 kg^{-1} in March, whereas at MU_MNBA χ was 9.5 ±5.0 $\times 10^{-8}$ m^3 kg^{-1} in November and 24.2±5.0 $\times 10^{-8}$ m^3 kg^{-1} in March (Fig. 2). The hysteresis loops were always saturated before 1.0 T. Leaves collected in November showed a mean (±SD) Ms. of 7.9±1.8 mAm^2 kg^{-1} and a mean (±SD) Mrs. of 0.5±0.1 mAm^2 kg^{-1}, with the highest values for the samples from OP (Ms. =13.8±2.4 mAm^2 kg^{-1} and Mrs. =0.92 ±0.1 mAm^2 kg^{-1}); in March, mean (±SD) Ms. was 19.3±2.1 mAm^2 kg^{-1} and mean (±SD) Mrs. was 1.2±0.1 mAm^2 kg^{-1}: Ms. increased by 144 % and Mrs. by 133 % from November 2022 to March 2023.

Table 2

Exposed to Unexposed (EU) ratios of trace element concentrations in lichen transplants at each exposure site. Different letters indicate statistically signifi- cant differences ($p < 0.05$) among sites.

Site		Al	Ba	Cd	Cr	Cu	Fe	Mn	Sb	Zn	χ
MNBA	**Unexposed**	468 ± 19	12.0 ± 1.8	0.05 ± 0.00	1.4 ± 0.3	5.7 ± 0.4	496 ± 109	27 ± 2	0.06 ± 0.01	27 ± 3	0.09 ± 0.02
	IH	499 ± 65	11.0 ± 1.5	0.05 ± 0.01	1.4 ± 0.1	5.6 ± 0.1	508 ± 17	24 ± 2	0.08 ± 0.00	20 ± 3	0.13 ± 0.01
	BH	478 ± 41	11.0 ± 1.5	0.06 ± 0.02	1.4 ± 0.1	6.0 ± 0.2	476 ± 80	26 ± 2	0.07 ± 0.00	18 ± 1	0.08 ± 0.01
	EH	386 ± 30	10.6 ± 0.7	0.06 ± 0.00	1.2 ± 0.1	5.6 ± 0.1	503 ± 125	27 ± 3	0.08 ± 0.01	20 ± 2	0.13 ± 0.03
	EW	421 ± 50	13.2 ± 0.4	0.13 ± 0.08	1.3 ± 0.1	6.2 ± 0.5	468 ± 50	28 ± 5	0.11 ± 0.02	30 ± 15	0.27 ± 0.04
	MU	603 ± 111	28.3 ± 4.4	0.55 ± 0.18	3.5 ± 0.7	9.9 ± 0.4	1247 ± 173	44 ± 6	0.48 ± 0.07	47 ± 5	1.6 ± 0.45
	OP	426 ± 101	24.0 ± 7.9	0.30 ± 0.15	2.6 ± 0.8	9.4 ± 2.3	911 ± 271	42 ± 7	0.47 ± 0.27	39 ± 13	1.51 ± 0.81
	PK	437 ± 111	18.6 ± 2.3	0.21 ± 0.04	2.2 ± 0.4	7.7 ± 0.3	800 ± 184	34 ± 3	0.27 ± 0.04	33 ± 3	0.89 ± 0.08
MHN	**H_1**	497 ± 94	11.2 ± 1.3	0.06 ± 0.02	1.5 ± 0.2	5.9 ± 0.4	539 ± 93	25 ± 1	0.08 ± 0.00	20 ± 2	0.11 ± 0.03
	H_2	485 ± 105	10.2 ± 1.6	0.05 ± 0.02	1.4 ± 0.3	5.6 ± 0.3	489 ± 128	25 ± 3	0.07 ± 0.01	35 ± 42	0.09 ± 0.04
	H_3	394 ± 34	20.1 ± 0.4	0.09 ± 0.03	1.8 ± 0.2	12.2 ± 6.4	643 ± 96	30 ± 2	0.18 ± 0.01	69 ± 43	0.08 ± 0.03
	EW	394 ± 9	20.1 ± 2.6	0.09 ± 0.01	1.8 ± 0.1	12.2 ± 0.3	643 ± 8	31.0 ± 2	0.18 ± 0.06	69 ± 2	0.52 ± 0.02
	MU	452 ± 15	39.1 ± 4.6	0.13 ± 0.01	2.8 ± 0.1	8.5 ± 0.6	1111 ± 14	49 ± 3	0.57 ± 0.10	50 ± 4	1.74 ± 0.31
	OP	423 ± 10	25.5 ± 0.6	0.12 ± 0.02	2.1 ± 0.1	7.5 ± 0.4	790 ± 21	42 ± 6	0.21 ± 0.01	45 ± 13	0.78 ± 0.02

Table 3

Mean concentration (±SD, N=3) of PTEs (µg/g) and magnetic susceptibility (χ, $10^{-8}m^3kg^{-1}$) in leaf samples of *Jacaranda mimosifolia* at 3 sites (OP, MU, PK) at MNBA and *Fraxinus americana* at 2 two sites (OP, MU) at MHN.

PTE	*J. mimosifolia*						*F. americana*			
	OP		MU		PK		OP		MU	
Fe	1041	± 227	1001	± 151	820	± 57	300	± 25	239	± 41
Al	299	± 119	298	± 89	354	± 97	165	± 49	118	± 12
Mn	55.0	± 7.8	48.2	± 10.3	34.0	± 0.2	41.7	± 2.5	38.7	± 24.4
Cu	16.7	± 1.3	19.4	± 2.3	15.0	± 0.8	8.2	± 1.2	10.2	± 3.7
Zn	41	± 6	47	± 3	38	± 2	19.5	± 1.1	22.3	± 7.7
Ba	30	± 3	31	± 4	22	± 2	25.8	± 4.1	14.9	± 10.1
Cr	3.41	± 0.70	3.03	± 0.45	2.59	± 0.06	0.79	± 0.06	0.65	± 0.05
Cd	0.40	± 0.15	0.45	± 0.07	0.27	± 0.02	0.02	± 0.00	0.02	± 0.01
Sb	1.00	± 0.08	0.79	± 0.11	0.62	± 0.03	0.29	± 0.05	0.15	± 0.03
χ	30	± 9	20	± 8	20	± 2	6	± 1	5	± 2

Table 4

LMEM results of magnetic susceptibility (χ, 10^{-8} m^3kg^{-1}) and concentration of PTEs (µg/g) of outdoor-indoor lichen transplants (lichen) and *J. mimosifolia* and *F. americana* leaves (leaf) (* = p<0.05, ** = p<0.01, *** = p<0.001)

		Al	Ba	Cd	Cr	Cu	Fe	Mn	Sb	Zn	χ
lichen	Estimate	-26.1	13.7	0.2	0.94	3.02	352.1	13.4	0.25	21.08	9.26E-08
	SE	28.20	2.02	0.1	0.19	0.84	71.03	2.1	0.047	7.36	2.30E-08
	p-value	> 0.05	***	**	***	***	***	***	***	**	***
leaf	Estimate	157	9.9	0.4	2.5	8.9	751	11.4	0.7	23	2.2
	SE	69	5.4	0.1	0.4	1.7	124	8.7	0.1	3.7	0.35
	p-value	*	> 0.05	***	***	***	***	> 0.05	***	***	***

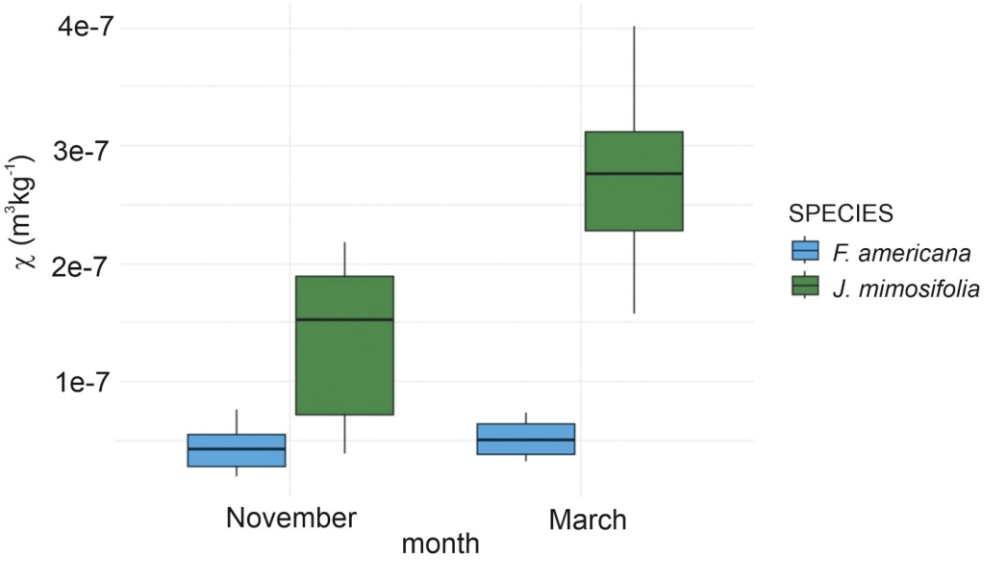

Figure 2. Magnetic susceptibility (χ, m^3 kg^{-1}) of *J. mimosifolia* and *F. americana* leaves in November 2022 and March 2023.

The mean Bc and Bcr were respectively 5.9±0.3 mT and 33.1±1.2 mT in November and 5.6±0.2 mT and 34.5±0.7 mT in March. At MHN, the χ of *F. americana* leaves differed on the two sides of the street in front of the museum. In November, the mean (±SD) χ in MU_MHN was 2.82 ±0.5 × 10^{-8} m^3 kg^{-1} and in OP_MHN 5.45±1.1 × 10^{-8} m^3 kg^{-1}. The leaves collected in March showed a χ of 4.55±1.4 × 10^{-8} m^3 kg^{-1} and 6.34±0.7 × 10^{-8} m^3 kg^{-1} respectively in MU_MHN and OP_MHN with temporal increases of 38% in MU and 14 % in OP_MHN. The leaves collected in November showed a lower mean (±SD) Ms. (2.3±0.4 mAm^2 kg^{-1}) and Mrs. (0.20±0.08 mAm^2 kg^{-1}) in MU compared to the mean observed in OP (Ms = 4.0±1.0 mAm^2 kg^{-1} and Mrs. = 0.3±0.0 mAm^2 kg^{-1}). The average values of Bc and Bcr, for the leaves collected in November, in MU_MHN were 7.2±1.8 mT and 29.0±4.2 mT respectively for Bc and Bcr, by the other side of the road, in OP_MHN, they were 6.5±1.2 mT and 31.0±6.4 mT respectively. In March, the averaged Ms. and Mrs. showed similar values after three months, notably in MU_MHN 2.9±0.0 mAm^2 kg^{-1} and 0.20±0.01 mAm^2 kg^{-1}, and in OP_MHN 4.1±0.1 mAm^2 kg^{-1} and 0.20±0.1 mAm^2 kg^{-1} for Ms. and Mrs. respectively. The mean values of Bc and Bcr were comparable after three months, namely 8.2±2.3 mT and 30.8±2.7 mT in MU_MHN and 6.6±0.5 mT and 34.6±3.3 mT, respectively in OP_MHN. Outdoors, lichen transplants accumulated similar amounts of magnetic particles at the two museums, and these values were higher than those in *F. americana* leaves at MHN, and lower than those in *J. mimosifolia* leaves at MNBA (Fig. 3).

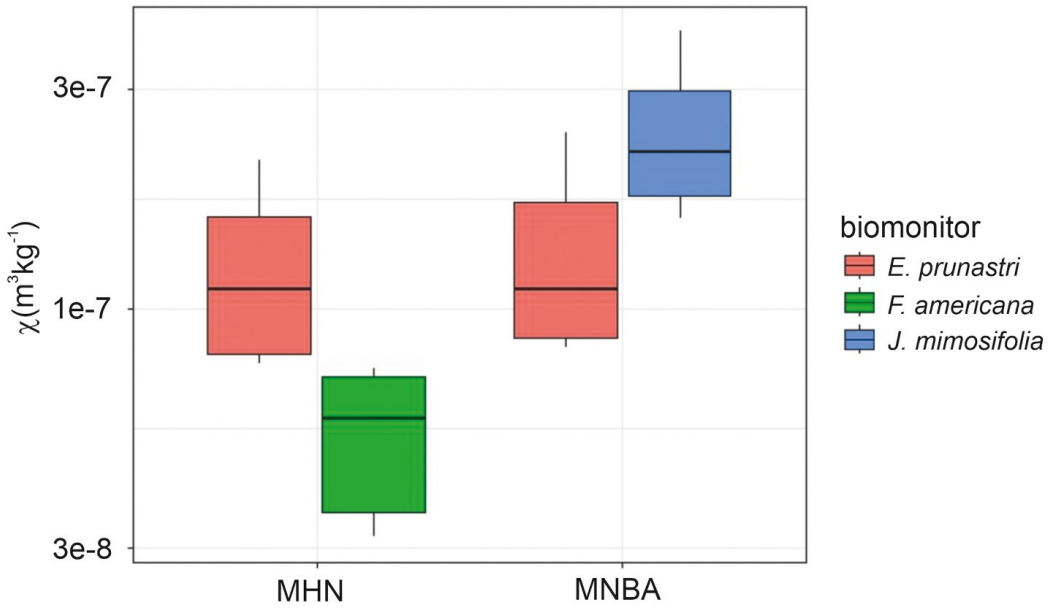

Figure 3. Magnetic susceptibility of the lichen *E. prunastri* (outdoor sites), *J. mimosifolia* and *F. americana* leaves at each museum (data from March 2023).

3.1.3. Magnetic grain-size of leaves and lichens

Ms. and χ are highly correlated for both lichens and leaves ($r > 0.90$, $p < 0.05$) showing that the gel caps used for the determination of hysteresis parameters were representative of the whole sample and that magnetic susceptibility and concentration dependent hysteresis parameters were carried by the same magnetic minerals. In the "Day plot", the site means progressively and roughly linearly shift from the central PSD region of the diagram for the indoor and the unexposed samples towards the low-right multidomain (MD) side of the plot for the outdoor lichens and leaves (Fig. 4).

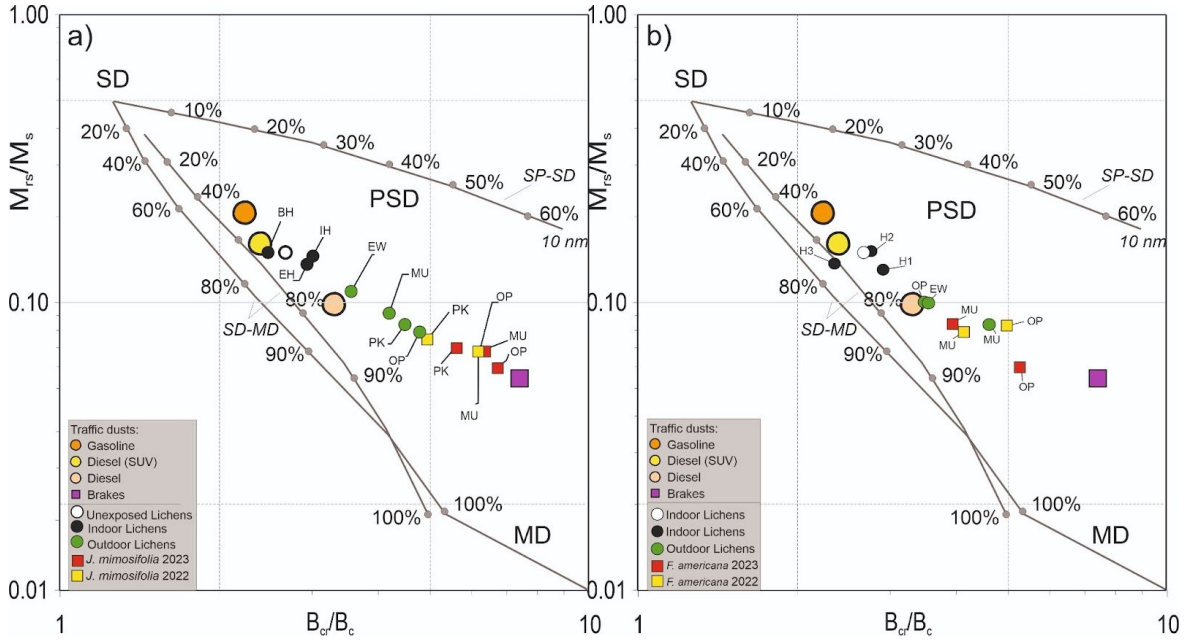

Figure 4. Biologarithmic "Day Plot" of the site mean ratios for lichens and *Jacaranda mimosifolia* leaves (MNBA - a) as well as lichens and *Fraxinus americana* leaves (MHN - b), along with the average points of fuel (orange, yellow and pink circles) and brake dust emissions (purple square) calculated from Sagnotti et al. (2009). The SD (single domain), PSD (pseudo-single domain) and MD (multidomain) fields and the theoretical mixing trends for SD-MD and SP-SD pure magnetite particles (SP, superparamagnetic) are from Dunlop (2002a, 2002b).

FORC diagrams reflected the same trend of the "Day plot": MD features prevailed for the OP outdoor lichen samples at both museums (Fig 5 a, c), shifting to prevalent low coercivity PSD/vortex magnetic components for the lichens exposed indoors (Fig. 5 b, d).

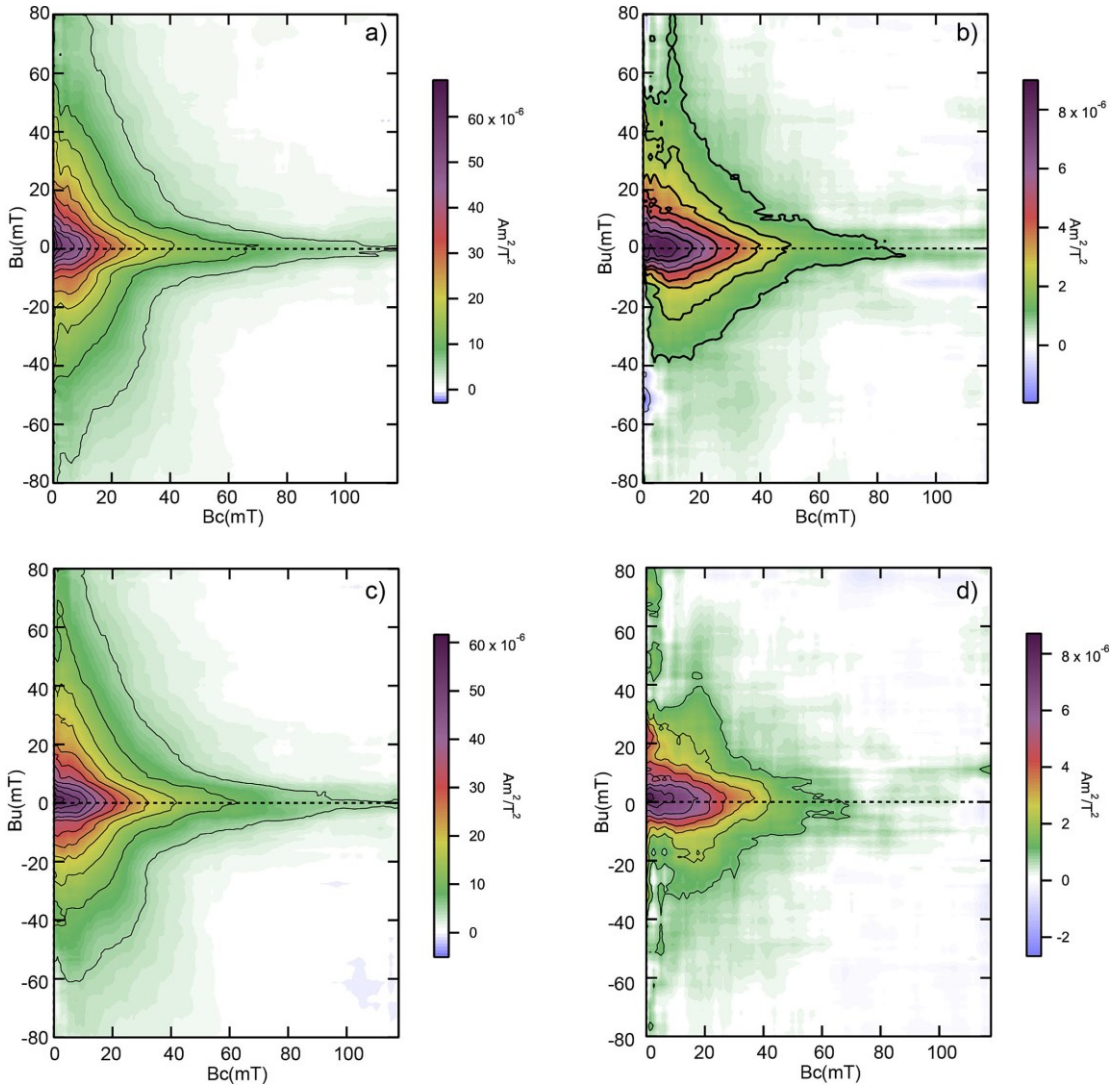

Figure 5. FORC diagrams for selected leaf and lichen samples. MNBA: (a) *Jacaranda mimosifolia* leaves sampled at the opposite side of the street (OP); (b) lichen bag at the entrance hall (EH). MHN: (c) *Fraxinus americana* leaves sampled at the opposite side of the street (OP); (d) lichen bag at the Hall 1 (H1).

3.2. Bioaccumulation of PTEs

3.2.1. Lichen samples

At both museums, lichen transplants exposed outdoors accumulated all PTEs but Al, while concentrations in lichen transplants exposed indoors were similar to unexposed samples, with slightly higher Cd and Sb values also indoors (Table 5). It is noteworthy that samples exposed just outdoors, at the external windows (EW), overall showed concentrations comparable to indoor and unexposed samples, with the notable exceptions of Cd and Sb, which were

intermediate between outdoors and indoors (Table 5). For these latter elements, at MNBA the exposed-to-unexposed (EU) ratios of outdoor stations (PK, OP, MU, EW) were on average 5.8±3.5 and 5.5±2.9, respectively, with notable values of 10.7±0.9 for Cd and 7.9±1.5 for Sb at MU. Similarly, average EU ratios of Cd and Sb for outdoor sites (OP, MU, EW) at MHN were 2.2±0.4 and 5.1±3.5, respectively, and notably 2.57 ±0.01 and 9.1±0.1, respectively, at MU (Fig. 6). The majority of PTEs were intercorrelated, with $r > 0.70$, except for Al, that was not correlated with any of the other PTEs. In some cases, correlations were very strong ($r > 0.90$), and also χ was correlated to all PTEs except Al (Fig. 7).

Table 5. Mean (±SD, μg/g) concentration of PTEs in lichen transplant exposed outdoors and indoors at MNBA and MHN.

	MNBA				**MHN**			
	outdoor		indoor		outdoor		indoor	
Al	472	± 88	454	± 60	423	± 29	489	± 23
Ba	21	± 7	11	± 1	28	± 10	11	± 1
Cd	0.30	± 0.18	0.06	± 0.01	0.11	± 0.02	0.06	± 0.01
Cr	2.4	± 0.9	1.4	± 0.1	2.2	± 0.5	1.4	± 0.2
Cu	8.3	± 1.7	5.7	± 0.2	9.4	± 2.5	5.7	± 0.3
Fe	857	± 321	496	± 17	848	± 240	506	± 74
Mn	37	± 8	26	± 2	41	± 9	25	± 1
Sb	0.33	± 0.18	0.08	± 0.01	0.32	± 0.22	0.07	± 0.01
Zn	38	± 8	19	± 1	55	± 13	30	± 20

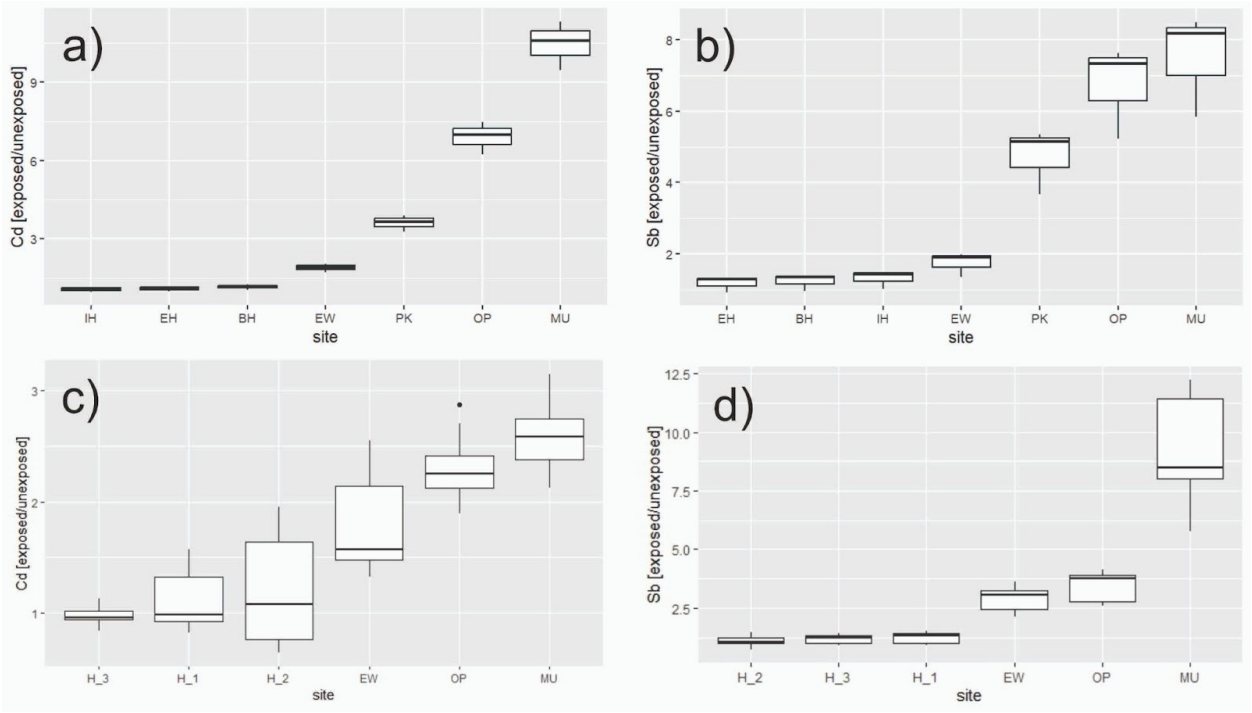

Figure 6. Lichen exposed-to-unexposed ratios for Cd and Sb at each site of MNBA (a, b) and Cd and Sb from MHN (c, d).

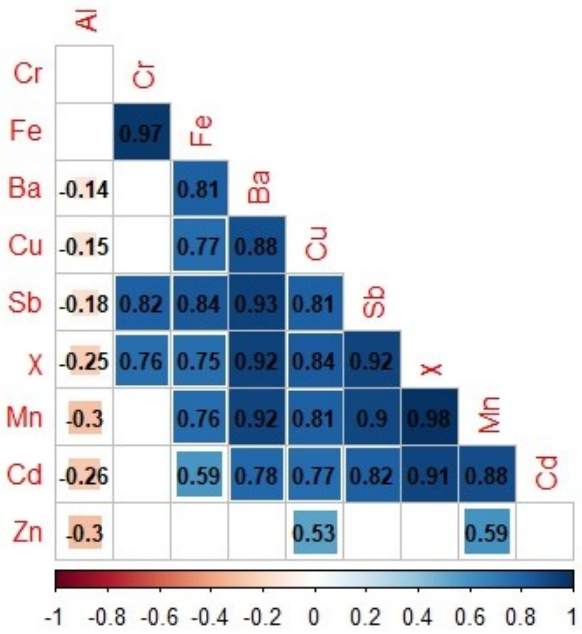

Figure 7. Correlation between PTEs and χ expressed as Spearman's rank correlation coefficient.

3.2.2. Leaf samples

Concentrations of PTEs in leaf samples were much higher in *J. mimosifolia* than in *F. americana* (Table 3). Conversely, the concentration of most PTEs, namely Al, Ba, Cd, Cr, Fe, Mn, Zn, in *J. mimosifolia* leaves were not significantly different from those in lichens at the same sites, while Cu and Sb levels were higher in leaves (Fig. 8).

4. Discussion

4.1. Magnetic and chemical properties of lichens

In this study, two museums of Buenos Aires were investigated to monitor their exposure to anthropogenic vehicular particles. Volume magnetic susceptibility values (k) were compared to those in Chaparro (2021). In this study, k values were within the same range of values observed for native lichens (i.e., lichens exposed to pollution during their lifetime) from urban sites of Tandil, a city in the province of Buenos Aires, namely k = 1.46–9.45 × 10^{-5} SI (Chaparro, 2021). Indeed, after three months, MNBA lichens' k was 2.11±0.1 × 10^{-5} SI at MU and 2.05 ±0.2 × 10^{-5} SI at OP; on the other hand for MHN lichens, k was 3.25 ±0.1 × 10^{-5} SI at MU and 1.35±0.03 × 10^{-5} SI at OP. Following the characterization of Chaparro (2021), lichens exposed three months in both areas evidenced a slightly polluted area (k = 1.10–2.79 × 10^{-5} SI), if compared to initial in situ magnetic susceptibility values of *Parmotrema pilosum, Punctelia hypoleucites* and *Dirinaria picta* native lichens whose exposure time was unknown. Regarding mass susceptibility, χ values were similar to those reported along a busy road of Rome using transplants of the same lichen species (Grifoni et al., 2024b). For MNBA, lichen χ was ten times higher than indoor one (statistically significant difference, Mann-Whitney z = 6.5 p = 7.4 × 10^{-11}), whose median was 1.24±0.05 (EU ratio) and it did not deviate significantly from the unexposed samples χ (Mann-Whitney z = 1.74 p = 0.08). On the other hand, the lichens exposed outside of MHN showed χ values approximately eight times higher than indoors (statistically significant difference, Mann-Whitney z = 3.5 p = 0.4 × 10^{-3}) whose χ did not differ significantly from the unexposed samples (Mann-Whitney z = 0.87 p = 0.38). In both study areas, the accumulation of magnetic particles was negligible indoors. The magnetic grain-size trend, qualitatively described by the "Day Plot", highlighted the gradual shifting from the MD coarser grain-sizes outdoors to the central PSD area of the plot indoors, roughly depending on the distance of the samples from the roadside. Such results are consistent with magnetic biomonitoring studies carried out in other Argentinian cities, such

as, in Tandil (province of Buenos Aires, Marié et al., 2016) and in San Salvador de Jujuy (province of Jujuy, Chaparro et al., 2024).

When compared with the average data obtained for fuel and brake emissions sampled in cars' exhaust pipes and wheel rims (Sagnotti et al., 2009; Sagnotti and Winkler, 2012) and recently revised (Letaïef et al., 2024), the outdoor samples - especially leaves - approached the "brake" data points (Fig. 4), consistently with magnetic biomonitoring surveys carried out on lichens transplanted in Milan and Rome, where multidisciplinary analyses pinpointed brake abrasion as the main source of urban PM near busy roads (Winkler et al., 2020; Winkler et al., 2022; Grifoni et al., 2024b). After three months, the points for leaves placed even closer to brake emissions, highlighting a further bioaccumulation of non-exhaust particles. The same results were confirmed by selected FORC diagrams, where the OP leaves showed prevailing MD features (Fig. 5a) with a minor PSD/vortex component (Fig. 5c) and a high coercivity tail extending beyond magnetite coercivities, that may reflect the presence of metallic Fe (Sheikh et al., 2022) and closely resemble those for brake dusts reported by Sagnotti et al. (2009) and Winkler et al. (2020). On the other hand, PSD/vortex components prevail in the noisier FORC distributions of indoor lichens (Fig. 5b and 5d), as a possible consequence of natural magnetic components preexisting to the lichen exposure and finer exhaust fuel emissions emerging when the contribution of brake emissions reduces. Overall, these results are compliant with Gonet et al., 2021, who concluded that non-exhaust vehicle brake wear is the major source of airborne magnetite in traffic-related contexts and estimated that, at the roadside of Lancaster and Birmingham, brake wear contributes 68–85% of the total airborne magnetite in the roadside environment, followed by diesel exhaust emissions (7–12%), petrol exhaust emissions (2–4%) and background dust (6–10%). Magnetite-like minerals dominated the magnetic mineralogy of the samples, which agrees with other magnetic biomonitoring in Argentinian cities, i.e., mean (±SD) Bcr values were 34.2±2.5 mT (Tandil, Marié et al., 2016); 36.3±1.6 mT (La Plata, Castañeda Miranda et al., 2018), 37.0±2.4 mT (Mar del Plata, Chaparro et al., 2020). The magnetite weight percentage fraction (wt%), with respect to the total mass of lichens and leaves was calculated dividing the grainsize independent magnetic parameter Ms. for the saturation magnetization of pure magnetite, Ms. = 90 $Am^2 kg^{-1}$. For lichens, the wt% of magnetite increased 10 and 9-fold with respect to the unexposed samples, respectively for MNBA and MHN at MU sites (Tables s1 and s2). These results were confirmed by chemical analyses. In fact, strong correlations were observed between χ and PTEs, such as Ba, Cd, Cu, Mn, Sb, Zn. Among these PTEs, Ba is used in several compounds

of car engine, brake pads and tires (Monaci and Bargagli, 1997), Cu and Zn are also tracers of exhaust emissions, tire wear and brakes (Steiner et al., 2007; Weckwerth, 2001). Sb compounds are used in the production of brake pads and are released within the fine particulate matter (Amereih et al., 2005; Gómez et al., 2005), similarly, Mn is present in brake pads and some rubber compounds, confirming non-exhaust emissions as the main source of particles (Hjortenkrans et al., 2006; Thorpe and Harrison, 2008). PTEs with the higher accumulation in lichens, i.e. Cd and Sb, are typical tracers of vehicular traffic (Matějka et al., 2011). Their diffusion from the roadside is well shown by the transplants deployed at increasing distances from the main road, particularly at MNBA, where Sb was accumulated in higher amounts at MU and OP and gradually decreased at PK and EW, at about 10 m from the road (Fig. 6b, d). This result is consistent with previous observations where χ values of leaves decreased to a 'magnetic background' level 20–30 m away from high-traffic roads (Szönyi et al., 2008; Winkler et al., 2022). Even if a very low bioaccumulation of Cd and Sb, much likely originated from the external vehicle traffic, was detected in lichen exposed indoors, the accumulation of all PTEs, except Al, was remarkably different from outdoors. These results showed that most magnetic particulate matter or PTEs present outdoors did not accumulate inside the museums.

4.2. Magnetic and chemical properties of leaves

Leaves of two tree species present on the sites MNBA and MHN, *J. mimosifolia* and *F. americana,* respectively, were collected approximately at the beginning of their vegetative phase (in November) and after three months. These species were characterized by an increase of χ values between the samplings of November and March. In particular, *J. mimosifolia* leaves had a significantly higher χ than *F. americana*. The bark of *J. mimosifolia* trunks, tested as magnetic biomonitor in trafficked roads of Lisbon, showed a magnetic susceptibility ($\chi = 33.03 \pm 20.42 \times 10^{-8}$ m^3 kg^{-1}) similar to our observations in leaves collected along the road ($\chi = 24.4 \pm 8.0 \times 10^{-8}$ m^3 kg^{-1}); the highest accumulation has been observed along the road on the opposite side of the museum (OP) with an increase of 43 % for χ. Leaf χ was not significantly correlated with lichen χ at the same sites, as an insignificant correlation was observed ($r = 0.56$, $p > 0.05$). Although *F. americana* leaf has proven to be a good biomonitor of Hg (Siwik et al., 2009) and ozone (Coulston et al., 2003), it has not yet been extensively studied for PM. In Buenos Aires, the bark of a tree species of the same genus, *F. pennsylvanica*, has been tested as biomonitor showing the highest enrichment factors for Cu,

Zn and Ba; the same study reported that Fe and Cu were significantly correlated in road dust samples, further suggesting that Cu derives from non-exhaust traffic emissions (Fujiwara et al., 2011). In the Argentinian city of Mar del Plata (province of Buenos Aires), the species *F. pensylvanica* and *F. excelsior* are urban trees well distributed. Chaparro et al. (2020) proved that tree bark of these species is an efficient biological collector of ubiquitous airborne particles in cities; they reported median χ values of 94.0 and 58.3 $\times 10^{-8}$ m^3 kg^{-1} in 2016 and 2017, respectively. In this study, the leaves of *F. americana* showed an accumulation of magnetic particles with a maximum percentage at MU (38%). At the same sites, leaves's χ was not correlated with lichen's. For both museums, the site MU recorded the highest χ values. At MNBA χ resulted highly correlated with Sb, a typical tracer of brake wear emissions. Wt% of magnetite increased 3.0 and 1.3-folds between November and March, respectively for *J. mimosifolia* and *F. americana* leaves sampled at the MU sites of MNBA (Tables s3 and s4) and MHN (Tables s5 and s6), highlighting a reduction of the bioaccumulation of magnetite 3.3 times for MNBA and 6.9 times for MHN with respect to the lichens exposed in the same time period. In addition to the biomonitor characteristics, this result can be explained by the different Ms. base level of unexposed lichens with respect to leaves that were already present at the sampling sites.

4.3. Comparison between magnetic and chemical properties of lichens and J. mimosifolia leaves

J. mimosifolia and *F. americana* leaves highlighted significantly different χ values (Fig. 3). The χ values of *E. prunastri* showed very similar values between the two investigated museums, thus implying that the different χ values among *J. mimosifolia* and *F. americana* leaves depended on the tree species and not on the site. This aspect was qualitatively confirmed by PM10 concentration data retrieved from "CORDOBA" and "LA BOCA" air quality stations, respectively the closest to MNBA (1.7 km) and MHN (0.4 km). In fact, even if it is improper to compare PM10 daily concentration to long term bioaccumulation data (three-months for lichens, seasonal for leaves), in 2024 they were on average 24.5±0.11 $\mu g/m^3$ and 23.8±0.13 $\mu g/m^3$ for "CORDOBA" and "LA BOCA", respectively, thus implying very similar average concentration of PM10 over the whole area, as consistently suggested by lichen data. This comparison was not possible for the three- month study period due to "CORDOBA data missing up to mid March 2023. The higher magnetic susceptibility values and PTEs accumulation observed in *J. mimosifolia* leaves relative to *F. americana* was likely

driven by species-specific leaf traits. In particular, *F. americana* has larger and thinner leaflets with respect to *J. mimosifolia*, thus resulting in a higher specific leaf area (SLA, ratio of leaf area to leaf biomass) values. In fact, Muhammad et al. (2019, 2022) previously showed with SIRM measurements applied to 96 different plant species that there is a significant and negative (p<0.001) relationship between SLA and PM accumulation. In Hamal et al. (2008), *J. mimosifolia* leaves from trees sampled in different polluted contexts had an average SLA value of 10.4 m^2/kg, with respect to 15.9 m^2/kg for *F. excelsior* in Muhammad, 2019. According to Muhammad et al., 2022, these two species would fall into two different PM accumulation efficiency classes with respect to their SLA values. Moreover, the presence of trichomes and increased surface roughness in *J. mimosifolia* leaves may enhance particle adhesion. In contrast, *F. americana* has smoother leaflets with lower microstructural complexity, limiting PM retention. Differences in cuticular properties and canopy architecture may also contribute to the greater PM accumulation efficiency of *J. mimosifolia*. At MNBA outdoor sites, χ of lichens was significantly lower than that of *J. mimosifolia* leaves (Mann-Whitney test, p <0.05) in March, but the two χ values became similar when considering the net accumulation of magnetic particles by leaves (i.e. subtracting the χ of leaves collected in March from the one of leaves collected in November). Moreover, the differential of wt% of magnetite between unexposed and exposed lichens after three months, as average among the MU and OP sites, was almost the same as that of *J. mimosifolia* leaves collected in November and March (Δwt%lichen =0.011% and Δwt%leaves =0.013%), despite the wt% of magnetite of unexposed lichens (0.001%) was seven times lower than that of leaves collected in November (0.007%). The positioning of *J. mimosifolia* in the Day Plot was more shifted towards the area of brakes with respect to lichens, probably due to pre-existing vehicular components in November 2022 leaves and a slightly higher accumulation of magnetite (+0.002%) in March 2023 samples (Fig. 4). Moreover, PTEs were accumulated in comparable concentrations by leaves of *J. mimosifolia* and *E. prunastri* with the exception of Al, Cu and Sb (Mann-Whitney test, p <0.05) (Fig. 8).

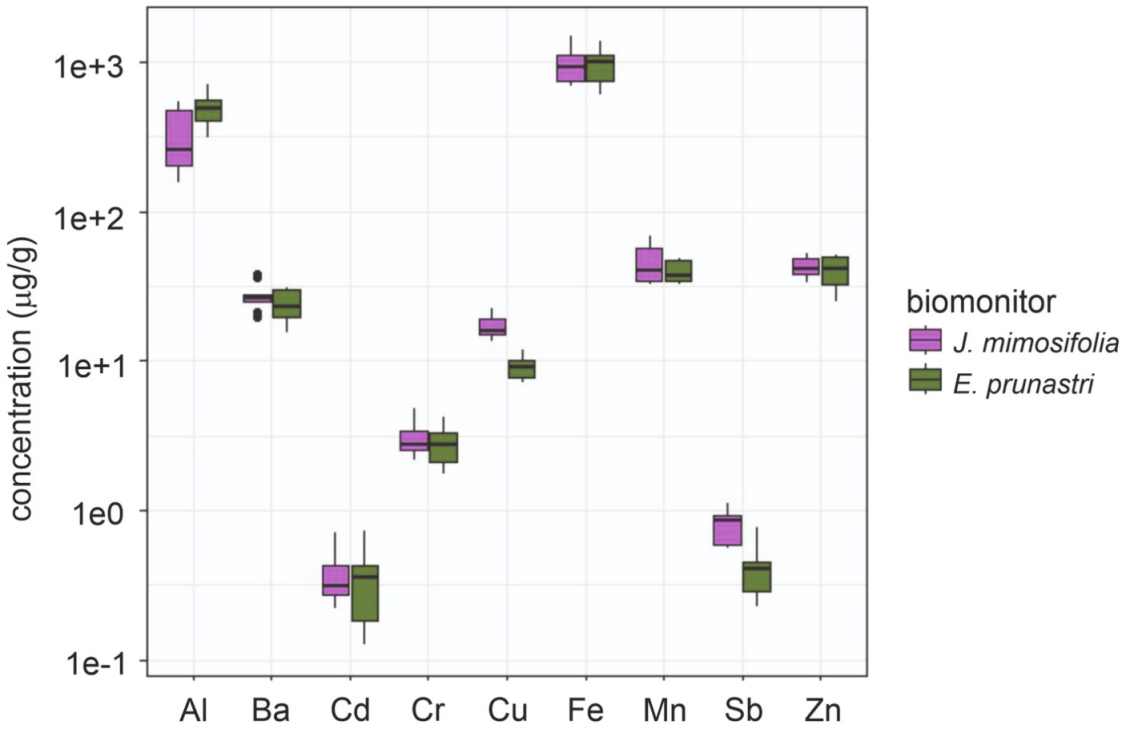

Figure 8. Comparison of the concentration of PTEs in outdoor lichen transplants and *J. mimosifolia* leaves.

Finally, the intense magnetic and chemical properties of *J. mimosifolia* leaves sampled in November suggest a limited removal of vehicular PM due to rainfall events. In fact, this study was preceded by an intense rainfall episode occurring in mid-November (>100 mm). On the other hand, the influence of rainfall was negligible during the lichen exposure, since there were only sparse events, cumulatively <90 mm/month up to late January and reducing to <45 mm/month up to early March.

5. Conclusions

The Museo Histórico Nacional and the Museo Nacional de Bellas Artes of Buenos Aires were selected for the biomonitoring of airborne particulate matter and potentially toxic elements. Lichen transplants and leaves were exposed and sampled for assessing the diffusion of vehicular PM from the busy outdoor roads towards the museum's indoor halls. Outdoors, the use of magnetic and chemical analyses demonstrated that the bioaccumulation of metallic PM depended on the distance from the road and was mainly related to brake emissions, as deduced from the magnetic grain-size and the concentration of elemental tracers as Sb, Cd and Ba. Indoors, the magnetic and chemical properties were similar to those of unexposed samples. Lichen exposure was useful to demonstrate that the outdoor bioaccumulation of

metallic PM was similar at both museum sites. Leaves of *J. mimosifolia* showed a valuable capability of accumulation of PM with respect to those of *F. americana*, thus demonstrating to be an efficient species for the provision of preventive conservation services at cultural heritage sites. This was the first application of a magnetic and chemical biomonitoring approach in museal settings outside Italy. Lichens and leaves demonstrated once again to be complementary for outlining the diffusion of vehicular particulate matter inside museums, expanding the dataset of plant species that are best suited for providing preventive conservation in addition to those already studied in the Mediterranean area.

Appendix – CHAPTER 3

Supplementary Material

Table s1: Magnetic susceptibility (χ), saturation magnetization by mass (Ms), saturation remanent magnetization by mass (Mrs), coercive force (Bc), coercivity of the saturation remanent magnetization (Bcr) and weight percentage of magnetite (wt%) of *E. prunastri* exposed at MNBA and unexposed.

Site		χ	Ms	Mrs	Bc	Bcr	wt
		10^{-8} m^3 kg^{-1}	mAm^2 kg^{-1}	mAm^2 kg^{-1}	mT	mT	%
PK	Mean	8.9	6.9	0.6	7.1	31	0.0077
	SE	0.4	1.2	0.1	0.8	1	0.0013
	Min	8.3	5.5	0.5	5.5	29	0.0061
	Max	9.7	9.5	0.8	8.1	32	0.0106
OP	Mean	15.1	10.6	0.8	6.7	3	0.0118
	SE	8.1	3.9	0.3	0.6	1	0.0043
	Min	2.4	7.4	0.6	6.1	31	0.0082
	Max	8.5	14.9	1.1	7.2	32	0.0166
MU	Mean	16.0	12	1.1	7.4	31	0.0133
	SE	2.6	2.5	0.2	0.4	1	0.0028
	Min	11.0	6.9	0.7	6.8	30	0.0077
	Max	19.9	14.6	1.3	8.1	32	0.0162
EW	Mean	2.7	2.2	0.2	8.1	29	0.0024
	SE	0.2	0.5	0.1	0.8	2	0.0006
	Min	2.5	1.4	0.1	7.1	25	0.0016
	Max	3.1	3.1	0.3	9.7	31	0.0034
EH	Mean	1.3	1.1	0.1	9.5	28	0.0012
	SE	0.2	0.4	0.0	1.1	3	0.0004
	Min	1.1	0.7	0.1	8.4	25	0.0008
	Max	1.5	1.5	0.2	10.5	31	0.0017
BH	Mean	0.8	0.8	0.1	9.7	24	0.0009
	SE	0.0	0.1	0.0	0.2	1	0.0001
	Min	0.8	0.6	0.1	9.4	22	0.0007
	Max	0.8	1.0	0.2	10.1	25	0.0011
IH	Mean	1.3	1.6	0.2	10.2	31	0.0018
	SE	0.1	0.3	0.1	0.2	1	0.0003
	Min	1.2	1.0	0.1	9.9	30	0.0011
	Max	1.5	2.1	0.2	10.5	33	0.0023
unexp	Mean	0.9	1.2	0.2	10.0	28	0.0013
	SE	0.0	0.1	0.0	0.0	1.3	0.0003
	Min	0.8	1.0	0.1	9.9	25	0.0011
	Max	1.1	1.4	0.2	10.1	30	0.0016

Table s2: Magnetic susceptibility (χ), saturation magnetization by mass (Ms), saturation remanent magnetization by mass (Mrs), coercive force (Bc), coercivity of the saturation remanent magnetization (Bcr) and weight percentage of magnetite (wt%) of *E. prunastri* exposed at MHN.

Site		**χ 10^{-8} m^3 kg^{-1}**	**Ms mAm^2 kg^{-1}**	**Mrs mAm^2 kg^{-1}**	**Bc mT**	**Bcr mT**	**wt %**
OP	Mean	9.0	6.1	0.6	8.7	30	0.0068
	SE	0.1	0.6	0.0	0.3	1	0.0007
	Min	7.6	5.1	0.5	8.2	29	0.0057
	Max	8.0	7.2	0.7	9.3	31	0.0080
MU	Mean	17.0	10.0	0.9	7.0	33	0.0111
	SE	1.8	0.7	0.0	0.2	1	0.0008
	Min	15.0	9.5	0.8	6.9	32	0.0106
	Max	21.0	11.7	0.9	7.5	34	0.0130
EW	Mean	5.2	3.9	0.4	9.0	30	0.0043
	SE	0.1	0.3	0.0	0.4	1	0.0003
	Min	5.0	3.5	0.4	7.9	29	0.0039
	Max	5.4	4.3	0.4	8.9	31	0.0048
H_1	Mean	1.1	1.1	0.2	10.0	27	0.0012
	SE	0.2	0.2	0.0	1.1	2	0.0002
	Min	0.8	0.9	0.1	7.37	25	0.0010
	Max	1.3	1.5	0.2	11.2	30	0.0017
H_2	Mean	0.9	1.0	0.1	10.0	26	0.0011
	SE	0.2	0.1	0.0	1.6	1	0.0001
	Min	0.4	0.7	0.1	7.0	25	0.0008
	Max	1.2	1.1	0.2	12.0	28	0.0012
H_3	Mean	0.8	0.8	0.1	10.0	24	0.0009
	SE	0.2	0.2	0.0	0.8	2	0.0002
	Min	0.5	0.3	0.1	9.0	19	0.0003
	Max	1.1	1.1	0.1	11.2	27	0.0012

Table s3: Magnetic susceptibility (χ), saturation magnetization by mass (Ms), saturation remanent magnetization by mass (Mrs), coercive force (Bc), coercivity of the saturation remanent magnetization (Bcr) and weight percentage of magnetite (wt%) of *J. mimosifolia* leaves collected nearby MNBA in November 2022.

Site		**χ 10^{-8} m^3 kg^{-1}**	**Ms mAm^2 kg^{-1}**	**Mrs mAm^2 kg^{-1}**	**Bc mT**	**Bcr mT**	**wt %**
OP	Mean	17.0	14.0	0.9	5.6	35	0.0156
	SE	2.3	1.5	0.9	0.2	1	0.0017
	Min	14.0	9.5	0.7	5.3	34	0.0106
	Max	21.0	17.9	1.2	5.9	36	0.0199
MU	Mean	9.5	6.4	0.4	5.8	35	0.0071
	SE	6.5	3.10	0.2	0.1	1	0.0034
	Min	3.8	3.6	0.2	5.3	33	0.0040
	Max	19.8	11.2	0.7	6.4	38	0.0124
PK	Mean	4.0	3.6	0.3	6.2	29	0.0040
	SE	1.3	1.1	0.1	1.2	1	0.0012
	Min	1.9	2.3	0.2	4.6	27	0.0026
	Max	5.1	5.1	0.3	7.5	32	0.0057

Table s4: Magnetic susceptibility (χ), saturation magnetization by mass (Ms), saturation remanent magnetization by mass (Mrs), coercive force (Bc), coercivity of the saturation remanent magnetization (Bcr) and weight percentage of magnetite (wt%) of *J. mimosifolia* leaves collected nearby MNBA in March 2023.

Site		**χ 10^{-8} m^3 kg^{-1}**	**Ms mAm^2 kg^{-1}**	**Mrs mAm^2 kg^{-1}**	**Bc mT**	**Bcr mT**	**wt %**
OP	Mean	31.0	24.0	1.4	5.3	36	0.0267
	SE	5.3	4.10	0.3	0.1	2	0.0046
	Min	22.0	16.6	0.9	5.1	32	0.0184
	Max	40.0	30.9	2.0	5.6	38	0.0343
MU	Mean	24.0	19.0	1.3	5.5	35	0.0211
	SE	4.6	4.1	0.2	0.2	0	0.0046
	Min	16.0	11.0	0.8	5.0	34	0.0122
	Max	25.0	25.0	1.5	5.8	35	0.0278
PK	Mean	19	15.0	1.1	5.9	33	0.0167
	SE	1.2	0.0	0.0	0.4	1	0.0000
	Min	17.0	15.1	1.0	5.3	32	0.0168
	Max	21.0	15.2	1.1	6.6	33	0.0169

Table s5: Magnetic susceptibility (χ), saturation magnetization by mass (Ms), saturation remanent magnetization by mass (Mrs), coercive force (Bc), coercivity of the saturation remanent magnetization (Bcr) and weight percentage of magnetite (wt%) of *F. americana* leaves collected nearby MHN in November 2022.

Site		**χ 10^{-8} m^3 kg^{-1}**	**Ms mAm^2 kg^{-1}**	**Mrs mAm^2 kg^{-1}**	**Bc mT**	**Bcr mT**	**wt %**
OP	Mean	5.5	4.0	0.3	6.6	31	0.0044
	SE	1.0	0.6	0.0	0.7	4	0.0006
	Min	4.2	3.5	0.3	5.1	25	0.0039
	Max	7.5	5.2	0.4	7.4	38	0.0058
MU	Mean	2.8	2.3	0.2	7.3	29	0.0026
	SE	0.5	0.4	0.1	1.1	2	0.0004
	Min	2.0	1.5	0.1	5.4	25	0.0017
	Max	3.7	2.8	0.2	9.1	33	0.0031

Table s6: Magnetic susceptibility (χ), saturation magnetization by mass (Ms), saturation remanent magnetization by mass (Mrs), coercive force (Bc) and coercivity of the saturation remanent magnetization (Bcr) of *F. americana* leaves collected nearby MHN in March 2023.

Site		**χ 10^{-8} m^3 Kg^{-1}**	**Ms mAm^2 kg^{-1}**	**Mrs mAm^2 kg^{-1}**	**Bc mT**	**Bcr mT**	**wt %**
OP	Mean	6.3	4.1	0.3	6.6	35	0.0046
	SE	0.7	0.31	0.1	0.3	2	0.0003
	Min	5.0	3.5	0.2	6.1	31	0.0039
	Max	7.4	4.6	0.3	7.1	37	0.0051
MU	Mean	4.6	2.9	0.2	8.3	31	0.0032
	SE	1.4	0.7	0.1	1.4	2	0.0008
	Min	3.2	1.5	0.1	6.6	28	0.0017
	Max	7.3	3.8	0.2	10.9	33	0.0042

Research article:

Science of the Total Environment 988 (2025) 179836

Contents lists available at ScienceDirect

Science of the Total Environment

journal homepage: www.elsevier.com/locate/scitotenv

Magnetic and chemical biomonitoring with lichens and vascular plants for the preservation of cultural heritage: A case study at two museums in a megacity (Buenos Aires, Argentina)

Lisa Grifoni [a,b], Aldo Winkler [a,*], Marcos A.E. Chaparro [c], Luigi Antonello Di Lella [b], Fernando Marte [d], Antonio Sgamellotti [e], Lilla Spagnuolo [a], Marcos Tascon [d], Daniela Buitrago Posada [c,f], Débora C. Marié [c,f], Martina Scoccimarro [d], Stefano Loppi [b]

[a] Istituto Nazionale di Geofisica e Vulcanologia, Rome, Italy
[b] Department of Life Sciences, University of Siena, Italy
[c] Centro de Investigaciones en Física e Ingeniería del Centro de la Provincia de Buenos Aires (CIFICEN, CONICET-UNCPBA), Argentina
[d] Centro de Estudios sobre Patrimonios y Ambiente, Universidad Nacional de San Martín, Buenos Aires, Argentina
[e] Accademia Nazionale dei Lincei, Rome, Italy
[f] Universidad Nacional del centro de la Provincia de Buenos Aires (UNCPBA), Facultad de Ciencias Exactas, IFAS, Pinto 399, 7000 Tandil, Buenos Aires, Argentina

***All the authors have agreed for the published article to be used as a chapter of this PhD thesis.**

Thesis conclusions

This PhD thesis explored a multidisciplinary approach for the preventive conservation of cultural heritage. Through the application of magnetic and chemical analysis, the studies investigated the distribution of PM and PTEs across distinct pollution sources and cultural heritage settings, demonstrating that lichen transplants provide a robust proxy for mapping airborne pollutants in both indoor and outdoor environments, thereby supporting prevention-oriented conservation strategies. Moreover, the research highlights the efficiency of different plant leaves to collect PM, offering ecosystem services to the area.

At Peggy Guggenheim Collection of Venice, where the pollution source was mainly diffused, the outdoor bioaccumulation of magnetic PM and PTEs was low in lichen (*E. prunastri*) and null in *P. tobira* leaves, with negligible concentrations detected in *E. prunastri* indoors. Magnetic analyses detected subtle variations of metallic magnetic particulate across the sites, confirming the sensitivity of magnetic parameters. Nevertheless, lichen transplants revealed specific point sources of pollution, such as the localized bioaccumulation of Zn within the museum interiors and Sb outdoors (chapter 1).

At the Palatine Hill in Rome, the study showed the bioaccumulation in lichens and leaves at two settings: along a busy road (via dei Cerchi) and in the adjacent archaeological area located ~8 m above the road level. The bioaccumulated PTEs and PM were directly derived from traffic, showing a decrease in concentrations with increasing distance from the road, and no influence from elevation. This finding highlights the importance of green barriers near traffic corridors for maximizing their ecosystem service function in mitigating pollutant exposure. The study highlighted a difference in PM accumulation: leaves were influenced by both airborne and resuspended particles, whereas lichens primarily bioaccumulated airborne PM with negligible influence from other sources (chapter 2). Magnetic measurements were so sensitive to reveal metallic particles of different magnetic grain size according to the different traffic regimes at via dei Cerchi.

In Buenos Aires, we realized the first application of magnetic and chemical biomonitoring at cultural heritage in a South American megacity. The study showed negligible bioaccumulation of metallic PM and PTEs inside the museums' halls. Conversely, the combined use of lichen transplants and plant leaves enabled the mapping of PM and PTEs

dispersion toward the museum interiors, higher along the street and lower close to the building. Leaves of *J. mimosifolia* exhibited remarkable PM and PTEs bioaccumulation capabilities, demonstrating higher effectiveness compared to the leaves of *F. americana*. These results confirmed the consistency of outdoor bioaccumulation linked to traffic pollution and expanded the dataset of suitable plant species for ecosystem services (chapter 3).

Overall, this thesis demonstrates the potential of biomonitoring using lichen transplants and plant leaves as a non-invasive tool for preventive conservation and highlights the need to select appropriate plants to mitigate the diffusion and consequently the deposition of PM on heritage. This thesis introduces a new framework in which biomonitoring is a key component of preventive conservation strategies.

Acknowledgements

My gratitude goes to my supervisors, Prof. Stefano Loppi and Dr. Aldo Winkler, who addressed me during these years. I am deeply grateful to my family, Edo and friends for their support and love. I would thank my collegues who have helped, taught and supported me throughout this journey.

References

- Accorinti, J., Allende, D., Puliafito, S.E., 2023. The impact on air quality of PM10 emissions from the bus fleet of Buenos Aires City. SN Appl. Sci. 5 (1). https://doi. org/10.1007/s42452-022-05231-5.

- Almeida, S.M., Canha, N., Silva, A., Freitas, M.D., Pegas, P., Alves, C., Evtyugina, M., Pio, C.A., 2011. Children exposure to atmospheric particles in indoor of Lisbon primary schools. Atmos. Environ. 45, 7594–7599.

- Amereih, S., Meisel, T., Scholger, R., Wegscheider, W., 2005. Antimony speciation in soil samples along two Austrian motorways by HPLC-ID-ICP-MS. J. Environ. Monit. 7, 1200–1206. https://doi.org/10.1039/b510321e.

- Ashley-Smith, J. (1999). *Risk assessment for object conservation*. Oxford: Butterworth-Heinemann.

- Baldantoni, D., de Nicola, F., Alfani, A., 2020. Potentially toxic element gradients in remote, residential, urban and industrial areas, as highlighted by the analysis of Quercus ilex leaves. Urban For. Urban Green. 47 https://doi.org/10.1016/j. ufug.2019.126522.

- Belfiore, C.M., Barca, D., Bonazza, A., Comite, V., la Russa, M.F., Pezzino, A., Ruffolo, S. A., Sabbioni, C., 2013. Application of spectrometric analysis to the identification of pollution sources causing cultural heritage damage. Environ. Sci. Pollut. Res. 20 (12), 8848–8859. https://doi.org/10.1007/s11356-013-1810-y.

- Blanusa, T., Fantozzi, F., Monaci, F., Bargagli, R., 2015. Leaf trapping and retention of particles by holm oak and other common tree species in Mediterranean urban environments. Urban For. Urban Green. 14 (4), 1095–1101. https://doi.org/ 10.1016/j.ufug.2015.10.004.

- Bonazza, A., Sabbioni, C., Ghedini, N., 2005. Quantitative data on carbon fractions in interpretation of black crusts and soiling on European built heritage. Atmos. Environ. 39 (14), 2607–2618. https://doi.org/10.1016/j.atmosenv.2005.01.040.

- Butler, R.F., Banerjee, S.K., 1975. Theoretical single-domain grain size range in magnetite and titanomagnetite. J. Geophys. Res. 80, 4049–4058. Canha, N., Almeida, S.M., Freitas,

M.C., Wolterbeek, H.T., 2014. Indoor and outdoor biomonitoring using lichens at urban and rural primary schools. J. Toxicol. Environ. Health Part A 77, 900–915. https://doi.org/10.1080/15287394.2014.911130, 14- 16.

- Calzoni, G. L., Antognoni, F., Pari, E., Fonti, P., Gnes, A., & Speranza, A. (2007). Active biomonitoring of heavy metal pollution using Rosa rugosa plants. *Environmental pollution (Barking, Essex : 1987)*, *149*(2), 239–245. https://doi.org/10.1016/j.envpol.2006.12.023
- Canha, N., Almeida-Silva, M., Freitas, M.C., Almeida, S.M., Wolterbeek, H.T., 2012. Lichens as biomonitors at indoor environments of primary schools. J. Radioanal. Nucl. Chem. 291 (1), 123–128. https://doi.org/10.1007/s10967-011-1259-8.
- Camuffo, D. (2014). *Microclimate for cultural heritage: Conservation, restoration, and maintenance of indoor and outdoor monuments* (2nd ed.). Elsevier.
- Castañeda Miranda, A.G., Chaparro, M.A.E., Marie, D.C., Chaparro, M.A.E., 2018. Uso de la epífita Tillandsia recurvata para biomonitoreo magnetico de contaminaci´on atmosferica en La Plata, Argentina [Use of Tillandsia recurvata for magnetic biomonitoring of atmospheric pollution in La Plata, Argentina]. Geos 38 (1), 79–80.
- Chaparro, M.A.E., Lavornia, J.M., Chaparro, M.A.E., Sinito, A.M., 2013. Biomonitors of urban air pollution: magnetic studies and SEM observations of corticolous foliose and microfoliose lichens and their suitability for magnetic monitoring. Environ. Pollut. 172, 61–69. https://doi.org/10.1016/j.envpol.2012.08.006.
- Chaparro, M.A.E., Chaparro, M.A.E., Castañeda Miranda, A.G., Marié, D.C., Gargiulo, J. D., Lavornia, J.M., Natal, M., B¨ohnel, H.N., 2020. Fine air pollution particles trapped by street tree barks: in situ magnetic biomonitoring. Environ. Pollut. 226 (1), 115229. https://doi.org/10.1016/j.envpol.2020.115229.
- Chaparro, M.A.E., 2021. Airborne particle accumulation and loss in pollution-tolerant lichens and its magnetic quantification. Environ. Pollut., 117807 https://doi.org/ 10.1016/j.envpol.2021.117807.
- Chaparro, M.A.E., Buitrago Posada, D., Chaparro, M.A.E., Molinari, D., Chiavarino, L., Alba, B., Marié, D.C., Natal, M., B¨ohnel, H.N., Vaira, M., 2024. Urban and suburban's airborne magnetic particles accumulated on Tillandsia capillaris. Sci. Total Environ. 907, 167890. https://doi.org/10.1016/J.SCITOTENV.2023.167890.
- Comite, V., Pozo-Antonio, J.S., Cardell, C., Rivas, T., 2019. Metals distributions within

black crusts sampled on the facade of an historical monument: The case study of the Cathedral of Monza (Milan, Italy). IMEKO TC4 International. In: Conference on Metrology for Archaeology and Cultural Heritage, MetroArchaeo: 4 through 6 December. International Measurement Federation Secretariat (IMEKO), pp. 73–78.

- Contardo, T., Vannini, A., Sharma, K., Giordani, P., Loppi, S., 2020. Disentangling sources of trace element air pollution in complex urban areas by lichen biomonitoring. A case study in Milan (Italy). Chemosphere 256. https://doi.org/10.1016/j.chemosphere.2020.127155.
- Coulston, J.W., Smith, G.C., Smith, W.D., 2003. Regional assessment of ozone sensitive tree species using bioindicator plants. Environ. Monit. Assess. 83, 113–127.
- Councell, T.B., Duckenfield, K.U., Landa, E.R., Callender, E., 2004. Tire-wear particles as a source of zinc to the environment. Environ. Sci. Technol. 38 (15), 4206–4214. https://doi.org/10.1021/es034631f.
- Day, R., Fuller, M., Schmidt, V.A., 1977. Hysteresis properties of titanomagnetites: grain-size and compositional dependence. Phys. Earth Planet. Inter. 13, 260–267. https://doi.org/10.1016/0031-9201(77)90108-X.
- Demková, L., Árvay, J., Bobulska, L., Oboňa, J. (2018). The Risk Elements Biomonitoring in the Ambient Air of an Underground Parking Lot. Polish Journal of Natural Science. 33. 545-559.
- Demková, L., Oboňa, J., Árvay, J., Michalková, J., & Lošák, T. (2019). Biomonitoring road dust pollution along streets with various traffic densities. *Polish Journal of Environmental Studies*, *28*(5), 3687–3696. https://doi.org/10.15244/pjoes/97354
- Dunlop, D.J., 2002a. Theory and application of the day plot (MRS/MS versus HCR/HC) 1. Theoretical curves and tests using titanomagnetite data. J. Geophys. Res. 107. https://doi.org/10.1029/2001JB000487.
- Dunlop, D.J., 2002b. Theory and application of the day plot (MRS/MS versus HCR/HC) 2. Application to data for rocks, sediments, and soils. J. Geophys. Res. 107. https://doi.org/10.1029/2001JB000486.
- Dunlop, D.J., Ozdemir, O., 1997. Rock Magnetism: Fundamentals and Frontiers. Cambridge University Press, Cambridge.

- Dzierzanowski, K., Popek, R., Gawronska, H., Sæbø, A., Gawronski, S.W., 2011. Deposition of particulate matter of different size fractions on leaf surfaces and in waxes of urban forest species. Int. J. Phytoremediation 13, 1037–1046.

- Fantozzi, F., Monaci, F., Blanusa, T., Bargagli, R., 2013. Holm Oak (Quercus ilex L.) canopy as interceptor of airborne trace elements and their accumulation in the litter and topsoil. Environ. Pollut. 183, 89–95. https://doi.org/10.1016/j. envpol.2012.11.037.

- Frati, L., Brunialti, G., Loppi, S., 2005. Problems related to lichen transplants to monitor trace element deposition in repeated surveys: a case study from central Italy. J. Atmos. Chem. 52 (3), 221–230. https://doi.org/10.1007/s10874-005-3483-5.

- Frati, L., Caprasecca, E., Santoni, S., Gaggi, C., Guttova, A., Gaudino, S., Pati, A., Rosamilia, S., Pirintsos, S.A., Loppi, S., 2006. Effects of NO2 and NH3 from road traffic on epiphytic lichens. Environ. Pollut. 142 (1), 58–64. https://doi.org/ 10.1016/j.envpol.2005.09.020.

- Formenton, G., Gregio, M., Gallo, G., Liguori, F., Peruzzo, M., Innocente, E., Lava, R., Masiol, M., 2021. PM10-bound arsenic emissions from the artistic glass industry in Murano (Venice, Italy) before and after the enforcement of REACH authorisation. J. Hazard. Mater. 406, 124294 https://doi.org/10.1016/j.jhazmat.2020.124294.

- Fusaro, L., Salvatori, E., Winkler, A., Frezzini, M.A., De Santis, E., Sagnotti, L., Canepari, S., Manes, F., 2021. Urban trees for biomonitoring atmospheric particulate matter: an integrated approach combining plant functional traits, magnetic and chemical properties. Ecol. Indic. 126 https://doi.org/10.1016/j. ecolind.2021.107707.

- Fujiwara, F.G., G´omez, D.R., Dawidowski, L., Perelman, P., Faggi, A., 2011. Metals associated with airborne particulate matter in road dust and tree bark collected in a megacity (Buenos Aires, Argentina). Ecol. Indic. 11 (2), 240–247. https://doi.org/ 10.1016/j.ecolind.2010.04.007.

- Georgeaud, V.M., Rochette, P., Ambrosi, J.P., Vandamme, D., Williamson, D., 1997. Relationship between heavy metals and magnetic properties in a large polluted catchment: the etang de berre (south of France). Phys.Chem. Earth 22 (1–2), 211–214. https://doi.org/10.1016/S0079-1946(97)00105-5.

- Gerhardt, A., Ingram, M. & Kang, I. J. & Ulitzur, S. (2006). In situ on-line toxicity biomonitoring in water: Recent developments. *Environmental toxicology and chemistry* / SETAC. 25. 2263-71. 10.1897/05-486R1.1.
- Gómez, D.R., Giné, M.F., Bellato, A.C.S., Smichowski, P., 2005. Antimony: a traffic-related element in the atmosphere of Buenos Aires, Argentina. J. Environ. Monit. 7 (12), 1162–1168.
- Gonçalves Da Silva, I., Ramos, C., Nunes, O., de Oliveira Costa, R., Eugˆenia, Pereira, C., Canela, M.C., 2021. Formaldehyde Exposure and Atmospheric Biomonitoring With Lichen Cladonia verticillaris in an Anatomy Laboratory. https://doi.org/10.1007/ s11356-021-14036-9.
- Gonet, T., Maher, B.A., 2019. Airborne, vehicle-derived fe-bearing nanoparticles in the urban environment—a review. Environ. Sci. Technol. 53, 9970–9991.
- Gonet, T., Maher, B.A., Kukutschová, J., 2021a. Source apportionment of magnetite particles in roadside airborne particulate matter. Sci. Total Environ. 752, 141828 https://doi.org/10.1016/j.scitotenv.2020.141828.
- Gonet, T., Maher, B.A., Nyirő-Kósa, I., P´osfai, M., Vaculík, M., Kukutschová, J., 2021b. Size-resolved, quantitative evaluation of the magnetic mineralogy of airborne brake-wear particulate emissions. Environ. Pollut. 288, 117808 https://doi.org/10.1016/j. envpol.2021.117808.
- Grifoni, L., Winkler, A., di Lella, L.A., Buemi, L.P., Sgamellotti, A., Spagnuolo, L., Loppi, S., 2024a. Magnetic and chemical biomonitoring of particulate matter at cultural heritage sites: the Peggy Guggenheim collection case study (Venice, Italy). Environ. Adv. 15. https://doi.org/10.1016/j.envadv.2023.100455.
- Grifoni, L., Winkler, A., Boldrighini, F., di Lella, L.A., Russo, A., Sgamellotti, A., Spagnuolo, L., Strano, G., Loppi, S., 2024b. Nature-based solutions for monitoring the impact of vehicular particulate matter and for the preventive conservation of the Palatine Hill archaeological site in Rome, Italy. Sci. Total Environ. 946, 174358. https://doi.org/10.1016/j.scitotenv.2024.174358.
- Hamal, J.P., Chettri, Mukesh, Kumar, 2008. Impact of heavy metals and biochemical parameters on specific leaf area of roadside trees in Kathmandu. NepalEco. Env. & Cons. 28 (3), 1108–1118.

- Harrison, R.J., Feinberg, J.M., 2008. FORCinel: An improved algorithm for calculating first-order reversal curve distributions using locally weighted regression smoothing. Geochem. Geophy. Geosy. 9 (5), 1987. https://doi.org/10.1029/2008GC001987.

- Hjortenkrans, D., Bergbäck, B., Häggerud, A., 2006. New metal emission patterns in road traffic environments. Environ. Monit. Assess. 117 (1–3), 85–98. https://doi.org/ 10.1007/s10661-006-7706-2.

- Hofman, J., Maher, B.A., Muxworthy, A.R., Wuyts, K., Castanheiro, A., Samson, R., 2017. Biomagnetic monitoring of atmospheric pollution: A review of magnetic signatures from biological sensors. Environ. Sci. Technol. 51, 6648–6664. https://doi.org/ 10.1021/acs.est.7b00832.

- Hulskotte, J.H.J., van der Gon, H.A.C.D., Visschedijk, A.J.H., Schaap, M., 2007. Brake wear from vehicles as an important source of diffuse copper pollution. Water Sci. Technol. 56 (1), 223–231. https://doi.org/10.2166/wst.2007.456.

- International Atomic Energy Agency, 1999. Reference material IAEA-336 - trace and minor elements in lichen. In: Reference Sheet (4 pp). Jeong, H., 2022. Toxic metal concentrations and Cu–Zn–Pb isotopic compositions in tires. J. Anal. Sci. Technol. 13 (1) https://doi.org/10.1186/s40543-021-00312-3.

- Keenan, T., Niinemets, Ü., Sabate, S., Gracia, C., Peñuelas, J., 2009. Process based inventory of isoprenoid emissions from European forests: model comparisons, current knowledge and uncertainties. Atmos. Chem. Phys. 9, 4053–4076.

- Lappe, S.C.L.L., Feinberg, J.M., Muxworthy, A., Harrison, R.J., 2013. Comparison and calibration of nonheating paleointensity methods: a case study using dusty olivine. Geochem. Geophys. Geosyst. 14 (7), 2143–2158. https://doi.org/10.1002/ ggge.20141.

- Larrasoaña, J.C., Pey, J., Zhao, X., Heslop, D., Mochales, T., Mata, P., Beamud, E., Reyes, J., Cerro, J.C., Perez, N., Castillo, S., 2021. Environmental magnetic fingerprinting of anthropogenic and natural atmospheric deposition over southwestern Europe. Atmos. Environ. 261, 118568 https://doi.org/10.1016/j. atmosenv.2021.118568.

- Lascu, I., Einsle, J.F., Ball, M.R., Harrison, R.J., 2018. The vortex state in geologic materials: a micromagnetic perspective. J. Geophys. Res. Solid Earth 123, 7285–7304.

https://doi.org/10.1029/2018JB015909.

- Letaïef, S., Carvallo, C., Franke, C., Isambert, A., Camps, P., 2024. Contributions and limitations of environmental magnetism to characterize traffic-related particulate matter sources. Geophys. J. Int. 237 (3), 1505–1525. https://doi.org/10.1093/gji/ ggae108.
- Levei, L., Cadar, O., Babalau-Fuss, V., Kovacs, E., Torok, A. I., Levei, E. A., & Ozunu, A. (2021). Use of black poplar leaves for the biomonitoring of air pollution in an urban agglomeration. *Plants*, *10*(3), 1–14. https://doi.org/10.3390/plants10030548
- Loppi, S., Pacioni, G., Olivieri, N., di Giacomo, F., 1998. Accumulation of trace metals in the lichen Evernia prunastri transplanted at biomonitoring sites in Central Italy. Bryologist 101 (3), 451–454. https://doi.org/10.2307/3244187.
- Loppi, S., Pirintsos, S.A., De Dominicis, V., 1999. Soil Contribution to the Elemental Composition of Epiphytic Lichens (Tuscany, Central Italy).
- Loppi, S., Paoli, L., 2015. Comparison of the trace element content in transplants of the lichen Evernia prunastri and in bulk atmospheric deposition: a case study from a low polluted environment (C Italy). Biologia 70, 460–466 (Bratisl).
- Loppi, S. 2019. May the diversity of epiphytic lichens be used in environmental forensics? In *Diversity* (Vol. 11, Issue 3). MDPI AG. https://doi.org/10.3390/D11030036
- Loppi, S., Ravera, S., Paoli, L., 2019a. Coping with uncertainty in the assessment of atmospheric pollution with lichen transplants. Environ. Forensics. https://doi.org/ 10.1080/15275922.2019.1627615.
- Loppi, S., Corsini, A., Paoli, L., 2019b. Estimating environmental contamination and element deposition at a urban area of Central Italy. Urban Sci. 3, 76. https://doi.org/ 10.3390/urbansci3030076.
- Lorenzini, G., Grassi, C., Nali, C., Petiti, A., Loppi, S., Tognotti, L., 2006. Leaves of Pittosporum tobira as indicators of airborne trace element and PM10 distribution: three case studies from Italy. Atmos. Environ. 40 (22), 4025–4036. https://doi.org/ 10.1016/j.atmosenv.2006.03.032.
- Maher, B.A., Moore, C., Matzka, J., 2008. Spatial variation in vehicle-derived metal pollution identified by magnetic and elemental analysis of roadside tree leaves. Atmos. Environ. 42, 364–373.

- Marié, D.C., Chaparro, M.A.E., Irurzun, M.A., Lavornia, J.M., Marinelli, C., Cepeda, R., Böhnel, H.N., Castañeda, M.A.G., Sinito, A.M., 2016. Magnetic mapping of air pollution in Tandil City (Argentina) using the lichen Parmotrema pilosum as biomonitor. Atmos. Pollut. Res. 7, 513–520. https://doi.org/10.1016/j. apr.2015.12.005.
- Matzka, J., & Maher, B. A. (1999). Magnetic biomonitoring of roadside tree leaves: identi"cation of spatial and temporal variations in vehicle-derived particulates. In *Atmospheric Environment* (Vol. 33).
- Masiol, M., Squizzato, S., Ceccato, D., Pavoni, B., 2014. The size distribution of chemical elements of atmospheric aerosol at a semi-rural coastal site in Venice (Italy). The role of atmospheric circulation. Chemosphere 119, 400–406. https://doi.org/10.1016/j. chemosphere.2014.06.086. PMID: 25063963.
- Matějka, V., Lu, Y., Matějková, P., Smetana, B., Kukutschová, J., Vaculík, M., Tomášek, V., Zlá, S., Fan, Y., 2011. Possible stibnite transformation at the friction surface of the semi-metallic friction composites designed for car brake linings. Appl. Surf. Sci. 258 (5), 1862–1868. https://doi.org/10.1016/j.apsusc.2011.10.063.
- Mitsos, D., Kantarelou, V., Palamara, E., Karydas, A.G., Zacharias, N., Gerasopoulos, E., 2022. Characterization of black crust on archaeological marble from the Library of Hadrian in Athens and inferences about contributing pollution sources. J. Cult. Herit. 53, 236–243. https://doi.org/10.1016/j.culher.2021.12.003.
- Monaci, F., Bargagli, R., 1997. Barium and other trace metals as indicators of vehicle emissions. Water Air Soil Pollut. 100, 89–98.
- Monaci, F., Moni, F., Lanciotti, E., Grechi, D., Bargagli, R., 2000. Biomonitoring of airborne metals in urban environments: new tracers of vehicle emission, in place of lead. Environ. Pollut. 107 (2000), 321–327. www.elsevier.com/locate/envpol.
- Monaci, F., Ancora, S., Paoli, L., Loppi, S., Franzaring, J., 2023. Air quality in post-mining towns: tracking potentially toxic elements using tree leaves. Environ. Geochem. Health 45 (3), 843–859. https://doi.org/10.1007/s10653-022-01252-6.
- Moreno, E., Sagnotti, L., Dinarès-Turell, J., Winkler, A., Cascella, A., 2003. Biomonitoring of traffic air pollution in Rome using magnetic properties of tree leaves. Atmos. Environ. 37 (21), 2967–2977. https://doi.org/10.1016/S1352-2310 (03)00244-9.
- Mori, J., Sæbø, A., Hanslin, H.M., Teani, A., Ferrini, F., Fini, A., Burchi, G., 2015.

Deposition of traffic-related air pollutants on leaves of six evergreen shrub species during a Mediterranean summer season. Urban For. Urban Green. 14 (2), 264–273. https://doi.org/10.1016/j.ufug.2015.02.008.

- Muhammad, S., Wuyts, K., Samson, R., 2019. Atmospheric net particle accumulation on 96 plant species with contrasting morphological and anatomical leaf characteristics in a common garden experiment. Atmos. Environ. 202, 328–344. https://doi.org/ 10.1016/j.atmosenv.2019.01.015.

- Muhammad, S., Wuyts, K., Samson, R., 2022. Selection of plant species for particulate matter removal in urban environments by considering multiple ecosystem (dis) services and environmental suitability. Atmosphere 13 (12), 1960. https://doi.org/ 10.3390/atmos13121960.
- Odabasi, M., Ozgunerge Falay, E., Tuna, G., Altiok, H., Kara, M., Dumanoglu, Y., ... & Elbir, T. (2015). Biomonitoring the spatial and historical variations of persistent organic pollutants (POPs) in an industrial region. *Environmental science & technology*, *49*(4), 2105-2114.
- Ozga, I., Ghedini, N., Giosuè, C., Sabbioni, C., Tittarelli, F., Bonazza, A., 2014. Assessment of air pollutant sources in the deposit on monuments by multivariate analysis. Sci. Total Environ. 490, 776–784. https://doi.org/10.1016/j. scitotenv.2014.05.084.
- Paoli, L., Munzi, S., Fiorini, E., Gaggi, E., Loppi, S., 2013. Influence of angular exposure and proximity to vehicular traffic on the diversity of epiphytic lichens and the bioaccumulation of traffic-related elements. Environ. Sci. Pollut. Res. 20, 250–259. https://doi.org/10.1007/s11356-012-0893-1.
- Paoli, L., Fǎckovcová, Z., Guttová, A., Maccelli, C., Kresáňová, K., Loppi, S., 2019. Evernia goes to school: bioaccumulation of heavy metals and photosynthetic performance in lichen transplants exposed indoors and outdoors in public and private environments. Plants 8, 125. https://doi.org/10.3390/plants8050125.

- Paoli, L., Bandoni, E., Sanità di Toppi, L., 2023. Lichens and Mosses as Biomonitors of Indoor Pollution. In Biology (Vol. 12, Issue 9). Multidisciplinary Digital Publishing Institute (MDPI). https://doi.org/10.3390/biology12091248
- Petrovský, E., Kapiˇcka, A., Jordanova, N., et al., 2000. Low-field magnetic susceptibility: a proxy method of estimating increased pollution of different environmental systems.

Environ. Geol. 39, 312–318. https://doi.org/10.1007/s002540050010.

- Pike, C.R., Roberts, A.P., Verosub, K.L., 1999. Characterizing interactions in fine magnetic particle systems using first order reversal curves. J. Appl. Phys. 85, 6660–6667.
- Popovicheva, O., Kireeva, E., Persiantseva, N., Timofeev, M., Bladt, H., Ivleva, N.P., Niessner, R., Moldanova, J., 2012. Microscopic´ characterization of individual particles from multicomponent ship exhaust. J. Environ. Monit. 14, 3101–3110.
- Prodi, F., Belosi, F., Contini, D., Santachiara, G., Di Matteo, L., Gambaro, A., Donateo, A., Cesari, D., 2009. Aerosol fine fraction in the Venice Lagoon: particle composition and sources. Atmos. Res. 92, 141–150.
- Protano, C., Owczarek, M., Antonucci, A., Guidotti, M., Vitali, A., 2017. Assessing indoor air quality of school environments: transplanted lichen Pseudovernia furfuracea as a new tool for biomonitoring and bioaccumulation. Environ. Monit. Assess. 189, 358. https://doi.org/10.1007/s10661-017-6076-2.
- Quero, J.L., Villar, R., Mara˜n´on, T., Zamora, R., 2006. Interactions of drought and shade effects on seedlings of four Quercus species: physiological and structural leaf responses. New Phytol. 170 (4), 819–834. https://doi.org/10.1111/j.1469- 8137.2006.01713.
- Querol, X., Alastuey, A., Ruiz, C. R., Viana, M., Minguillón, M. C., Castillo, S., & López-Soler, A. (2004). Speciation and origin of PM10 and PM2.5 in Spain. Atmos. Environ., 38(36), 6383–6395. DOI: 10.1016/j.atmosenv.2004.08.003
- R Core Team, 2025. R: A Language and Environment for Statistical Computing. R Foundation for Statistical Computing, Vienna. Avaliable in: https://www.R-project. org(Accessed on March 30, 2025).
- Roberts, A.P., Pike, C.R., Verosub, K.L., 2000. First-order reversal curve diagrams: a new tool for characterizing the magnetic properties of natural samples. J. Geophys. Res. Solid Earth 105 (B12), 28461–28475. https://doi.org/10.1029/2000jb900326.
- Roberts, A.P., Heslop, D., Zhao, X., Pike, C.R., 2014. Understanding fine magnetic particle systems through use of first-order reversal curve diagrams. Rev. Geophys. 52 (4), 557–602. https://doi.org/10.1002/2014RG000462.
- Roberts, A.P., Almeida, T.P., Church, N.S., Harrison, R.J., Heslop, D., Li, Y., et al., 2017. Resolving the origin of pseudo-single domain magnetic behavior. J. Geophys. Res. Solid

Earth 122 (12), 9534–9558. https://doi.org/10.1002/2017JB014860.

- Sæbø, A., Popek, R., Nawrot, B., Hanslin, H. M., Gawronska, H., & Gawronski, S. W. (2012). Plant species differences in particulate matter accumulation on leaf surfaces. *Science of the Total Environment*, *427–428*, 347–354. https://doi.org/10.1016/j.scitotenv.2012.03.084
- Sagnotti, L., Macrì, P., Egli, R., Mondino, M., 2006. Magnetic properties of atmospheric particulate matter from automatic air sampler stations in Latium (Italy): Toward a definition of magnetic fingerprints for natural and anthropogenic PM10 sources. J. Geophys. Res. 111, B12. https://doi.org/10.1029/2006JB004508.
- Sagnotti, L., Taddeucci, J., Winkler, A., Cavallo, A., 2009. Compositional, morphological, and hysteresis characterization of magnetic airborne particulate matter in Rome, Italy geochem. Geophys. Geosyst. 10 (8) https://doi.org/10.1029/2009GC002563.
- Sagnotti, L., Winkler, A., 2012. On the magnetic characterization and quantification of the superparamagnetic fraction of tra c-related urban airborne PM in Rome, Italy. Atmos. Environ. 59, 131–140
- Salo, Hanna, 2014. Preliminary comparison of the suitability of three sampling materials to air pollution monitoring. Fennia 192 (2), 154–163. ISSN 1798-5617.
- Salo, H., Mäkinen, J., 2019. Comparison of traditional moss bags and synthetic fabric bags in magnetic monitoring of urban air pollution. Ecol. Indic. 104, 559–566. https://doi.org/10.1016/j.ecolind.2019.05.033.
- Schmid, T., Ubbens, A., Mühlethaler, C., Kuebler, S. M., & Lutz, H. (2021). A review of metal formates on heritage objects. *Heritage Science*, 9, 118. https://doi.org/10.1186/s40494-021-00499-z
- Sgrigna, G., Sæbø, A., Gawronski, S., Popek, R., Calfapietra, C., 2015. Particulate matter deposition on Quercus ilex leaves in an industrial city of central Italy. Environ. Pollut. 197, 187–194. https://doi.org/10.1016/j.envpol.2014.11.030.
- Sheikh, H.A., Maher, B.A., Karloukovski, V., Lampronti, G.I., Harrison, R.J., 2022. Biomagnetic characterization of air pollution particulates in Lahore, Pakistan. Geochem. Geophys. Geosyst. 23, e2021GC010293 https://doi.org/10.1029/ 2021GC010293.

- Sheikh, H.A., Maher, B.A., Woods, A.W., Tung, P.Y., Harrison, R.J., 2023. Efficacy of green infrastructure in reducing exposure to local, traffic-related sources of airborne particulate matter (PM). Sci. Total Environ. 903 https://doi.org/10.1016/j. scitotenv.2023.166598.
- Smith, B.J., Gomez-Heras, M., McCabe, S., 2008. Understanding the decay of stone-built cultural heritage. Prog. Phys. Geogr. Earth Environ. 32 (4), 439–461. https://doi. org/10.1177/0309133308098119.
- Sotiropoulou, S., Sciutto, G., Tenorio, A. L., Mazurek, J., Bonaduce, I., Prati, S., Mazzeo, R., Schilling, M., & Colombini, M. P. (2018). Advanced analytical investigation on degradation markers in wall paintings. *Microchemical Journal*, *139*, 278–294. https://doi.org/10.1016/j.microc.2018.03.007
- Szönyi, M., Sagnotti, L., Hirt, A.M., 2007. On leaf magnetic homogeneity in particulate matter biomonitoring studies. Geophys. Res. Lett. 34, L06306. https://doi.org/ 10.1029/2006GL029076.
- Szönyi, M., Sagnotti, L., Hirt, A.M., 2008. A refined biomonitoring study of airborne particulate matter pollution in Rome, with magnetic measurements on quercus ilex tree leaves. Geophys. J. Int. 173, 127–141. https://doi.org/10.1111/j.1365-246X.2008.03715.x.
- Tittarelli, F., Moriconi, G., Bonazza, A., 2008. Atmospheric deterioration of cement plaster in a building exposed to a urban environment. J. Cult. Herit. 9 (2), 203–206. https://doi.org/10.1016/j.culher.2007.09.005.
- Ugolini, F., Tognetti, R., Raschi, A., Bacci, L., 2013. Quercus ilex L. as bioaccumulator for heavy metals in urban areas: effectiveness of leaf washing with distilled water and considerations on the trees distance from traffic. Urban For. Urban Green. 12 (4), 576–584. https://doi.org/10.1016/j.ufug.2013.05.007.
- Varotsos, C., Tzanis, C., Cracknell, A., 2009. The enhanced deterioration of the cultural heritage monuments due to air pollution. Environ. Sci. Pollut. Res. 16 (5), 590–592. https://doi.org/10.1007/s11356-009-0114-8.
- Vannini, A., Paoli, L., Russo, A., Loppi, S., 2019. Contribution of submicronic (PM1) and coarse (PM>1) particulate matter deposition to the heavy metal load of lichens transplanted along a busy road. Chemosphere 231, 121–125.
- Winkler, A., Caricchi, C., Guidotti, M., Owczarek, M., Macrì, P., Nazzari, M., Amoroso,

A., di Giosa, A., Listrani, S., 2019. Combined magnetic, chemical and morphoscopic analyses on lichens from a complex anthropic context in Rome, Italy. Sci. Total Environ. 690, 1355–1368. https://doi.org/10.1016/j. scitotenv.2019.06.526.

- Winkler, A., Contardo, T., Vannini, A., Sorbo, S., Basile, A., Loppi, S., 2020. Magnetic emissions from brake wear are the major source of airborne particulate matter bioaccumulated by lichens exposed in Milan (Italy). Appl. Sci. 10, 2073. https://doi. org/10.3390/app10062073.

- Winkler, A., Amoroso, A., Di Giosa, A., Marchegiani, G., 2021. The effect of Covid-lockdown on airborne particulate matter in Rome, Italy: a magnetic point of view. Environ. Pollut. 291, 118191 https://doi.org/10.1016/j.envpol.2021.11819.

- Winkler, A., Contardo, T., Lapenta, V., Sgamellotti, A., Loppi, S., 2022. Assessing the impact of vehicular particulate matter on cultural heritage by magnetic biomonitoring at Villa Farnesina in Rome, Italy. Sci. Total Environ. 823 https://doi.org/10.1016/j.scitotenv.2022.153729.